AN EVALUATION OF THE EUTROPHICATION PREVENTION POTENTIAL OF HIGH RATE ALGAE PONDS THROUGH THE DEVELOPMENT OF A DETERMINISTIC DESIGN MODEL

by
Izak Schalk Willem van der Merwe

Thesis presented in fulfilment of the requirements for the degree of Master of Engineering in the Faculty of Civil Engineering at Stellenbosch University

Supervisor: Dr IC Brink

December 2016

DECLARATION

By submitting this thesis electronically, I declare that the entirety of the work contained therein is my own, original work, that I am the sole author thereof (save to the extent explicitly otherwise stated), that reproduction and publication thereof by Stellenbosch University will not infringe any third party rights and that I have not previously in its entirety or in part submitted it for obtaining any qualification.

ISW van der Merwe

Date

ABSTRACT

Wastewater treatment is a major problem in South Africa. South Africa generally has the wastewater treatment infrastructure in place but often lacks the labour skills to operate these plants efficiently. The increasing eutrophication in South African water bodies is an indication that this problem needs to be rectified.

The characteristics of a High Rate Algal Pond (HRAP) make it an attractive option for effluent polishing in South Africa. It has the potential of simultaneous nutrient removal and nutrient recovery from the partially or poorly treated effluent of wastewater treatment works. Its simple operation would ensure that it is less susceptible to the poor operation practices in South Africa. It is also relatively inexpensive to construct and operate, but the large footprint of these ponds makes its feasibility largely dependent on the availability and cost of land.

A scale model HRAP was operated under laboratory conditions to investigate the nutrient removal potential of these ponds. The nutrient removal measured during the laboratory experiments was believed to be modest, due to a lack of the high-intensity sunlight that the algae require for photosynthesis. However, these were promising indications that the HRAP might be effective in the warm and sunny climate of South Africa despite the modest nutrient removals measured in the laboratory experiments.

A deterministic design model for an HRAP was developed. The deterministic design was programmed into Microsoft Excel with the use of Microsoft Visual Basics for Applications (VBA). The deterministic equations were solved numerically in the computational model. The results obtained from the laboratory experiments were used to calibrate the computational HRAP model. The calibrated computational model accurately predicted the ammonia and nitrate/nitrite concentrations. It was unsatisfactory in predicting the soluble reactive phosphorus (SRP) concentration since it did not account for phosphate precipitation. The model only gave an estimation of the SRP assimilated by algae.

The calibrated HRAP model was used to investigate the nutrient removal potential of an HRAP in South Africa. It was established that shallow ponds with long retention times, and consequently large surface areas, are required to achieve satisfactory nutrient removal. The area requirement of an HRAP was estimated at approximately 60 square meters per cubic meter of daily flow to achieve roughly 100% Total Inorganic Nitrogen removal. The estimated area requirement for roughly 100% ammonia removal was approximately 20 m^2/m^3/day. It was also established that HRAPs has the prospect of notable SRP removal.

The theoretical calculations of the deterministic HRAP model indicated that an HRAP could potentially achieve sufficient nutrient removal for effective eutrophication prevention. However, the large surface area requirements might not make the HRAP practically feasible for effluent polishing in most cases.

OPSOMMING

Die suiwering van rioolwater is 'n groot probleem in Suid-Afrika. Suid-Afrika het oor die algemeen die nodige infrastruktuur vir rioolwater suiwering, maar het dikwels nie die vaardighede om hierdie rioolsuiweringsaanlegte doeltreffend te bestuur nie. Die toenemende eutrofikasie in die Suid-Afrikaanse varswaterbronne is 'n aanduiding dat hierdie probleem aangespreek moet word.

Die eienskappe van 'n Hoë Konsentrasie Alg Dam (HKAD) maak dit 'n gewenste opsie vir die polering van die afvloeiwater van oneffektiewe rioolsuiweringsaanlegte in Suid-Afrika. Dit het die potensiaal om voedingstowwe (hoofsaaklik stikstof en fosfor) te verwyder asook te herwin uit die gedeeltelike of swak behandelde afvloeiwater van hierdie rioolsuiweringsaanlegte. Die eenvoudige bestuur van die HKAD sal verseker dat dit minder vatbaar is vir die slegte bestuurspraktyke in Suid-Afrika. Dit is ook relatief goedkoop om ŉ HKAD te bou en te bedryf, maar die groot voetspoor van hierdie poele maak sy lewensvatbaarheid grootliks afhanklik van die beskikbaarheid en koste van grond.

Die voedingstofverwyderingspotensiaal van ŉ skaalmodel HKAD is onder laboratorium toestande ondersoek. Die gemete voedingstofverwyderingspotensiaal was matig weens 'n gebrek aan die hoë intensiteit sonlig wat die alge benodig vir fotosintese. Daar was wel aanduidings dat ŉ HKAD moontlik effektief in die warm en sonnige klimaat van Suid-Afrika kan wees.

ŉ Deterministiese model is ontwikkel om ŉ HKAD voor te stel. Die deterministiese model is geprogrammeer in Microsoft Excel met die gebruik van Microsoft Visual Basics for Applications (VBA). Die deterministiese vergelykings is numeries opgelos in die rekenaar model. Die resultate van die eksperimente in die laboratorium is gebruik om die rekenaar HKAD model te kalibreer. Die gekalibreerde rekenaar model het die ammoniak en nitraat/nitriet konsentrasies akkuraat voorspel. Die model was onbevredigend in die voorspelling van die oplosbare reaktiewe fosfor (ORF) konsentrasie, aangesien dit nie die presipitasie van fosfor in berekening gebring het nie. Die model het slegs 'n beraming van die ORF gegee, wat deur die alge geassimileer is.

Die gekalibreerde HKAD model is gebruik om die voedingstofverwyderingspotensiaal van 'n HKAD in Suid-Afrika te ondersoek. Daar is vasgestel dat ŉ HKAD vlak, ŉ lang retensietyd en gevolglik met ‘n groot oppervlakte moet hê om bevredigende voedingstofverwydering te bereik. Dit is beraam dat om ongeveer 100% Totaal Anorganiese Stikstof verwydering te bereik, die oppervlak van die HKAD in die omgewing van 60 vierkante meter per kubieke meter van die daaglikse vloei moet wees. Ammoniak verwydering vereis 'n kleiner area van ongeveer 20 m^2/m^3/dag vir 100% ammoniak verwydering. Dit is ook vasgestel dat HRAPs het die vooruitsig van noemenswaardige ORF verwydering.

Die teoretiese berekeninge van die deterministiese HKAD model het aangedui dat 'n HKAD potensieel voldoende voedingstofverwydering vir effektiewe eutrofikasie voorkoming kan

bereik. Die groot oppervlakte vereistes vir hierdie voedingstofverwydering maak die HKAD moontlik nie prakties uitvoerbaar vir die polering van afvloeiwater nie.

ACKNOWLEDGEMENTS

Firstly, I would like to express my sincere gratitude to my supervisor, Dr IC Brink, for her continuous support and guidance in the completion of my master's thesis. I would also like to thank Mr W Kamish for his supervision during the first year of my master's program.

I would additionally like to thank Mr J Nieuwoudt and Mr C Visser for their assistance during my laboratory experiments.

I would also like to acknowledge my siblings, Sunelle and Johann van der Merwe, and my friends for their support and encouragement.

Finally, I would like to express my profound gratitude to my parents, Schalk and Seugnet van der Merwe, and my girlfriend, Michelle Krogscheepers: my father for his advice and guidance, and my mother and girlfriend for their love and unfailing support throughout writing this thesis.

TABLE OF CONTENTS

LIST OF TABLES

LIST OF FIGURES

NOMENCLATURE

Abbreviations

ANO/s	Ammonia Oxidising Organism/s
BOD	Biochemical Oxygen Demand
Chl$a$	Chlorophyll a
CMFR/s	Continuously Mixed Flow Reactor/s
COD	Chemical Oxygen Demand
CSIR	Council for Scientific and Industrial Research
CSTR	Continuously Stirred Tank Reactor
DWS	Department of Water and Sanitation of South Africa
EBRU	Environmental Biotechnology Group at Rhodes University
HRAP/s	High Rate Algae Pond/s
HRT/s	Hydraulic Retention Time/s
IAPS	Integrated Algal Ponding System
NNO/s	Nitrite Oxidising Organism/s
OHO/s	Ordinary Heterotrophic Organism/s
PFR/s	Plug Flow Reactor/s
SRP	Soluble Reactive Phosphorus
TIN	Total Inorganic Nitrogen
TKN	Total Kjeldahl Nitrogen
VSS	Volatile Settable Solids
WWTWs	Wastewater Treatment Works

Alphabetical Symbols

A	Exposed surface area per volume (cm^2/L)
APE	Average percentage error (%)
a	Algae concentration (mgChl$a$/L)
a_{ca}	Ratio of carbon to chlorophyll a in phytoplankton biomass (mgC/mgChla)
a_{na}	Ratio of nitrogen to chlorophyll a in algal biomass (mgN/mgChl$a$)
a_{nc}	Ratio of nitrogen to organic carbon (mgN/mgC)
a_{nv}	Ratio of nitrogen to VSS in OHOs and ANOs (mgN/mgVSS)
a_{pa}	Ratio of phosphorus to algae (mgP/mgChl$a$)
a_{pc}	Ratio of phosphorus to organic carbon (mgP/mgC)
a_{pv}	Phosphorus to VSS ratio in OHOs and ANOs (mgP/mgVSS)
$a_{t-\Delta t}$	Algal concentration at the end of the previous interval (mgChl$a$/L)
a_u	Algae concentration in an upper layer (mgChl$a$/L)
b_A	Endogenous respiration rate (mgVSS/mgVSS/day)
$b_{A,20}$	Endogenous respiration rate at 20 °C (mgVSS/mgVSS/day)
b'_H	Rate of active mass loss due to organism die-off in death regeneration (day^{-1})

b_H	Endogenous mass loss (death) rate (mgVSS/mgVSS/day)
$b_{H,20}$	Endogenous respiration rate at 20 °C (mgVSS/mgVSS/day)
BOD_{ult}	Fully oxidised BOD loading in the influent (mgBOD/L)
C	Carbon concentration to be removed (mgC/L)
C	Concentration of reactant in the reactor (mg/L)
$c_{adjusted}$	Concentration of substance after evaporation correction was applied (mg/L)
C_c	Algal concentration (mg/L)
c_d	Dissolved organic carbon concentration (day^{-1})
$C_{d_{t-\Delta t}}$	Soluble biodegradable organics concentration at the end of the previous interval (mgCOD/L)
c_{d,in_t}	Influent soluble biodegradable organic concentration during time interval (mgCOD/L)
C_{gh}	Herbivorous zooplankton grazing rate at 20 °C with no algae limitation (L/mgC/d)
C_{gc}	Carnivorous zooplankton grazing rate at 20 °C with no herbivore limitation (L/mgC/d)
c_m	Represent all the measured concentrations of parameter (mg/L)
c_{m_i}	Measured concentration of parameter at date i (mg/L)
c_p	Particulate biodegradable organic concentration (mgCOD/L)
$c_{p_{t-\Delta t}}$	Particulate biodegradable organic concentration at the end of the previous time step (mgCOD/L)
c_{p,in_t}	Influent particulate biodegradable organic concentration during that time interval (mgCOD/L)
c_s	Represent all the simulated concentrations of parameter (mg/L)
c_{s_i}	Simulated concentration of parameter at date i (mg/L)
D	Concentration of non-algal volatile suspended solids (or detritus) (mg/L)
d	Depth (m)
DO	Dissolved oxygen concentration (mg/L)
F	Photosynthetic efficiency
f	Light saturation limiting factor
F_{am}	Ammonium preference factor
f_{cv}	COD/VSS ratio of the biomass (mgCOD/mgVSS)
f_H	Endogenous residue fraction of endogenous mass loss
f'_H	Endogenous residue fraction for death regeneration model
f_{ld}	Photoperiod (fraction of day with light/sunshine)
F_{max}	Maximum quantum yield factor
f_{onc}	Ratio of organically bound nitrogen to COD in the influent biodegradable organics (mgN/mgCOD)
f_{opc}	Organically bound phosphorus to COD ratio for the influent biodegradable organics (mgP/mgCOD)
f_r	Maximum ratio of stored substrate to active heterotrophic organisms
f_{va}	Ratio of VSS to algal biomass (mgVSS/mgChl$a$)

h	Heat combustion in microalgae (cal/mg)
H_0	Depth at top of layer under consideration (m)
H_1	Depth at bottom of layer under consideration (m)
I	Visible light intensity (cal/cm^2/min)
I_a	Average light intensity (W/m^2)
I_d	Light intensity at depth d (cal/cm^2/min)
I_m	Maximum light intensity measured at the surface (W/m^2)
I_s	Saturation light intensity (cal/cm^2/min)
I_0	Incident light intensity at surface (cal/cm^2/min)
K	Rate of substrate entering the storage (L/mgVSS/d)
k_{dc}	Rate of mass loss due to higher organism grazing (day^{-1})
k_e	Light extinction coefficient (m^{-1})
k_e'	Light extinction due to other factors than phytoplankton/algae (m^{-1})
k_{ea}	Algal excretion rate (day^{-1})
k_{ew}	Light extinction in pure and particle-free water (0.04 m^{-1})
k_{ga}	Algal growth rate (day^{-1})
$k_{ga,20}$	Algal growth rate at 20 °C with no light or nutrient limitation (day^{-1})
k_{gc}	Rate of mass loss due to carnivorous zooplankton grazing (day^{-1})
k_{gh}	Rate of losses due to zooplankton grazing (day-1)
k_h	Rate of dissolved organic carbon hydrolysis (day^{-1})
k_{Hm}	Maximum substrate utilisation rate (mgCOD/mgVSS/d)
K_{m2}	Maximum stored substrate utilisation rate (mgCOD/mgVSS/d)
k_{ma}	Non-predatory mortality rate (day^{-1})
K_n	Half-saturation coefficient for the growth of ANOs on ammonia (mgN/L)
$K_{n,20}$	Ammonia half-saturation concentration at 20 °C (mgN/L)
k_n	Nitrification rate (day^{-1})
K_o	Half-saturation concentration for dissolved oxygen (mg/L)
k_p	Rate of particulate organic carbon dilution (day^{-1})
k_{ra}	Algal respiration rate (day^{-1})
k_{rc}	Carnivorous zooplankton respiration (and excretion) rate (day^{-1})
k_{rea}	Rate of losses due to respiration and excretion (day^{-1})
$k_{rea,20}$	Algal respiration rate at 20 °C (day^{-1})
k_{rh}	Herbivorous zooplankton respiration (and excretion) rate (day^{-1})
k_{sa}	Algal settling rate (day^{-1})
K_S	Half-saturation constant (mgCOD/L)
K_{s2}	Half-saturation coefficient for OHO growth from stored substrate (mgCOD/L)

k_{sga}	Half-saturation constant for herbivorous zooplankton grazing on algae (mgChla/L)
k_{sam}	Half-saturation constant for ammonium preference (mgN/L)
k_{sh}	Half-saturation coefficient for grazing on herbivorous zooplankton (mgC/L)
k_{si}	Half-saturation coefficient for nutrient (mg/L)
N	Concentration of non-volatile suspended solids (mg/L)
N	Nitrogen concentration to be removed (mgN/L)
n_a	Ammonium-N concentration (mgN/L)
$n_{a,in}$	Ammonia concentration in the influent (mgN/L)
n_{a,in_t}	Influent ammonia concentration during the interval (mgN/L)
n_{a_m}	Measured ammonia concentration at date i (mgN/L)
n_{a_s}	Simulated ammonia concentration at date i (mgN/L)
$n_{a_{t-\Delta t}}$	Ammonia concentration at the end of the previous interval (mgN/L)
n_i	Nitrate-N/nitrite-N concentration (mgN/L)
$n_{i,in}$	Influent nitrate concentration (mgN/L)
n_{i,in_t}	Influent nitrate concentration during the interval (mgN/L)
n_{i_m}	Measured nitrate/nitrite concentration at date i (mgN/L)
n_{i_s}	Simulated nitrate/nitrite concentration at date i (mgN/L)
$n_{i_{t-\Delta t}}$	Nitrate concentration at the end of the previous interval (mgN/L)
$N_{t-\Delta t}$	Phosphorus, nitrogen and ammonia concentrations at the end of the previous interval (mg/L)
P	Phosphorus concentration to be removed (mgP/L)
p	Concentration of SRP (mgP/L)
p_{in}	Influent SRP concentration (mgP/L)
p_{in_t}	Influent SRP concentration during the interval (mgP/L)
p_m	Measured SRP concentration at date i (mgP/L)
p_s	Simulated SRP concentration at date i (mgP/L)
$p_{t-\Delta t}$	SRP concentration at the end of the previous interval (mgP/L)
Q	Flow (L/d)
Q_t	Flow rate during the interval (L/d)
r	Reaction rate (mg/L/d)
S	Photosynthetically available solar energy (cal/cm^2/day)
S	Soluble substrate (COD) concentration (mgCOD/L)
T	Temperature (°C)
t	Time (day)
V	Reactor volume (L)
V	Pond volume (L)
WL_m	Water level when the sample was taken for measurement (mm)
WL_{full}	Water level when the HRAP is full (mm)
X_a	Active heterotrophic organism concentration (mgVSS/L)

$X_{a_{t-\Delta t}}$	OHO concentration at the end of the previous interval (mgVSS/L)
X_e	Endogenous residue concentration (mgVSS/L)
$X_{e_{t-\Delta t}}$	Endogenous residue concentration at the end of the previous interval (mgVSS/L)
X_n	ANOs concentration (mgVSS/L)
$X_{n_{t-\Delta t}}$	ANO concentration at the end of the previous interval (mgVSS/L)
X_s	Stored substrate concentration (mgVSS/L)
Y_A	Nitrifier yield coefficient (mgVSS/mgN)
Y_{Hv}	Yield of OHO biomass (mgVSS/mgCOD)
Y_{COD}	Portion of COD utilised for anabolism
z_c	Carnivorous zooplankton concentration (mgC/L)
z_h	Herbivorous zooplankton concentration (mgC/L)

Greek symbols

α	Light absorption constant (L/mg/cm)
Δa	Change in algal concentration over time interval (mgChla/L)
Δc_d	Change in the soluble biodegradable organic concentration over a time interval (mgCOD/L)
Δc_p	Change in the particulate biodegradable organic concentration over a time interval (mgCOD/L)
Δn_a	Change in ammonia concentration over the interval (mgN/L)
Δn_i	Change in nitrate concentration over the interval (mgN/L)
Δp	Change in SRP concentration over the interval (mgP/L)
Δt	Duration of the interval (days)
ΔX_a	Change in OHO concentration over the time interval (mgVSS/L)
ΔX_e	Change in endogenous residue concentration during interval (mgVSS/L)
ΔX_n	Change in ANO concentration over the time interval (mgVSS/L)
ε_c	Grazing efficiency factor
ε_h	Grazing efficiency factor
θ	Hydraulic retention time (days)
θ_{ga}	Temperature factor for algal growth rate
θ_{gc}	Temperature factor for carnivorous zooplankton grazing
θ_{gh}	Temperature correction factor
θ_{gX_a}	Temperature coefficient for the maximum specific growth rate of OHOs
θ_{gX_n}	Temperature coefficient for the maximum specific growth rate of ANOs
θ_{K_n}	Temperature coefficient of ammonia half-saturation concentration
θ_{rea}	Temperature factor for algae respiration rate
θ_{rX_a}	Temperature coefficient OHO endogenous respiration
θ_{rX_n}	Temperature coefficient ANO endogenous respiration
λ_I	Multiplier for growth limiting due to light
λ_N	Multiplier for growth limiting due to nutrients

λ_{n_i}	Growth-limiting multiplier for a specific nutrient
λ_T	Multiplier for growth limiting/increase due to temperature
μ_{Am}	Maximum specific growth rate of ANOs (mgVSS/mgVSS/day)
$\mu_{Am,20}$	Maximum specific growth rate of ANOs at 20 °C (mgVSS/mgVSS/day)
μ_{Hm}	Maximum specific growth rate of OHOs (mgVSS/mgVSS/day)
$\mu_{Hm_{20}}$	Maximum specific growth rate at 20 °C (mgVSS/mgVSS/day)
μ_m	Maximum specific growth rate (mgVSS/mgVSS/day)
Φ_i	Nutrient concentration (mg/L)

1 INTRODUCTION

1.1 Background Information

The discharge of untreated or poorly treated wastewater is a major problem in developing countries (Mara, 2004; Henze, et al., 2008). This practice holds a major threat to human health and the environment. Untreated wastewater transmits excreta-related diseases to humans. Besides the risk to human health, untreated or partially treated wastewater is also a cause for high levels of pollution in receiving water bodies which cause serious harm to the environment (Mara, 2004).

Developing countries generally do not have the financial capacity and expertise to implement advanced wastewater treatment systems such as the activated sludge system. (Mara, 2004). Besides the capital investment and expertise required for the design and construction of these wastewater treatment systems, developing countries struggle to educate and employ skilled labourers to maintain and operate these plants properly (Henze, et al., 2008). Waste stabilisation ponds are used as a cost-effective and simple alternative for wastewater treatment in developing countries (Mara, 2004). The low cost and simple operation of waste stabilisation ponds, also makes it an attractive option for effluent polishing from poorly operated existing advanced treatment works in developing countries.

The High Rate Algae Pond (HRAP) is a type of waste stabilisation pond that was designed for enhanced nutrient removal from wastewaters through the nutrient assimilation into algal biomass (Craggs, 2005b). An HRAP also has the advantage of nutrient recovery through harvesting the algal biomass (Craggs, 2005b). An HRAP may consequently be an appropriate solution when nutrient removal and nutrient recovery are required.

1.2 Problem Statement

Eutrophication is a major problem in South Africa with an estimated 62% of the 50 largest water bodies in South Africa classified as hypertrophic, which means that they are even more nutrient-rich than eutrophic water bodies (Matthews & Bernard, 2015). Eutrophication is destructive to the ecology of a natural water body, because it has the potential to deoxygenate the water body and it causes toxic blue-green algae blooms (Foehrenbach, 1972). Other effects of eutrophication include high turbidity and odour release (Foehrenbach, 1972).

It is believed that the discharge of untreated or partially treated wastewater is a major contributor to eutrophication in South Africa. A recent study showed that only 26% of South Africa's wastewater is sufficiently treated. The rest is discharged into the receiving water bodies as untreated or partially treated wastewater (Turton, 2015). South Africa's wastewater is not sufficiently treated due to a combination of poor operating practices at existing wastewater treatment works (WWTWs), high discharge standards (in terms of nutrient

removal) compared to the available dilution and the ineffective implementation of these discharge standards. These issues are discussed in further detail in sections 2.1, 2.2 and 2.3.

In the current state of South African wastewater treatment, waste stabilisation ponds and HRAPs in particular, may serve as viable options for effluent polishing from underperforming WWTWs. The nutrient removal and nutrient recovery capabilities of HRAPs make them particularly promising for effluent polishing. The pond can potentially serve as a buffer between the underperforming plant and the receiving water body, and thus reduce eutrophication in the receiving water body.

1.3 Thesis Statement

"Effluent polishing with High Rate Algal Ponds can reduce eutrophication in receiving water bodies."

1.4 Research Objectives

Four main objectives which served as the basis for the investigation of the thesis statement, were established. The first objective was to measure the water treatment capability of a scale model HRAP, fed with effluent quality wastewater under laboratory conditions. The second research objective was to develop a deterministic design model that incorporated the kinetics involved in an HRAP. The deterministic model was then calibrated with the results obtained from the laboratory experiment, for the third research objective. The fourth research objective involved the use of the calibrated deterministic model to investigate the eutrophication prevention potential of HRAPs in South Africa.

1.5 Delineations and Limitations

The delineations of the study were as follows:

1. The study focussed on HRAPs only.
2. Only ideal reactors were considered for the deterministic model.
3. Only the kinetics of two selected parent deterministic models, the activated sludge model and an algal water quality model, served as the basis for the development of the deterministic model.
4. The potential of treatment was determined for HRAPs, fed only with effluent quality wastewater.
5. The practical implementation of an HRAP would require a settling pond or a different method that can remove the suspended solids from the HRAP effluent before discharge. The removal of the suspended solids from the HRAP effluent did not form part of the scope of the research.

The major limitations of the study were as follows:

1. The study was limited to one HRAP setup.
2. All the laboratory experiments were conducted at the same pond depth.
3. Experimentation and sampling were limited by time and funding.

1.6 Major Assumptions

A number of assumptions were made in the development of the deterministic HRAP model. These are listed below. These assumptions together with other less significant assumptions are discussed further in section 3.2.

1. Completely mixed conditions exist within the pond.
2. Ammonia volatilisation and phosphate precipitation are negligible.
3. Zooplankton are not present in the system.
4. The endogenous respiration model can be applied for algal respiration.
5. Evaporation losses are negligible.
6. There are no rapid variations in the influent.

A major assumption was also made in the calibration of the deterministic model. Since the rates and constants applicable to the model could not be measured individually, the optimum combination of rates and constants were estimated through an iterative calibration process. The assumption was made that the combination of calibrated rates and constants are representative of the kinetics in the HRAP system. This assumption is discussed further in section 4.2.

The calibrated deterministic model was used in the investigation of HRAPs' eutrophication prevention potential in South Africa. This required the assumption that the calibrated HRAP model is valid for environmental conditions that differ from the environmental conditions in which the model was calibrated. This assumption is discussed further in section 4.3.

1.7 Thesis Layout

A literature review was performed in Chapter 2 to investigate and evaluate the need for HRAPs in South Africa, the current design method, and the equations required for the development of the deterministic model. Chapter 3 encompasses the methodology of the experimental HRAP and the development of the deterministic HRAP model. In Chapter 4, the results of the laboratory experiment, the model calibration process, and the investigation of the use of HRAPs for nutrient removal in South Africa are discussed. The thesis is concluded in Chapter 5. The recommendations established from this research are discussed in Chapter 6.

2 LITERATURE REVIEW

In this chapter, the current state of wastewater treatment in South Africa and its possible link to the eutrophication in South African water bodies, are discussed. Further, HRAP technologies were investigated in view of effluent polishing. This includes an outlay of advantages and disadvantages of the HRAP technologies, the current design method, and design and operation guidelines. The last part of the literature review describes the basics of reactor kinetics, and the kinetics of two existing deterministic models that were used for the development of the deterministic HRAP model in section 3.2.

2.1 State of Wastewater Treatment in RSA

Wastewater treatment is a growing problem in South Africa and other countries that experience rapid urban growth. Conventional activated sludge treatment systems, commonly used in South Africa, require a high degree of expertise to operate and are frequently neglected or poorly maintained (Mara, 2004; Department of Water Affairs, 2014).

The Department of Water and Sanitation of South Africa (DWS) has a system in place to monitor the performance of all the wastewater treatment works (WWTWs) in South Africa. This system is called the Green Drop System. It evaluates the condition of WWTWs according to various categories such as wastewater quality monitoring, wastewater quality compliance, and operational staff. According to the 2013 Green Drop Report, 30% of South Africa's WWTWs are in critical condition, 20% are in poor condition, and only 16% are in good or excellent condition (Department of Water Affairs, 2014). The remaining WWTWs were classified as being in average condition. A 2013 investigation on the state of wastewater treatment in South Africa, with data obtained under the Promotion of Access to Information Act of 2000, concluded that of the 4 901 million litres of wastewater that are received per day in South Africa, only 1 259 million litres (26%) are sufficiently treated. The rest is discharged into the receiving water bodies as untreated or partially treated wastewater (Turton, 2015).

The Green Drop System has a webpage that indicates the compliance of WWTWs to effluent standards in four categories. These are monitoring compliance, physical compliance, chemical compliance and microbiological compliance. Monitoring compliance indicates whether WWTWs submitted the required samples to determine the compliance with the other three categories. Physical compliance monitors WWTWs adherence to the limits set for the pH, electrical conductivity and suspended solids in the effluent. Chemical compliance determines WWTWs compliance with limits set for the concentration of ammonia, COD, Nitrate, Nitrite and phosphate in the effluent. Lastly microbiological compliance monitors WWTWs compliance with the limit set for E. coli or faecal coliforms in the effluent discharged from the WWTWs (Department of Water Affairs, 2011).

In 2015, according to the Green Drop System web page, only 45% of the WWTWs in South Africa submitted enough effluent samples to achieve monitoring compliance. From these submitted samples, 42% achieved physical compliance, 38% achieved chemical compliance and 31% achieved microbiological compliance (Department of Water and Sanitation, 2015).

South Africa has a 22.2% surplus capacity at the existing WWTWs (Department of Water Affairs, 2014). This indicates that the South African wastewater treatment problem is not due to a lack of treatment facilities, but rather due to poor operational practices at existing WWTWs.

2.2 South African Discharge Standards

South African water users, which include WWTWs, are divided into two main groups. Different discharge regulations are assigned to each group. The first group uses water under general authorisation and the second group operates under a water use licence.

General authorisation water users are allowed to discharge up to 2 ML on any given day and they do not require a water use licence (Department of Water Affairs, 2013). These water users must comply with the discharge limits given in Table 2.1. Most users are restricted by the general limit shown in Table 2.1. The special limit only applies if a water user discharges into a water body that was classified as environmentally sensitive. A water body that is classified as sensitive is generally in a eutrophic state or may possibly become eutrophic in the near future.

Table 2.1 - Compliance limits for the effluents from WWTWs that operate under a general authorisation (Department of Water Affairs, 2013)

Substance/Parameter	**General Limit**	**Special Limit**
Chemical Oxygen Demand (mg/L)	75*	30*
Suspended Solids (mg/L)	25	10
Ammonia (ionised and un-ionised) as Nitrogen (mg/L)	6	2
Nitrate/Nitrite as Nitrogen (mg/L)	15	1.5
Ortho-phosphate as phosphorus (mg/L)	10	1 (median) & 2.5 (maximum)
*after algae removal		

When water users or WWTWs discharge more than 2 ML on any given day, a water use licence must be acquired (Department of Water Affairs, 2011). The standards set in the Government Gazette of 18 May 1984 for this type of water user are given in Table 2.2. These standards serve only as a guideline because the discharge standards for each WWTWs (or water user) are individually determined with the issuing of its water use licence. These standards are mainly dependent on the sensitivity of the receiving water body (Department of Water Affairs, 2011).

Table 2.2 – Compliance limits for the effluent from WWTWs that operates under a Water Use licence (Department of Water Affairs and Forestry, 1984)

Substance/Parameter	**General Limit**	**Special Limit**
Chemical Oxygen Demand (mgCOD/L)	75	30
Suspended Solids (mg/L)	25	10
Ammonia (ionised and un-ionised) as Nitrogen (mgN/L)	10	1
Nitrate/Nitrite as Nitrogen (mgN/L)	-	1.5
Ortho-phosphate as phosphorus (mgP/L)	-	1

The European Union has legislation in place that specifies the quality of the treated effluent from WWTWs. This EU legislation is summarised in Table 2.3 (Official Journal of European Communities, 1991). This legislation differentiates between large and small WWTWs according to the population equivalent (p.e.) that it serves. It is estimated that one person generates a waste flow of between 216 and 316 litres per day (Mayer, et al., 1999).

Table 2.3 - European standards for the discharge of treated wastewater (Official Journal of European Communities, 1991)

Parameter	**Concentration**	**Minimum percentage of reduction**
Biochemical oxygen demand (BOD_5 at 20 °C) without nitrification	25 mgO_2/L	70-90
Chemical oxygen demand (COD)	125 mgO_2/L	75
Total Suspended Solids	35 mg/L (>10 000 p.e.) 60 mg/L (2000-10 0000 p.e.)	90 (>10 000 p.e.) 70 (2000-10 0000 p.e.)
Additional requirements for discharge to a sensitive area		
Total Phosphorus	2 mgP/L (10 000 - 100 000 p.e.) 1 mgP/L (>100 000 p.e.)	80
Total Nitrogen	15 mgN/L (10 000-100 000 p.e.) 10 mgN/L (>100 000 p.e.)	70-80

The South African discharge standards of Table 2.1 and Table 2.2 compare well with the European discharge standards given in Table 2.3. The South African discharge standards are even more strict than those of the European Union, for most parameters. As with the European Union, the South African discharge standards only really require nutrient removal when the receiving water body is classified as sensitive. In this case, the special limits of Table 2.1 and

Table 2.2 would apply. Frequent and thorough assessment of receiving water bodies is consequently required to ensure that sufficient nutrient removal takes place at the WWTWs.

It was already mentioned that eutrophication is a problem in South Africa. The discharge standards for nutrient removal should therefore commonly apply. However, the poor operating practices discussed in section 2.1 and the severe eutrophication are indications that these discharge restrictions are not met.

The discharge standards discussed in this section were used to develop a synthetic wastewater for the laboratory experiments. The development of the synthetic wastewater is discussed further in section 3.1.1.

2.3 Eutrophication in South Africa

The major nutrients of concern with respect to eutrophication in natural water bodies are phosphorus, nitrogen and carbon (Oswald, 1978). Algae uses carbon dioxide as its main source of carbon. Since carbon dioxide is abundant in the air and can always enter a water body through various processes, eutrophication can be prevented by reducing the nitrogen and phosphorus concentrations.

In a study of the relationship between phosphorus concentration and the growth of *Chlorella pyrenoidosa* (a type of algae), it was found that a phosphorus concentration above 200 µg/L did not limit the algal growth rate (Oswald, 1978). A similar study for nitrogen showed that a concentration above 3000 µg/L did not limit algal growth (Oswald, 1978). Algal growth can start at phosphorus and nitrogen concentrations as low as 10 µg/L and 300 µg/L respectively (Oswald, 1978). Therefore, in order to completely prevent algal growth in a water body, the nitrogen concentration should be below 300 µg/L or the phosphorus concentration should be below 10 µg/L. In addition, algal growth and thus eutrophication can be limited with nitrogen concentrations below 3000 µg/L and phosphorus concentrations below 200 µg/L.

The discharge standards, given in Table 2.1 and Table 2.2 above, are high when compared with the concentrations mentioned in the previous paragraph, especially for phosphorus. It can be argued that the discharge standards of Table 2.1 and Table 2.2 take dilution into account. Dilution plays an important role in wastewater treatment and if the dilution by the receiving wastewater is sufficient, high discharge standards are defendable (Mara, 2004). However, South Africa is considered to be an arid to semi-arid region which means that the required level of dilution is not always available (CSIR, 2010).

Eutrophication is therefore a major problem in South Africa, but eutrophication prevention still has a relatively low priority in South Africa (CSIR, 2010; Matthews & Bernard, 2015). The high level of eutrophication in South African water bodies indicates that the discharge

standards discussed in section 2.2 are generally not reached. It also suggests that the discharge standards might be too low for the dilution that is available in South Africa.

The low discharge standards compared to the available dilution, the ineffective enforcement of these standards, and the poor operational practises discussed in section 2.1 all indicate that nutrient removal from wastewater is not as high a priority in South Africa as it should be.

2.4 High Rate Algae Ponds for Eutrophication Prevention

The High Rate Algae Pond (HRAP) is a shallow pond where wastewater is driven along a circuit or raceway by a paddlewheel. This type of pond was developed with the purpose of simultaneously treating wastewater as well as recovering nutrients in algal biomass (Craggs, 2005b). This section looks at the advantages and disadvantages of the use of HRAPs for effluent polishing.

Figure 2.1 - High Rate Ponds that is part of an AIWPS plant located at the Rhodes University Environmental Biotechnology Experimental Field Station (Rose, et al., 2002)

2.4.1 Advantages

HRAPs have several advantages that make this technology an attractive option for effluent polishing in South Africa. These advantages include enhanced nutrient removal, simplicity, cost and disinfection.

2.4.1.1 Enhanced nutrient removal

High Rate Algae Ponds (HRAPs) depend on natural processes to reduce the nutrient concentrations in wastewater. These processes include assimilation into algal and bacterial biomass, precipitation of phosphate, volatilisation of ammonia and nitrification (Craggs, 2005a). Nutrient removal in HRAPs is typically a result of a combination of these processes.

2.4.1.1.1 Assimilation

A relatively large component of algal and bacterial cells consists of nutrients such as nitrogen and phosphorus. Nutrients are consequently removed from wastewater by assimilation through algal and bacterial growth. The effectiveness of this process depends on the density of the algal or bacterial cells, their composition and the growth rate. Other factors such as the organic material loading, nutrient concentration, hydraulic retention time, pH, hardness and temperature also affect the assimilation of nutrients (Craggs, 2005a).

Green, et al., (1996) stated that a typical formula for the cell composition of microalgae is $C_{106}H_{181}O_{45}N_{16}P$. The empirical formula for the active biomass that is found in wastewater treatment processes was approximated as $C_{60}H_{87}O_{23}N_{12}P$ (Comeau, 2008). These formulas indicate that algae and bacteria have a nitrogen to phosphorus ratio (by weight) of 7:1 and 5:1 respectively. The nitrogen to phosphorus ratio of domestic wastewater is usually about 4:1 (Craggs, 2005a). Theoretically, wastewater does not have sufficient nitrogen for complete phosphorus removal through assimilation. However, the true ratio of nitrogen to phosphorus in algal biomass can vary between 4:1 and 40:1. This ratio depends on the type of algae species in the pond and the nutrient availability (Park, et al., 2011). It is therefore possible that phosphorus removal through assimilation can still be efficient at low nitrogen to phosphorus ratios.

Craggs (2005a) approximated an equation for the synthesis of algae by assuming that ammonium is the source of nitrogen, phosphate is the source of phosphorus and water the source of oxygen and hydrogen:

$$\mathbf{106CO_2 + 16NH_4^+ + HPO_4^{2-} + 236H_2O \xrightarrow{Light+Alga} C_{106}H_{181}O_{45}N_{16}P + 118O_2 + 171H_2O + 14H^-}$$

The growth of aerobic heterotrophic bacteria on a carbon source (glucose in this case) was approximated as follows (Comeau, 2008):

$$\mathbf{C_6H_{12}O_6 + O_2 + NH_3 + \textit{other nutrients} \rightarrow C_5H_7O_2N + CO_2 + H_2O}$$

It is generally considered that algae are more effective at nutrient assimilation than the bacteria. Bacteria require a significant number of organics as a carbon source for growth. Organics are normally depleted rapidly and the bacteria growth is thereby limited before a significant number of nutrients can be assimilated. Algae, however, uses carbon dioxide as its carbon source. Since carbon dioxide is abundant in the atmosphere, algae can grow until a nutrient (commonly nitrogen or phosphorus) is depleted.

The HRAP technology was specifically developed to promote algae growth and therefore to achieve enhanced nitrogen and phosphorus removal through assimilation (Craggs, 2005b; Mara, 2004). It is this attribute that makes the HRAP attractive for eutrophication prevention. The algal biomass can then be harvested for multiple uses. Uses for algal biomass include

fertilisation, animal feed, biofuels as well as vitamin and pigment extraction (Shilton, 2005; Park, et al., 2011).

2.4.1.1.2 Precipitation of phosphate

Phosphates (PO_4^{3-}, HPO_4^{2-} and $H_2PO_4^-$) can bind with cations (Ca^{2+}, Mg^{2+}, Al^{3+}, and Fe^{3+}) to form insoluble compounds. These compounds are removed from the wastewater through precipitation and subsequent sedimentation. The efficiency of this process depends on pH, temperature and the cation concentration (Craggs, 2005a). Phosphate precipitation is most effective at a high pH and elevated cation concentrations (Craggs, 2005a). Elevated pH is common in HRAPs and it has been suggested that phosphate precipitation plays an important role in phosphate removal from these ponds (Craggs, 2005a).

2.4.1.1.3 Ammonia Volatilisation

Nitrogen can be removed from wastewater through ammonia gas that escapes through the pond water surface. This process is called volatilisation. The rate at which volatilisation occurs depends on the pH, temperature, mixing conditions and the free ammonia concentration. Ammonia volatilisation can be the dominant process for nitrogen removal at the optimum pH and temperature. Ammonia volatilisation typically requires a pH between 7 and 9 and temperatures between 22 and 28 °C. This process has been accounted for 75 to 98% of nitrogen removal in WSPs (Craggs, 2005a).

2.4.1.1.4 Nitrification

Nitrification is an aerobic process where nitrifying bacteria oxidise ammoniacal-N to nitrite and later nitrate. Nitrification is enhanced by a dissolved oxygen concentration greater than 1 g/m^3, a temperature greater than 8 ^oC and a pH between 6 and 9 (Craggs, 2005a). Nitrification is restricted by solar-UV light and the slower nitrifying bacteria dominate when exposed to sunlight (Craggs, 2005a). Nitrification is consequently limited in an HRAP due to the high UV exposure (Craggs, 2005a).

Denitrification is an anaerobic process where denitrifying bacteria oxidise organic matter by reducing nitrite to nitrous oxide (N_2O) and nitrogen (N_2) gases. Denitrification is prevented in completely aerobic conditions such as in an HRAP.

2.4.1.2 Simplicity

An HRAP is considered to be a relatively complicated type of waste stabilisation pond (Mara, 2004). However, its construction and operation are relatively simple when compared to more advanced systems such as activated sludge. HRAPs also have the additional benefit of resource recovery (Craggs, 2005b). The performance of an HRAP does not depend so much on the operator and it is normally hassle free (Craggs, 2005b). HRAPs should therefore not be as susceptible to the poor operational practices of existing WWTWs in South Africa.

2.4.1.3 Cost

The simplicity of an HRAP means that capital costs are relatively low, especially when the cost of the land is considered as an investment (Craggs, 2005b). The operational cost for an HRAP is also significantly lower than in-tank mechanical treatment systems such as activated sludge. The operational cost includes the electricity cost required for the paddlewheel as well as the personnel cost. However, the motor of the paddlewheel uses much less electricity than mechanical aerators. Less-skilled, and consequently less expensive personnel are also required for the operation of an HRAP (Craggs, 2005b).

2.4.1.4 Disinfection

HRAPs are effective in terms of virus and pathogen removal due to the elevated pH levels, high exposure to the UV in solar radiation, and the high dissolved oxygen concentration in these ponds (Mara, 2004). The use of an HRAP for effluent polishing therefore has the added benefit of significant disinfection.

2.4.2 Disadvantages

Although HRAPs seem to be a very promising solution for effluent polishing and eutrophication prevention, there are disadvantages that can inhibit the implementation and effectiveness of these ponds. These disadvantages include design uncertainty, unpredictable performance and the footprint of the pond.

2.4.2.1 Design Uncertainty

Waste stabilisation ponds are highly complex biological systems and the large amount of biological processes in the pond make the design of ponds challenging.

Current design methods usually use “black-box” approaches (Mara, 2004; Shilton, 2005; Oswald, 1978). The design equations for these ponds are empirically determined from experimental data. The universal applicability of these design equations is unclear, since it does not account for all the parameters that might have an influence on the pond performance. The experimental data used to develop the design equations are not always from representative locations. Mara (2004), for example, gave a design for a facultative pond, where the temperature is the only external factor that influences the pond performance. The empirical design equations for this method were developed from the performance data obtained from ponds in Germany and northeast Brazil (Mara, 2004). Since only two locations were used to derive the empirical equations, the applicability of these equations elsewhere is questionable. The design equations for HRAPs are not entirely empirical, but they are also limited in terms of relating the design to a specific parameter. This is discussed in section 2.5 with reference to the HRAP design method that was found to be most widely used.

A deterministic design model has the potential to significantly reduce the uncertainty associated with the design of the ponds. It will allow the designer to base the design of an

HRAP on all the parameters that have a significant effect on the performance of an HRAP. These parameters can also be measured as site-specific data, which will ensure that the design corresponds with the location of the pond.

2.4.2.2 Unpredictable and fluctuating performance

The effectiveness of algae-based wastewater treatment is often criticised due to inconsistent effluent quality measured from operational algal pond systems. This was also the case for a pilot scale Integrated Algal Ponding System (IAPS) operated by the Environmental Biotechnology Group at Rhodes University (EBRU). The IAPS had an average performance over a 25-week study period of stable operation as shown in Table 2.4 (Rose, et al., 2002).

Table 2.4 - Performance of EBRU IAPS over 25-week study period (Rose, et al., 2002)

Parameter	**Average Removal before filtration**	**Average Removal after filtration**
COD	92%	94%
TKN	82%	91%
Ammonia	100%	100%
Nitrate	57%	71%
Phosphate	43%	57%

Table 2.4 indicates that the IAPS at EBRU had an acceptable performance for COD, TKN and ammonia removal and a less satisfactory performance for nitrate and phosphate removal when averaged over the study period. However, one must be careful in judging the IAPS's performance in terms of average effluent quality due to significant variations in the effluent quality over the study period. Figure 2.2 indicates how the performance of the IAPS in terms of phosphate removal, fluctuated over the study period.

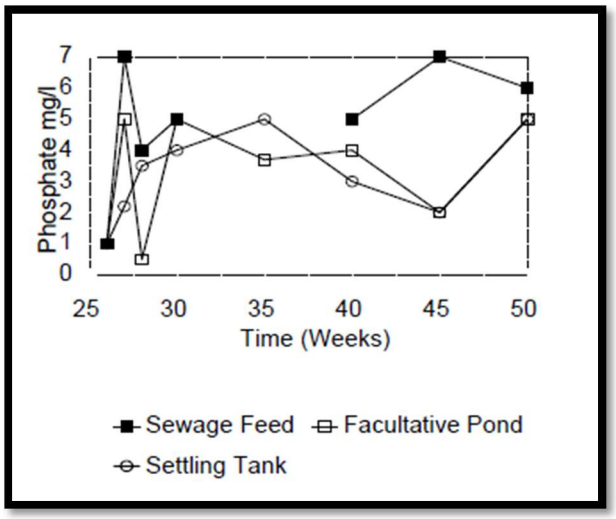

Figure 2.2 - Phosphate removal in IAPS at EBRU over a 25-week study period (Rose, et al., 2002)

Although the average phosphate removal was 43%, the actual phosphate removal varied between approximately 20% and 80% of the influent phosphate concentration. The COD, TKN, ammonia and nitrate also fluctuated over the study period but to a lesser extent. There are various reasons for these fluctuations, most likely changing environmental conditions and fluctuating influent concentrations.

The empirical design approach additionally, does not allow accurate prediction of such fluctuations. An operator or designer consequently has limited assistance in operating the system for extraordinary conditions. A deterministic design model, however, will allow a designer to simulate the pond's response to various extraordinary conditions and consequently incorporate these conditions into the design. An existing pond can theoretically also be calibrated with a deterministic model to investigate the pond's response to extraordinary conditions, and to optimise the operation of the pond.

2.4.2.3 Footprint

Waste stabilisation ponds, including HRAPs, needs to be shallow to allow sufficient sunlight penetration for algal photosynthesis. The ponds consequently require a large surface area and therefore occupy a significant portion of land (Mara, 2004). This large footprint of HRAPs is problematic in some circumstances. Developed countries and large cities often do not have sufficient free space to build large ponds for wastewater treatment. HRAPs are therefore not a suitable solution for densely populated areas where land is expensive. However, in many of the smaller cities and towns in developing countries, including South Africa, land is relatively inexpensive and widely available (Shilton, 2005; Mara, 2004).

2.5 Current Design Method

The HRAP design approach that was found to be the most widely recommended design method, is based on an energy balance between the energy stored within an algal population and the solar energy supplied for the growth of the population (Oswald, 1978; Craggs, 2005b). This design therefore assumes that light is the only limiting factor in algal growth (Oswald, 1978). Light energy is an important limitation to algal growth, but there are various other factors such as nutrient availability and temperature that can also limit algal growth (Bowie, et al., 1985). This design approach does therefore not incorporate the effects of nutrient and temperature changes. It is clear that this assumption can be problematic when the responses to nutrient and temperature changes are desired for the design and operation phases.

The energy balance given by Oswald (1978) for the design of HRAP is shown in Equation 2.1.

$$hC_c = FSA\theta \qquad \text{Equation 2.1}$$

Where

h = heat combustion in microalgae (cal/mg)

C_c = algal concentration (mg/L)
F = photosynthetic efficiency
S = photosynthetically available solar energy (cal/cm^2/day)
A = exposed surface area per volume (cm^2/L)
θ = hydraulic retention time (days)

The exposed surface area (A) used in Equation 2.1 can be simplified with the knowledge that one litre is equal to 1000 cm^3. The exposed surface area per litre is consequently equal to 1000 cm^3 divided by the depth (d) of the pond. This condition was added to Equation 2.1 and then upon rearrangement, Equation 2.2 was formed.

$$\frac{d}{\theta} = \frac{1000FS}{hC_c} \qquad \text{Equation 2.2}$$

Equation 2.2 is used to calculate the ratio of depth over hydraulic retention time $\left(\frac{d}{\theta}\right)$ and it is termed the hydraulic loading (Oswald, 1978). However, since it is a ratio, Equation 2.2 holds for various combinations of d and θ. Therefore, in solving Equation 2.2, either d or θ must be fixed and the other one is solved accordingly. The depth (d) is generally fixed as the depth that the light energy penetrates the water containing the selected algae concentration. The algae concentration (C_c) is selected according to the level of treatment required in the pond. The photosynthetically available solar energy (S) and the photosynthetic efficiency (F) depend on the location of the pond as well as other climate related factors. It is recommended to choose the heat combustion (h) of microalgae as 5.5 cal/mg for this design approach (Oswald, 1978; Craggs, 2005b).

The following paragraphs explain how the variables in Equation 2.2 are selected or calculated.

2.5.1 Algae Concentration

The algae concentration is selected according to the treatment requirements of the ponds. If the only purpose of the pond is to supply oxygen to heterotrophic bacteria for BOD removal, then an algal concentration should be selected that satisfies the oxygen demand. If the pond is designed for nutrient removal, then the algal concentration should be determined according to the desired number of nutrients to be removed.

The stoichiometric equation in section 2.4.1.1.1 indicates that approximately 1.6 grams of oxygen are produced for each gram of algal biomass grown. This relationship was used to develop Equation 2.3, which can be used to calculate the required algae concentration supply oxygen for the degradation of a certain BOD concentration (Craggs, 2005b; Oswald, 1978).

$$C_c = \frac{3}{2} BOD_{ult} \qquad \text{Equation 2.3}$$

Where

BOD_{ult} = fully oxidised BOD loading in the influent (mgBOD/L)

Equations 2.4, 2.5 and 2.6 can be used to calculate the required algae concentration for carbon, nitrogen and phosphorus removal (Oswald, 1978). These equations were also developed from the stoichiometric equation in section 2.4.1.1.1 with a safety factor included.

$$C_c = 2.5C \quad \text{Equation 2.4}$$

$$C_c = 10N \quad \text{Equation 2.5}$$

$$C_c = 100P \quad \text{Equation 2.6}$$

Where

C = carbon concentration to be removed (mgC/L)

N = nitrogen concentration to be removed (mgN/L)

P = phosphorus concentration to be removed (mgP/L)

It can be argued that Equation 2.3 to 2.6 approaches the design from the wrong side. The design is based on what one desires to remove instead of what can be removed. For example, it was stated in section 2.4.1.1.1 that algae have a nitrogen to phosphorus ratio of approximately 16:1. Therefore, if 5 mg/L phosphorus is to be removed, at least 35 mg/L nitrogen has to be available to reach the required algal concentration (C_c). The algal concentration selected with Equation 2.3 to 2.6 might therefore not always be practically attainable.

2.5.2 Available solar energy

The intensity of solar energy changes throughout the day. In order to compensate for these fluctuations during each day, the daily solar radiation intensity is defined with Equation 2.7 (Oswald, 1978).

$$S = \int_0^{1440} I dt \quad \text{Equation 2.7}$$

Where

I = visible light intensity (cal/cm^2/min)

It is critical to select the solar intensity correctly to achieve a correct design. Oswald (1978) gave a table to select the visible solar intensity as a function of latitude as well as the month of the year as shown in Table 2.5. However, this table is only applicable to the northern hemisphere. The available solar intensity is also an input parameter for the HRAP deterministic model developed in section 3.2. The deterministic model requires the maximum

daily solar intensity and the photoperiod. These parameters are then used in the equations in section 2.8.2.1.1.3 to determine the average daily solar intensity.

Table 2.5 – Probable values of visible solar energy (Oswald, 1978)

North Latitude		Month											
		Jan	Feb	Mar	Apr	May	Jun	Jul	Aug	Sep	Oct	Nov	Dec
0	max	255	266	271	266	249	236	238	252	269	265	256	253
	min	210	219	206	188	182	103	137	167	207	203	202	195
10	max	223	244	264	271	270	262	265	266	266	248	228	225
	min	179	184	193	183	192	129	158	176	196	181	176	162
20	max	183	213	246	271	284	284	282	272	252	224	190	182
	min	134	140	168	170	194	148	172	177	176	150	138	120
30	max	136	176	218	261	290	296	289	271	231	192	148	126
	min	76	96	134	151	184	163	178	166	147	113	90	70
40	max	80	130	181	181	286	298	288	258	203	152	95	66
	min	30	53	95	125	162	173	172	147	112	72	42	24
50	max	28	70	141	210	271	297	280	236	166	100	40	26
	min	10	19	58	97	144	176	155	125	73	40	15	7
60	max	7	32	107	176	249	294	268	205	126	43	10	5
	min	2	4	33	79	132	174	144	100	38	26	3	1

2.5.3 Photosynthetic efficiency

The photosynthetic efficiency represents the fraction of the available solar radiation that can be utilised for algal growth. The photosynthetic efficiency (F) is limited thermodynamically and by the light saturation of the algae cells as shown in Equation 2.8 (Oswald, 1978).

$$F = F_{max} \cdot f \qquad \text{Equation 2.8}$$

Where

F_{max} = maximum quantum yield factor

f = light saturation limiting factor

The maximum quantum yield factor (F_{max}) represents the thermodynamic limit by which light energy can be used by photosynthetic systems. This factor depends on the wavelength as well as the quanta required to fix a mole of CO_2 (Oswald, 1978). Figure 2.3 is used to determine the maximum quantum yield factor (F_{max}) from these dependencies.

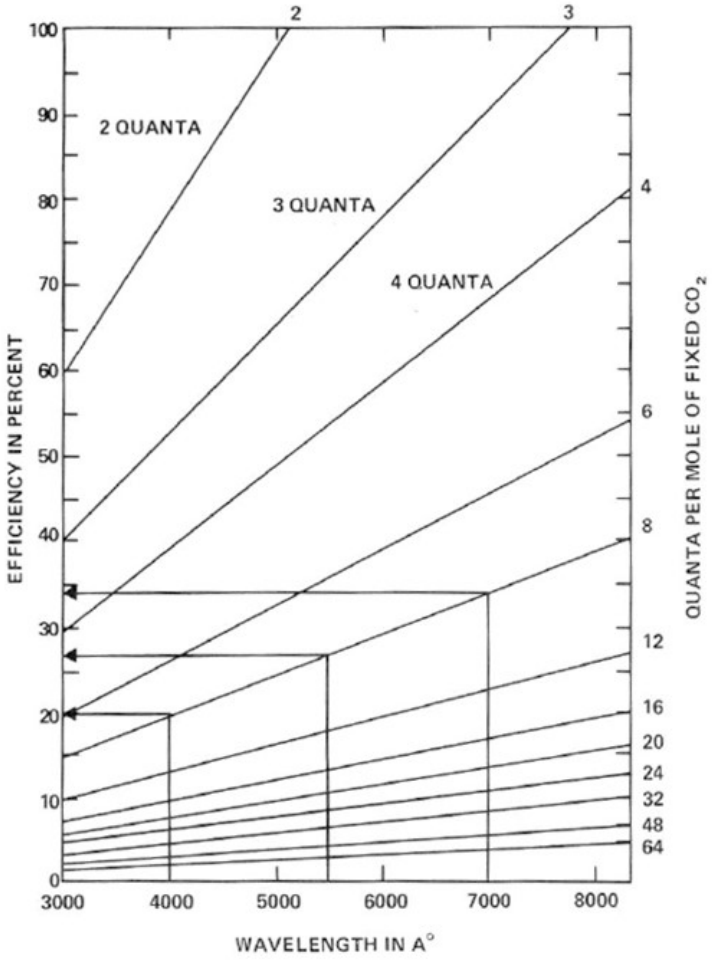

Figure 2.3 - Theoretical energy conversion efficiency as a function of wavelength and quanta required per mole CO_2 fixed (Oswald, 1978)

In examining Figure 2.3, one should keep in mind that only light in the visible range (with a wavelength between 400 and 700 nm) can be used for photosynthesis. It is also known that between 4 and 8 quanta are required to fix one mole of carbon dioxide (Oswald, 1978). In the design equations, 8 quanta are preferred as a more conservative value (Oswald, 1978). The quantum yield factor is consequently between 20% and 34% as shown in Figure 2.3.

The photosynthetic efficiency is also limited by the light saturation of the algae. The biochemical transformations in algae cells are saturated at relatively low light intensities. Light intensities that are higher or lower than the saturation light intensity, decrease the photosynthetic efficiency further. Equation 2.9 is used to determine the light saturation limiting factor (f) (Oswald, 1978).

$$f = \frac{I_s}{I_0}\left(\ln\left(\frac{I_0}{I_s}\right) + 1\right) \qquad \text{Equation 2.9}$$

Where

I_s = saturation light intensity (cal/cm^2/min)

I_0 = incident light intensity at surface (cal/cm^2/min)

It is recommended to apply a factor of safety after the photosynthetic efficiency has been determined with Equation 2.8. Typical photosynthetic efficiencies are between 3% and 4% (Oswald, 1978).

Park *et al.* (2011) used a more theoretical approach to estimate the photosynthetic efficiency. They used CH_2O as a very simplified formula for algal biomass and stated that one mole of CH_2O has an approximate energy content of 468 kJ. A photon of red light contains approximately 176 kJ of energy. In order for the algae to achieve complete photosynthesis, eight photons are required. Algae cells therefore only store 33.2% of the solar energy utilised during photosynthesis as algal biomass. Only 48% of the total solar energy that reaches the earth's surface is "photosynthetically available solar radiation" (PAR). Another 10% to 20% of the solar energy is lost, due to refraction on the pond's surface. The theoretical photosynthetic efficiency of algae is consequently between 12.8% and 14.4%. However, the prevalent algae species is light saturated at 10% to 17% of the summer or winter sunlight intensities. The actual photosynthetic efficiency of common algae cells is therefore only in the range of 1.3% to 2.4% (Park, et al., 2011).

The method, given by Oswald (1978), was accepted to be scientifically more valid since it is based on sound scientific principles where Park *et. al.* (2011) gives more a general approximation of the photosynthetic efficiency. However, both of these approaches fail to acknowledge the loss of solar radiation over the depth of the pond. The available solar intensity (S) used in Equation 2.2, is the solar intensity at the surface of the pond. However, due to shading and adsorption from particulates, the algae deeper in the pond would be exposed to a much lower solar intensity. The algal water quality model described in section 2.8.2 and used in the development of the deterministic HRAP model, incorporates the effect of light extinction over the depth of the pond into the design equations.

2.5.4 Pond depth

The depth of the pond is selected as the depth at which 99.9% of the light is absorbed (Oswald, 1978). With this requirement in mind, the depth can be calculated with Equation 2.10 (Oswald, 1978).

$$d = \frac{\ln I_0 - \ln I_d}{C_c \alpha} \qquad \text{Equation 2.10}$$

Where

I_0 = light intensity at the surface (cal/cm^2/min)
I_d = light intensity at depth d (cal/cm^2/min)
α = light absorption constant (L/mg/cm)

I_d is consequently equal to 0.1% of I_0 for the design requirement given by Oswald (1978). The light absorption constant ranges from 7×10^{-4} L/mg/cm to 13×10^{-4} L/mg/cm. A value of

1×10^{-3} L/mg/cm is therefore commonly used for the light absorption constant (Oswald, 1978).

Craggs (2005b) simplified Equation 2.10 to form Equation 2.11, which can also be used to determine the depth. The constant that forms the numerator of Equation 2.11 is dependent on the insolation and light attenuation over the pond depth. In cloudy areas for ponds with a high concentration of non-algal suspended solids, this constant takes the value of 6000 $\frac{mg \cdot cm}{L}$. At the other end of the scale, the constant is 9000 $\frac{mg \cdot cm}{L}$ for sunny areas with ponds mainly containing algae (Craggs, 2005b).

$$d = \frac{6000}{C_c} \; to \; \frac{9000}{C_c} \qquad \text{Equation 2.11}$$

Most wastewaters require HRAP depths between 0.3 m to 0.5 m for sufficient treatment. Shallower depths can, however, be required for wastewaters with poor turbidity but the pond depth should be at least 0.2 m (Craggs, 2005b; Oswald, 1978). The pond depth is further discussed in section 2.6.1.

2.6 Design and Operation Guidelines

2.6.1 Depth

The depth of an HRAP is one of the most significant variables in its design. Depths for HRAPs typically range between 0.2 m and 1 m with 0.3m to 0.5 m being most common (Craggs, 2005b; Oswald, 1978). A pond that is too deep prevents sunlight from reaching the bottom. Algae photosynthesis is consequently limited and the pond might become anaerobic at greater depths. A pond that is too shallow is unstable due to temperature fluctuations (Craggs, 2005b). Shallow ponds also limit the algae's ability to adjust its vertical position according to the sunlight exposure it requires (Mara, 2004).

Studies have shown that when insolation and water temperature vary between seasons, it might be necessary to alter the pond's depth and hydraulic retention time (HRT). In winter, when the algae density is lower than in summer, the pond may have a greater depth because light penetration will be deeper (Craggs, 2005b).

2.6.2 Hydraulic Retention Time

An HRAP typically has a retention time that varies between 2 and 8 days (Blanc & Leshem, 2013; Craggs, 2005b). Due to the relatively slow growth rate of algae (Bowie, et al., 1985), the hydraulic retention time is a very important parameter in the design and operation of these ponds. The hydraulic retention time is generally directly proportional to the mass of algae that synthesises (Bowie, et al., 1985; Chapra, 2008). A longer hydraulic retention time consequently means that more nutrients are removed through assimilation.

2.6.3 Paddlewheel

The paddlewheel in an HRAP is an efficient method to ensure that the algae stay in suspension as well as to prevent thermal stratification. A constant horizontal water velocity of 5 cm/s is sufficient to prevent thermal stratification (Oswald, 1978). However, a horizontal water velocity of at least 30 cm/s is required for one to two hours a day to ensure that large flocculated bacteria particles stay in suspension (Oswald, 1978). Park *et. al.* (2011) recommends that the paddlewheel should induce a mean velocity of 0.15 to 0.3 m/s to the water. This generally ensures that the lowest velocity at all locations in the pond is not below 0.05 m/s.

2.6.4 CO_2 addition

Carbon is often a limiting source in HRAPs especially if the ponds are further down the process chain in wastewater treatment processes. This problem can be reduced by adding carbon dioxide to the pond water. Maximum efficiency is achieved by maintaining the maximum pH in the water below 8 through CO_2 addition (Park, et al., 2011).

Besides being an additional carbon source, CO_2 addition also ensures a lowered pond pH. Most ammoniacal-N is in the form of saline ammonium (NH_4^+) at a pH of 8 thus reducing the toxic effect of free ammonia (NH_3). However, a low pH reduces the efficiency of other processes such as phosphate precipitation and ammonia volatilisation. Studies have shown that CO_2 addition can double the algal productivity and the reduced efficiency of phosphate precipitation and ammonia volatilisation is outweighed by increased assimilation (Park, et al., 2011).

2.6.5 Controlling algal predators

Predators that feed on algae can exist in HRAP. Zooplankton are such an example. Zooplankton grazers can be controlled through various physical and chemical methods. Increasing the pond pH to greater than 11, has proven to be the most practical method of control (Park, et al., 2011).

2.6.6 Discharge

HRAPs normally have an uninterrupted discharge. Studies have shown that effluent quality can be improved by only discharging during the day or by implementing batch operations (Craggs, 2005b). These discharge strategies reduce the adverse effect of algae respiration during the night. During the night, nutrients are released from the algal cells (Chapra, 2008). The water discharged during the night, consequently has a higher nutrient concentration.

2.7 Reactor Kinetics

A deterministic model can be developed from the basic reactor kinetics. To develop a deterministic model for the HRAP, the types of reactors that can be used to approximate an HRAP, should first be investigated. Each type of reactor also has a basic mass balance equation that coincides with the assumptions of the reactor.

2.7.1 Mass balance equation

Reactor kinetics can be used to model physical and biological processes within a system. The defining principle of reactor kinetics is described by the general mass balance equation that is given below as Equation 2.12 (Howe, et al., 2012).

$$\begin{bmatrix} rate\ of\ mass \\ change\ in \\ the\ system \end{bmatrix} = \begin{bmatrix} rate\ of\ mass \\ flow\ into \\ the\ system \end{bmatrix} - \begin{bmatrix} rate\ of\ mass \\ flow\ out\ of \\ the\ system \end{bmatrix} + \begin{bmatrix} rate\ of\ mass \\ increase\ due\ to \\ biological\ processes \end{bmatrix} - \begin{bmatrix} rate\ of\ mass \\ decrease\ due\ to \\ biological\ processes \end{bmatrix} \quad \text{Equation 2.12}$$

The general mass balance equation is based on the principle of the conservation of mass. Mass cannot be created or destroyed and therefore Equation 2.12 should hold for any component in any system. This mass balance equation can consequently also serve as the base for the development of a deterministic model for an HRAP.

2.7.2 Types of Reactors

Reactors can be categorised into ideal and real reactors. Ideal reactors are simplified approximations of real reactors. Assumptions that define ideal reactors include perfect homogeneity throughout the entire reactor and no diffusion and dispersion within the reactor. Real reactors attempt to simulate what realistically happen in a reactor and they usually include complex hydraulic and mixing conditions. This research has been focused on ideal reactors only. There are three main types of ideal reactors, namely batch reactors, completely mixed flow reactors and plug flow reactors (Howe, et al., 2012).

2.7.2.1 Batch reactors

Batch reactors are characterised by phased operation with no flow in or out of the reactor during a phase. In modelling batch reactors, the reactor is seen as a completely closed system with no outside influences i.e., the volume of the reactor stays the same. Instantaneous and uniform mixing is assumed in batch reactors and therefore variables including concentrations and the temperature are consistent throughout the reactor. The assumption of uniformity also specifies that the reaction rate is the same in the entire reactor. A diagrammatic representation of a batch reactor is shown in Figure 2.5 (Howe, et al., 2012).

The basic mass balance equation applicable to a batch reactor is shown in Equation 2.13 (Howe, et al., 2012). Since there is no inflow and outflow, the rate of change in mass in the reactor depends only on the biological processes.

$$V\frac{dC}{dt} = Vr \qquad \text{Equation 2.13}$$

Where

C = concentration of reactant in the reactor (mg/L)

V = reactor volume (L)

r = reaction rate (mg/L/d)

t = time (d)

Since an HRAP needs to have inflow and outflow, a batch reactor model is not a suitable approximation for these ponds. However, a batch operation was used for the calibration of a deterministic model.

2.7.2.2 Plug Flow Reactor

A Plug Flow Reactor (PFR) is an ideal reactor, which follows the assumption that no mixing occurs within the reactor. The reactor is divided into infinitely small elements or plugs and the plugs do not mix with one another. If a new element is added through the inflow, the last element in the series must leave through the outflow. The concentrations of reactants in a PFR would decrease along the length of the reactor. A diagrammatic representation of a PFR is shown in Figure 2.5 (Howe, et al., 2012).

Since the conditions within a PFR are not uniform, the total volume of the PFR cannot be used as the control volume for the mass balance analysis. The control volume is then chosen as the differential element or "one plug" as shown in Figure 2.4.

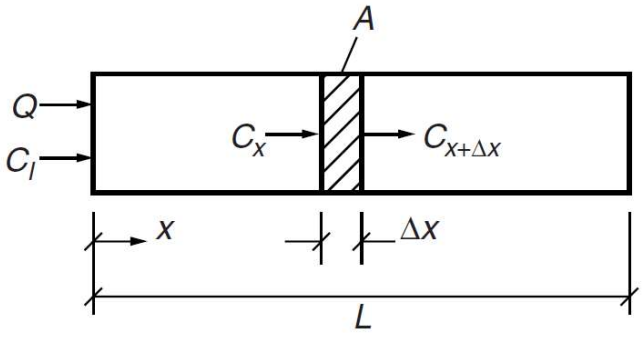

Figure 2.4 - Control volume definition for the mass balance analysis of a PFR (Howe, et al., 2012)

The mass balance equation can therefore only be defined for one element or "plug" in the PFR and is given as Equation 2.14 (Howe, et al., 2012).

$$V\frac{dC_{x+\Delta x}}{dt} = QC_x - QC_{x+\Delta x} + Vr \qquad \text{Equation 2.14}$$

Where

C_x = the concentration entering the plug (mg/L)

$C_{x+\Delta x}$ = concentration in the plug (mg/L)

V = volume of the plug (L)

By analysing the definition of a PFR with Equation 2.14, it can be seen that a PFR is simply a collection for completely mixed flow reactors (CMFRs) (discussed in section 2.7.2.3) in series. The assumption of uniformity therefore still applies for one plug, which implies that the effluent concentration is always equal to the concentration within the plug.

A plug flow approximation can be the preferred option for most types of waste stabilisation ponds. However, the paddle wheel mixing of an HRAP violates the plug flow assumption that no mixing occurs in the horizontal direction. A plug flow assumption would therefore not be a suitable approximation for an HRAP.

2.7.2.3 Continuously Mixed Flow Reactors

Continuously Mixed Flow Reactors (CMFRs) are very similar to batch reactors. The only difference is that a CMFR has an inflow and an outflow. It is assumed that the inflow into a CMFR is instantaneously and completely mixed within the reactor. The CMFR model has the same assumptions of the batch reactor in terms of uniformity and reaction rate. The effluent concentration should always be the same as the concentration within the reactor, due to the uniformity assumption. A diagrammatic representation of a CMFR is shown in Figure 2.5 (Howe, et al., 2012).

The basic mass balance equation for a CMFR reactor is given as Equation 2.15 (Howe, et al., 2012).

$$V\frac{dC}{dt} = QC_I - QC + Vr \qquad \text{Equation 2.15}$$

Where

Q = flow rate (L/day)

V = reactor volume

C_I = influent concentration (mg/L)

C = effluent concentration/concentration in the reactor (mg/L)

r = reaction rate at the effluent concentration (mg/L/day)

Equation 2.15 accounts for the inflow and outflow of mass. Due to the assumption of uniform concentration in the reactor, the effluent concentration is always equal to the concentration in the reactor at that point in time.

The description of the CMFR approximation is the best representation of the conditions within an HRAP when compared with the batch and plug flow reactor. It was assumed that the

paddle wheel mixing and the turbulence in the pond would ensure sufficient mixing for a uniform concentration in the vertical and horizontal directions.

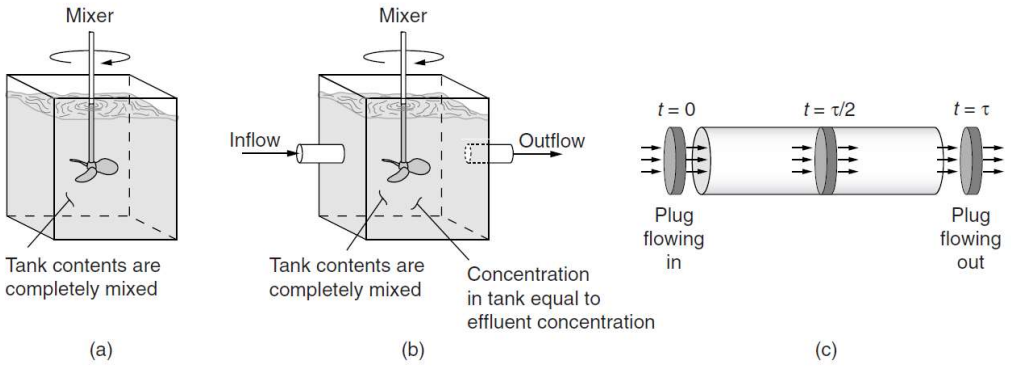

Figure 2.5 - Representations of ideal reactors: (a) batch reactor, (b) CMFR, and (c) PFR (Howe, et al., 2012)

2.8 Biological Processes within an HRAP

Algae-based wastewater treatment is defined by the symbiosis between the heterotrophic bacteria and algae. This mutualistic relationship between the algae and bacteria is called 'photosynthetic oxygenation' (Craggs, 2005b). Mara (2004) explained this relationship by referring to facultative and maturation ponds. Mara (2004) described these ponds as "photosynthetic ponds" i.e. the oxygen required for organic degradation is supplied by algae through photosynthesis, and in return the bacteria produce the carbon dioxide in the organic degradation required by the algae for photosynthesis. The use of algae therefore eliminates the need for aeration, which is a large expense in conventional activated sludge plants. This relationship is represented Figure 2.6.

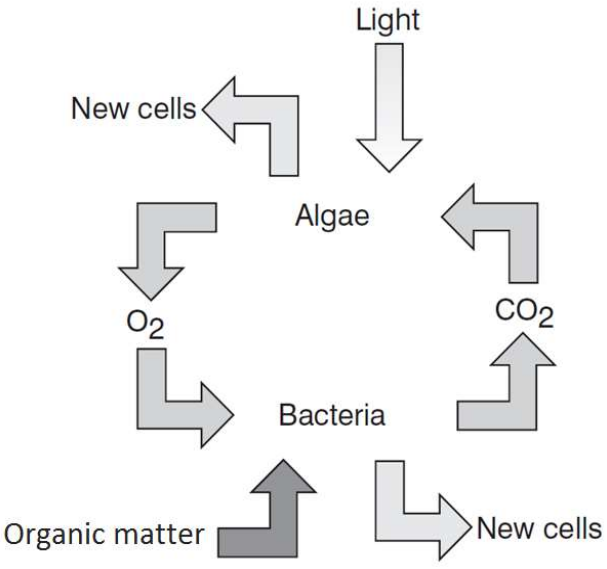

Figure 2.6 - The mutualistic relationship between algae and bacteria (adapted from Mara, 2004).

The mutualistic relationship described by Mara (2004) is applicable for many types of algae-based wastewater treatment systems including HRAPs. It was therefore deemed acceptable to base a deterministic model of an HRAP on this relationship between bacteria and algae.

Bacteria have been extensively used in wastewater treatment and the Activated Sludge model is widely used for heterotrophic and ammonia oxidising bacteria modelling (Ekama & Wentzel, 2008a; Tchobanoglous, et al., 2003). Algal modelling is mostly part of surface water quality models. Bowie *et. al.* (1985) developed a surface water quality model that included algae. This model and variations thereof are also widely used in water quality modelling (Chapra, 2008; Cole & Wells, 2013). A combination of these models has the prospect of a representative deterministic model of an HRAP. This section discusses these existing deterministic models used for the bacteria and algal modelling.

2.8.1 Activated Sludge Model

The Activated Sludge Model attempts to simulate the growth of Ordinary Heterotrophic Organisms (OHOs) on soluble biodegradable organics as well as the growth of Ammonia Oxidising Organisms (ANOs) on ammonia. In this section, the kinetics of these processes and their application in HRAPs are discussed in further detail.

2.8.1.1 Ordinary Heterotrophic Organisms

2.8.1.1.1 Cell Growth

Ordinary Heterotrophic Organisms (OHOs) oxidise biodegradable organic material to produce energy and new cell mass. Wastewaters normally have a very high organic content and OHOs are important to reduce the amount of organics in wastewater.

The rate at which the ordinary heterotrophic organisms (OHOs) grow is a function of the number of heterotrophic organisms already in the reactor. The more heterotrophic organisms present in the reactor, the faster the growth would occur. The heterotrophic organisms, however, need a substrate to generate energy and cell mass. The substrate in the reactor is the limiting nutrient for the growth. The heterotrophic organism growth can be accurately modelled by using the Monod equation. The mathematical model for the growth of heterotrophic organisms is given in Equation 2.16 (Marais & Ekama, 1976; Tchobanoglous, et al., 2003).

$$\frac{dX_a}{dt} = \frac{\mu_{Hm}(T)S}{K_S + S} X_a \qquad \text{Equation 2.16}$$

Where

X_a = active heterotrophic organism concentration (mgVSS/L)

S = soluble substrate (COD) concentration (mgCOD/L)

$\mu_{Hm}(T)$ = maximum specific growth rate as a function of temperature

(mgVSS/mgVSS/day)

K_S = half-saturation constant (mgCOD/L)

The Monod relationship can be better understood by examining the following conditions.

$$\text{If } S \gg K_s \text{ then } \frac{S}{K_S+S} \to 1 \text{ and if } S \ll K_s \text{ then } \frac{S}{K_S+S} \to 0.$$

The expressions above indicate that if the substrate is in abundance, growth will occur rapidly, but as soon as the nutrient concentration becomes smaller than the half-saturation constant, the growth will be limited. The half-saturation constant (K_S) is the substrate concentration at which the heterotrophic organisms' growth rate would be half of the maximum.

The maximum specific growth rate (μ_{Hm}) is the maximum growth rate that the heterotrophic organisms can achieve if food or substrate is abundant. The maximum specific growth rate is temperature dependent and can be determined with Equation 2.17 (Tchobanoglous, et al., 2003).

$$\mu_{Hm}(T) = \mu_{Hm,20}\theta_{gX_a}^{T-20} \qquad \text{Equation 2.17}$$

Where

$\mu_{Hm,20}$ = maximum specific growth rate at 20 °C (mgVSS/mgVSS/day)

θ_{gX_a} = temperature coefficient for the maximum specific growth rate of OHOs

T = temperature (°C)

The rates and kinetics of Equation 2.16, model the growth of heterotrophic bacteria on readily biodegradable or soluble substrate. If substrate was only available in a particulate form, Equation 2.16 would not apply.

Marais and Ekama (1976) stated that Equation 2.16 only applies when steady-state conditions are of interest. Heterotrophic organisms can only utilise substrate once it has been absorbed into its storage. The substrate concentration in storage is equal to the ambient substrate concentration when steady-state conditions exist. However, under dynamic conditions with large and regular variations in the substrate concentration, the substrate concentration in the storage differs from the ambient substrate concentration. This phenomenon occurs because the heterotrophic organisms need time to develop additional adsorption sites to synchronise the stored substrate concentration with the ambient substrate concentration. Equation 2.16 assumes that the ambient and stored substrate concentrations are always the same. The heterotrophic organisms' response to a changed ambient substrate concentration is therefore far too rapid if it is modelled with Equation 2.16.

Ekama and Marais (1977) developed equations to model heterotrophic organisms under dynamic conditions. They added a parameter to represent the stored substrate concentration

(measured as part of the VSS). Equation 2.18 was derived to determine the synthesis of heterotrophic organisms in a dynamic environment (Ekama & Marais, 1977).

$$\frac{dX_a}{dt} = Y_{Hv}\frac{K_{m2}X_s f_{cv}}{K_{s2} + X_s f_{cv}}X_a \qquad \text{Equation 2.18}$$

Where

X_s = stored substrate concentration (mgVSS/L)

K_{m2} = maximum stored substrate utilisation rate (mgCOD/mgVSS/d)

K_{s2} = half-saturation coefficient for OHO growth from stored substrate (mgCOD/L)

Y_{Hv} = the yield of biomass (mgVSS/mgCOD)

f_{cv} = the COD/VSS ratio of the biomass (mgCOD/mgVSS)

In the development of Equation 2.18, Ekama and Marais (1977) essentially only changed the substrate concentration on which the OHO synthesis occur to the stored substrate concentration, instead of the ambient substrate concentration as in Equation 2.16.

Ekama and Marais (1977) also developed Equation 2.19 for the rate of change in the stored substrate concentration. The stored substrate increase by entering the substrate storage through the adsorption sites on the heterotrophic organisms as shown by the first term of Equation 2.19. The stored substrate decrease through utilisation for cell synthesis that is represented by the second term of Equation 2.19.

$$\frac{dX_s}{dt} = KSX_a\left(f_r - \frac{X_s}{X_a}\right)\frac{1}{f_{cv}} - \frac{K_{m2}X_s}{K_{s2} + X_s f_{cv}}X_a \qquad \text{Equation 2.19}$$

Where

K = rate of substrate entering the storage (L/mgVSS/d)

f_r = maximum ratio of stored substrate to active heterotrophic organisms

The rate of substrate entering the storage is limited by a maximum ratio (f_r). The ratio represents the maximum amount of substrate that the heterotrophic organisms can store before it is saturated.

In an HRAP environment, the approach that includes substrate storage has the advantage of an accurate response to rapid changes in the influent substrate concentration. However, in the design of wastewater treatment systems, the approach without substrate storage is preferred (Ekama & Wentzel, 2008a; Tchobanoglous, et al., 2003). Due to the preference of the approach without substrate storage, more research has been done on the rates and constants associated with this approach (Tchobanoglous, et al., 2003; Ekama & Wentzel, 2008a; Comeau, 2008; Marais & Ekama, 1976). Therefore, the applicable rates and constants can be better estimated by applying the approach without substrate storage to the HRAP.

2.8.1.1.2 Endogenous mass loss

It is generally believed that all the organisms in a biological process, experience some kind of mass loss due to internal energy requirements for cell maintenance processes. This process is the most prominent when oxygen consumption continues, although there is a decrease in active mass and all the external substrate has been consumed (Ekama & Wentzel, 2008b). There are two different approaches that can be used to model this process, namely "endogenous respiration" and "death regeneration" (Ekama & Marais, 1977).

In the endogenous respiration method, a black box approach is followed. Only the net reduction in the active mass is taken into account. All the different processes that cause this net reduction are consequently ignored. The causes for this net reduction in active mass are then attributed to the energy requirements of the endogenous respiration process and the unbiodegradable residue that forms during endogenous respiration (Ekama & Marais, 1977).

The death regeneration approach tries to separate all the different processes that lead to the net reduction in active mass. This approach follows the assumption that the active mass lost, is due to organism die-off. A small fraction of this mass loss is attributed to unbiodegradable endogenous residue, while the rest returns to the system as biodegradable substrate. The substrate can then be stored by the heterotrophic organisms and can eventually be consumed to produce energy and form new cell mass (1977).

These two approaches yield identical results under steady-state conditions when the substrate storage process does not have an influence on the system. However, under dynamic conditions where the substrate storage process plays a bigger role, the two approaches yield slightly different results, because the endogenous respiration method does not take the substrate storage process into account (Ekama & Marais, 1977). Ekama and Marais (1977) did state that there is no significant difference between the two approaches and suggested that the difference between the approaches might be negligible.

The loss of active mass due to endogenous respiration can be determined with Equation 2.20 (Ekama & Marais, 1977).

$$\frac{dX_a}{dt} = -b_H(T)X_a \qquad \text{Equation 2.20}$$

Where

$b_H(T)$ = endogenous mass loss (death) rate as a function of temperature (mgVSS/mgVSS/day)

The rate of endogenous mass loss is temperature dependent and is calculated with Equation 2.21 (Tchobanoglous, et al., 2003; Ekama & Wentzel, 2008a).

$$b_H(T) = b_{H,20}\theta_{rX_a}^{T-20} \qquad \text{Equation 2.21}$$

Where

$b_{H,20}$ = endogenous respiration rate at 20 °C (mgVSS/mgVSS/day)

θ_{rX_a} = temperature coefficient OHO endogenous respiration

The unbiodegradable endogenous residue accumulation due to endogenous respiration can consequently be modelled using Equation 2.22 (Ekama & Marais, 1977).

$$\frac{dX_e}{dt} = f_H b_H(T) X_a \qquad \text{Equation 2.22}$$

Where

X_e = endogenous residue concentration (mgVSS/L)

f_H = endogenous residue fraction of endogenous mass loss

Equation 2.20 and Equation 2.22 are applicable to the endogenous respiration approach. These equations essentially stay the same for the death regeneration approach. The only difference would be the value used for the endogenous respiration rate (b_H) and the endogenous residue fraction (f_H) as shown in Equation 2.23 and Equation 2.24.

$$\frac{dX_a}{dt} = -b'_H(T) X_a \qquad \text{Equation 2.23}$$

$$\frac{dX_e}{dt} = f'_H b'_H(T) X_a \qquad \text{Equation 2.24}$$

Where

b'_H = rate of active mass loss due to organism die-off in death regeneration model (mgVSS/mgVSS/d)

f'_H = endogenous residue fraction for death regeneration model

Both of these approaches can be used to model endogenous mass loss in an HRAP. As stated previously, the results obtained from these approaches differ only slightly if substrate storage is taken into account (Ekama & Marais, 1977). The endogenous respiration approach is normally preferred in the design of wastewater treatment systems and consequently it also has the advantage of better-researched estimations of the rates and constants (Tchobanoglous, et al., 2003; Ekama & Wentzel, 2008a). Due to this availability of the rates and constants of the endogenous respiration model, it was decided to use this model in the deterministic HRAP model.

2.8.1.2 Substrate

The kinetics that determines the increase and decrease in the substrate concentrations are dependent on the type of approach that is used to model the OHOs. As explained for the OHOs in section 2.8.1.1, the kinetics of the substrate concentration depend on whether the substrate storage is included and if the endogenous respiration of the death regeneration model

was chosen. The kinetics for each of these approaches are discussed in further detail in the following paragraphs.

2.8.1.2.1 Substrate utilisation/storage

Heterotrophic organisms consume substrate for two processes namely catabolism and anabolism. Anabolism is the process where the substrate is transformed into cell mass. Catabolism is the process of energy generation required for the anabolic process. Since only approximately two-thirds of the substrate used are transformed into biomass (anabolism), Equation 2.16 should be adjusted to model the substrate utilisation. The substrate is measured in terms of Chemical Oxygen Demand (COD) and heterotrophic organisms are measured in terms of Volatile Settable Solids (VSS). Therefore, Equation 2.16 should also be multiplied by a conversion factor to transform the units from VSS to COD. Equation 2.25 is used to determine the yield of biomass (in VSS) for each unit of substrate that was utilised (Tchobanoglous, et al., 2003).

$$Y_{Hv} = \frac{Y_{COD}}{f_{cv}} \qquad \text{Equation 2.25}$$

Where

Y_{Hv} = the yield of biomass (mgVSS/mgCOD)

Y_{COD} = the portion of COD utilised for anabolism

f_{cv} = the COD/VSS ratio of the biomass (mgCOD/mgVSS)

By using the yield coefficient (Y_{Hv}), a maximum substrate utilisation rate can be calculated from the maximum specific growth rate (μ_m). Equation 2.26 shows how this is done (Tchobanoglous, et al., 2003).

$$k_{Hm} = \frac{\mu_{Hm}}{Y_{Hv}} \qquad \text{Equation 2.26}$$

Where

k_{Hm} = maximum substrate utilisation rate (mgCOD/mgVSS/d)

μ_{Hm} = maximum specific growth rate (mgVSS/mgVSS/day)

The maximum substrate utilisation rate can then be used together with the Monod equation to derive an equation for substrate utilisation within a reactor. Equation 2.27 is the equation that is used to model the utilisation of substrate in a reactor (Marais & Ekama, 1976).

$$\frac{dS}{dt} = -\frac{k_{Hm}S}{K_S + S}X_a \qquad \text{Equation 2.27}$$

Where

S = soluble substrate (COD) concentration (mgCOD/L)

X_a = active biomass concentration (mgVSS/L)

K_S = half-saturation constant (mgCOD/L)

Equation 2.27 pairs with Equation 2.16 and also ignores the substrate storage process. Equation 2.27 would consequently not apply when there are large and frequent variations in the ambient substrate concentration (Marais & Ekama, 1976).

If the substrate storage process is accounted for, the reduction in the substrate concentration is due to substrate entering the storage and not due to direct utilisation by the heterotrophic organism for growth as in Equation 2.27. Equation 2.40 describes the decrease in the substrate concentration due to substrate storage (Ekama & Marais, 1977).

$$\frac{dS}{dt} = -KSX_a\left(f_r - \frac{X_s}{X_a}\right) \qquad \text{Equation 2.28}$$

2.8.1.2.2 Substrate release

The death regeneration approach is responsible for an increase in the substrate concentration, as a fraction of the organism mass loss returns to the system as biodegradable substrate. The rate of this increase in the substrate concentration for the death regeneration approach is shown in Equation 2.29 (Ekama & Marais, 1977).

$$\frac{dS}{dt} = f_{cv}(1 - f'_H)b'_H X_a \qquad \text{Equation 2.29}$$

2.8.1.3 Ammonia Oxidising Organisms

Ammonia Oxidising Organisms (ANOs) oxidise ammonia into nitrite according to the equation below (Ekama & Wentzel, 2008b).

$$NH_4^+ + \frac{3}{2}O_2 \rightarrow NO_2^- + H_2O + 2H^+$$

Nitrite Oxidising Organisms (NNOs) oxidise the nitrite further to form nitrate as shown below (Ekama & Wentzel, 2008b).

$$NO_2 + \frac{1}{2}O_2 \rightarrow NO_3^-$$

The total oxidation reaction for ammonia can then be written as shown below.

$$NH_4^+ + 2O_2 \rightarrow NO_3^- + 2H^+ + H_2O$$

In most nitrification systems operated below 28 °C, the ammonia oxidising bacteria are rate limiting in the complete nitrification of ammonia to nitrate (Tchobanoglous, et al., 2003). Consequently, nitrite is almost immediately oxidised into nitrate in most wastewater treatment systems (Ekama & Wentzel, 2008b). The only case where the NNOs might limit the rate of nitrification, is at very low dissolved oxygen concentrations (below 0.5 mg/L) (Tchobanoglous, et al., 2003). It is therefore generally safe to ignore NNOs from a nitrifying system provided that the system operates at dissolved oxygen concentrations above 0.5 mg/L. Consequently,

in the design of activated sludge systems, the assumption is made that the rate of complete nitrification only depends on the kinetics of the ANOs (Ekama & Wentzel, 2008b; Tchobanoglous, et al., 2003).

In section 2.4.1.1.4, it was stated that nitrification would be limited in an HRAP environment because the UV-light penetration in these shallow ponds inhibits the growth of the nitrifying organisms. This can possibly cause the nitrification rate in these ponds to be slower than expected.

2.8.1.3.1 Growth

The growth of the ANOs follows the same approach as the growth of the OHOs. Equation 2.25 is a mathematical representation of the growth of ANOs (Ekama & Wentzel, 2008b).

$$\frac{dX_n}{dt} = \frac{\mu_{Am}(T) n_a}{K_n(T) + n_a} X_n \qquad \text{Equation 2.30}$$

Where

X_n = ANOs concentration (mgVSS/L)

n_a = ammonia concentration (mgN/L)

$\mu_{Am}(T)$ = maximum specific growth rate of ANOs as a function of temperature (mgVSS/mgVSS/day)

$K_n(T)$ = half-saturation coefficient for the growth of ANOs on ammonia (mgN/L)

Nitrification has a high oxygen requirement as shown in the stoichiometric equations above. In an environment with a low dissolved oxygen concentration, nitrification is inhibited regardless of the ammonia concentration. Equation 2.31 is the rate of change in ANO concentration where the dissolved oxygen concentration is limiting (Tchobanoglous, et al., 2003).

$$\frac{dX_n}{dt} = \left(\frac{\mu_{Am}(T) n_a}{K_n(T) + n_a}\right)\left(\frac{DO}{K_o + DO}\right) X_n \qquad \text{Equation 2.31}$$

Where

DO = dissolved oxygen concentration (mg/L)

K_o = half-saturation concentration for dissolved oxygen (mg/L)

The maximum specific growth rate (μ_A) and the half-saturation constant are temperature dependent (K_n) and are calculated with Equation 2.32 and 2.33 respectively.

$$\mu_{Am}(T) = \mu_{Am,20}\theta_{gX_n}^{T-20} \qquad \text{Equation 2.32}$$

$$K_n(T) = K_{n,20}\theta_{K_n}^{T-20} \qquad \text{Equation 2.33}$$

Where

$\mu_{Am,20}$ = maximum specific growth rate of ANOs at 20 °C (mgVSS/mgVSS/day)

θ_{gX_n} = temperature coefficient for the maximum specific growth rate of ANOs
$K_{n,20}$ = ammonia half-saturation concentration at 20 °C (mgN/L)
θ_{K_n} = temperature coefficient of ammonia half-saturation concentration

2.8.1.3.2 Endogenous Respiration

Endogenous respiration for ANOs follows exactly the same mathematical equation as in the case of OHOs. Equation 2.26 represents the rate of change in the ANO concentration due to endogenous respiration (Ekama & Wentzel, 2008b).

$$\frac{dX_n}{dt} = -b_A(T)X_n \qquad \text{Equation 2.34}$$

Where
$b_A(T)$ = endogenous respiration rate as a function of temperature (mgVSS/mgVSS/day)

The endogenous respiration rate of ANOs is also temperature dependant and is adjusted for temperature according to Equation 2.35.

$$b_A(T) = b_{A,20}\theta_{rX_n}^{T-20} \qquad \text{Equation 2.35}$$

Where
$b_{A,20}$ = endogenous respiration rate at 20 °C (mgVSS/mgVSS/day)
θ_{rX_n} = temperature coefficient ANO endogenous respiration

2.8.1.4 Ammonia and Nitrate

The ANOs and NNOs oxidise ammonia into nitrate. Since the assumption was made that ANOs are rate limiting, the rate of nitrification is directly proportional to the growth rate of ANOs described in section 2.8.1.3. The equations for the rates of change in the ammonia and nitrate concentrations, given in Equation 2.36 and 2.37 respectively, were consequently developed from the equation for the growth rate of ANOs (Ekama & Wentzel, 2008b).

$$\frac{dn_a}{dt} = -\frac{1}{Y_A}\frac{\mu_{Am}(T)n_a}{K_n(T)+n_a}X_n \qquad \text{Equation 2.36}$$

$$\frac{dn_i}{dt} = \frac{1}{Y_A}\frac{\mu_{Am}(T)n_a}{K_n(T)+n_a}X_n \qquad \text{Equation 2.37}$$

Where
n_i = nitrate concentration (mgN/L)
Y_A = nitrifier yield coefficient (mgVSS/mgN)

2.8.2 Algal Water Quality Model

This section discusses the surface water quality model used by Chapra (2008). Chapra's (2008) model primarily focuses on the interaction between the algae and the nutrients in the water. This model was based on the surface water quality model developed by Bowie *et. al.* (1985). The model attempts to simulate the interactions between algae, zooplankton, nutrients and non-living organic carbon.

2.8.2.1 Algae

The algae concentration is affected by various processes. The process responsible for algae growth is called photosynthesis. Processes responsible for a loss in algal mass include respiration, settling, mortality, grazing, and excretion. The relationship among all these processes is shown in Figure 2.7. The labile DOM and POM of Figure 2.7 represent readily biodegradable dissolved and particulate organic matter.

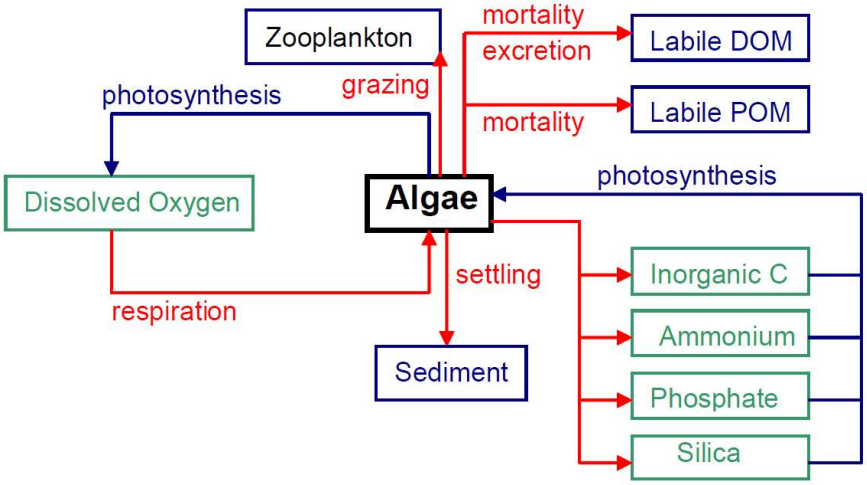

Figure 2.7 - Factors affecting algal concentration (Cole & Wells, 2013)

Figure 2.7 is mathematically represented by Equation 2.38 (Bowie, et al., 1985). Equation 2.38 can thus be used to model all the above-mentioned processes responsible for a change in algal mass.

$$\frac{da}{dt} = (\mathrm{k_{ga}} - k_{ra} - k_{ea} - k_{sa} - k_{ma})a - k_{gh} \qquad \text{Equation 2.38}$$

Where

a = algae concentration (mgChl$a$/L)
k_{ga} = algal growth rate (day^{-1})
k_{ra} = algal respiration rate (day^{-1})
k_{ea} = algal excretion rate (day^{-1})
k_{sa} = algal settling rate (day^{-1})
k_{ma} = non predatory mortality rate (day^{-1})

k_{gh} = rate of losses due to zooplankton grazing as a function of temperature, algae concentration and zooplankton concentration (day^{-1})

Chapra (2008) adapted Equation 2.38 by combining certain terms to provide an equation that makes use of more measurable rates. In Chapra's simplification, the respiration and excretion rates were combined and the algal mortality rate was excluded.

Equation 2.39 was derived by Chapra (2008) to model microalgae growth and decay in water.

$$\frac{da}{dt} = k_{ga}(T,N,I)a - k_{rea}(T)a - k_{gh}(T,a,z_h)a + v_a A_t a_u - v_a A_t a \qquad \text{Equation 2.39}$$

Where

$k_{ga}(T,N,I)$ = algal growth rate as a function of temperature, nutrients and solar radiation (day^{-1})

$k_{rea}(T)$ = rate of losses due to respiration and excretion (day^{-1})

$k_{gh}(T,a,z_h)$ = rate of losses due to zooplankton grazing as a function of temperature, algae concentration and zooplankton concentration (day^{-1})

z_h = herbivorous zooplankton concentration (mgC/L)

a_u = algae concentration in an upper layer (mgChl$a$/L)

Most of the rates in Equation 2.38 and Equation 2.39 vary with different environmental condition as well as for the algae strain that is present. Experimental procedures are followed to get an estimate of a base rate under certain conditions. The base rate is then adjusted to be applicable for changing environmental conditions.

2.8.2.1.1 Algae growth rate

As mentioned previously, the algae growth rate depends on the temperature and the availability of light and nutrients. Equation 2.40 can be used to calculate the applicable growth rate (Chapra, 2008).

$$k_{ga} = \lambda_N \lambda_I \lambda_T k_{ga,20} \qquad \text{Equation 2.40}$$

Where

$k_{ga,20}$ = algal growth rate at 20 °C with no light or nutrient limitation (day^{-1})

λ_T = multiplier for growth limiting/increase due to temperature

λ_I = multiplier for growth limiting due to light

λ_N = multiplier for growth limiting due to nutrients

Equation 2.40 uses multipliers to adjust the algal growth rate at 20 °C when there is no limitation due to nutrient or light. Each multiplier is calculated as shown in the sections 2.8.2.1.1.1 to 2.8.2.1.1.3.

2.8.2.1.1.1 Temperature Multiplier

The Arrhenius relationship is commonly used to calculate the temperature multiplier as indicated in Equation 2.41 (Chapra, 2008; Bowie, et al., 1985). This relationship adjusts the base growth rate at 20 °C for temperature effects. Temperatures higher than 20 °C will result in a temperature multiplier (λ_T) larger than one and consequently an increased growth rate. Temperatures lower than 20 °C will result in a temperature multiplier (λ_T) less than one and consequently a decreased growth rate.

$$\lambda_T = \theta_{ga}^{T-20} \qquad \text{Equation 2.41}$$

Where

T = temperature of media (°C)

θ_{ga} = temperature factor for algal growth rate

Epperly (1972) suggested that θ must be equal to 1.066 based on a study that included a wide variety of algae strains.

Algae growth is not only inhibited by low temperatures, but also by temperatures higher than the optimal growth temperature (Chapra, 2008). The temperature dependence of various strains of algae can be seen in Figure 2.8. A limitation of the Arrhenius relationship is that it does not allow for growth limitation at temperatures above the optimum. However, when a mixed population of algae is considered, there will always be a certain strain of algae that will grow at any reasonable temperature. Therefore, the Arrhenius relationship can be accurately applied to model a mixed population (Chapra, 2008).

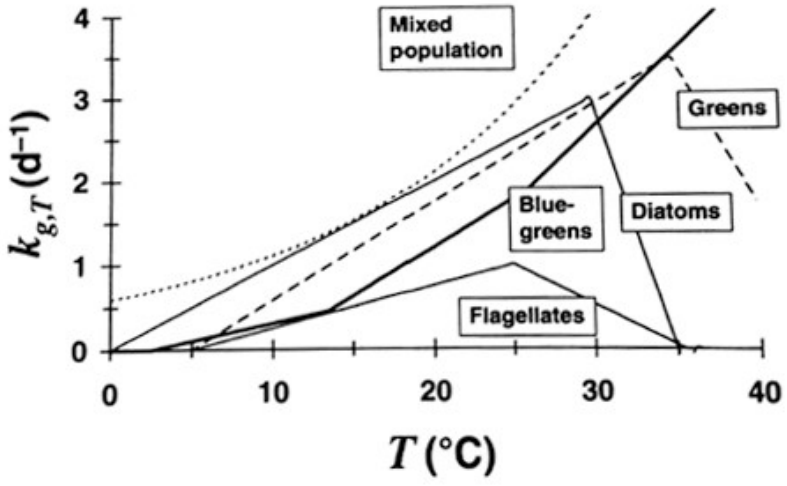

Figure 2.8 - Growth rate dependence on temperature for various strains of algae (Chapra, 2008)

2.8.2.1.1.2 Nutrient Multiplier

Algae require nutrients in order to grow. The major nutrients required for the growth of most microalgae are carbon, nitrogen, and phosphorus. Various other micronutrients and trace elements are also required for algal growth.

The nutrient limiting factors can be computed using the Monod relationship as shown in Equation 2.42 (Cole & Wells, 2013).

$$\lambda_{n_i} = \frac{\Phi_i}{K_{si} + \Phi_i} \qquad \text{Equation 2.42}$$

Where

λ_{n_i} = growth limiting factor for a specific nutrient

Φ_i = nutrient concentration (mg/L)

k_{si} = half-saturation coefficient for nutrient (mg/L)

As mentioned above, algal growth depends on a number of nutrients. More than one nutrient can therefore be responsible for growth limitation. A *minimum* approach is most commonly used to incorporate more than one type of nutrient. This approach calculates a nutrient limiting multiplier for each nutrient (with Equation 2.42) and then chooses the minimum value to be used as the multiplier for nutrient limitation in Equation 2.40. Equation 2.43 can be used to calculate the limiting nutrient multiplier in the case where more than one nutrient is considered (Chapra, 2008). This approach also allows one to incorporate all the nutrients that might be limiting into the algal growth kinetics.

$$\lambda_N = \min(\lambda_{n_i}, \lambda_{n_{i+1}}, \dots) \qquad \text{Equation 2.43}$$

2.8.2.1.1.3 Light Multiplier

Chapra (2008) and Bowie *et al.* (1985) provided Equation 2.44 for the calculation of growth rate limitation due to light. Equation 2.44 is the result of an integration over time and depth in order to obtain the mean value for light limitation (Chapra, 2008; Bowie, et al., 1985).

$$\lambda_I = \frac{2.718 f_{ld}}{k_e d}(e^{-\alpha_1} - e^{-\alpha_0}) \qquad \text{Equation 2.44}$$

Where

f_{ld} = photoperiod (fraction of day with light/sunshine)

k_e = light extinction coefficient (m^{-1})

d = depth (m)

The light multiplier given in Equation 2.44 does not only depend on the light intensity but also on the duration of the sunlight in each day, the turbidity of the water and the depth of the water. Light extinction differs over the depth of the pond and the light multiplier in Equation 2.44 is consequently calculated as an average over the depth of the pond.

The variables α_1 and α_0 of Equation 2.44 are used to simplify the equation and can be calculated with Equation 2.45 and Equation 2.46.

$$\alpha_0 = \frac{I_a}{I_s} e^{-k_e H_0} \quad \text{Equation 2.45}$$

$$\alpha_1 = \frac{I_a}{I_s} e^{-k_e H_1} \quad \text{Equation 2.46}$$

Where

I_a = average light intensity (W/m^2)
I_s = optimal light intensity (W/m^2)
H_0 = depth at top of layer under consideration (0 if the top is the water surface) (m)
H_1 = depth at bottom of layer under consideration (m)

The average light intensity (I_a) is calculated by adjusting the maximum light intensity according to a half-sinusoid approximation that represents the light variation of the sun. The calculation for this adjustment is shown in Equation 2.47.

$$I_a = I_m \left(\frac{2}{\pi}\right) \quad \text{Equation 2.47}$$

Where

I_m = the maximum light intensity measured at the surface (W/m^2)

The light extinction coefficient (k_e) incorporates the loss of light intensity with water depth due to light absorbance of particles in the water as well as reflection from the water surface. The light extinction coefficient is determined with Equation 2.48 (Riley, et al., 1956).

$$k_e = k_e' + 0.0088a + 0.054a^{\frac{2}{3}} \quad \text{Equation 2.48}$$

Where

a = algal concentration (µgChl$a$/L)
k_e' = light extinction due to other factors than phytoplankton/algae (m^{-1})

In pure and particle-free water, the light extinction is 0.04 m^{-1} (Riley, et al., 1956). However, algae rarely occur alone and are normally accompanied by other non-algal volatile solids and non-volatile suspended solids. The light extinction due to other factors than algae (k_e') can either be directly measured or Equation 2.49 can be used to calculate it from the concentrations of other non-algal suspended solids (Di Toro, 1978; Chapra, 2008).

$$k_e' = k_{ew} + 0.052N + 0.174D \quad \text{Equation 2.49}$$

Where

k_{ew} = light extinction in pure and particle free water (0.04 m^{-1})

N = concentration of non-volatile suspended solids (mg/L)

D = concentration of non-algal volatile suspended solids (or detritus) (mg/L)

2.8.2.1.2 Algal respiration and excretion rate

The algal respiration and excretion rates are normally combined to obtain a rate that accounts for all metabolic losses. The respiration and excretion rate consequently represents the difference between the gross and the net algal growth (Bowie, et al., 1985).

The rate of algal respiration and excretion is temperature dependent and is mathematically represented by Equation 2.50 (Chapra, 2008; Bowie, et al., 1985).

$$k_{rea} = \theta_{rea}^{T-20} k_{rea,20} \qquad \text{Equation 2.50}$$

Where

$k_{rea,20}$ = algal respiration rate at 20 °C (day^{-1})

θ_{rea} = temperature factor for algae respiration rate

2.8.2.1.3 Grazing rate

Zooplankton are microscopic aquatic animals. Zooplankton are often identified as drifters since they are suspended in natural waters and ordinarily move with the currents (Clesceri, et al., 1998). Herbivorous zooplankton are predators that use algae as their main food source. Herbivorous zooplankton cause a reduction in algal concentration through grazing (Chapra, 2008).

The rate of algal mass loss due to the grazing of herbivorous zooplankton can be calculated with Equation 2.51 (Chapra, 2008).

$$k_{gh}(T, a, z_h) = \frac{a}{k_{sga} + a} \theta_{gh}^{T-20} C_{gh} z_h \qquad \text{Equation 2.51}$$

Where

z_h = herbivorous zooplankton concentration (mgC/L)

C_{gh} = herbivorous zooplankton grazing rate at 20 °C with no algae limitation (L/mgC/d)

k_{sga} = half-saturation constant for herbivorous zooplankton grazing on algae (mgChl*a*/L)

θ_{gh} = temperature correction factor

Equation 2.51 limits the grazing rate with the Michaelis-Mentis (Monod) term. The same principle was applied in the algal growth limitation due to nutrients in section 2.8.2.1.1.2.

2.8.2.2 Zooplankton

It was already mentioned that herbivorous zooplankton consume algae. It is therefore important to model the concentration of herbivorous zooplankton since it has a major influence on the algal concentration. However, herbivorous zooplankton are in return grazed upon by

carnivorous zooplankton. The algal concentration is therefore also indirectly dependent on the carnivorous zooplankton concentration. An accurate model would consequently require for both the herbivorous and carnivorous zooplankton to be modelled.

2.8.2.2.1 Herbivorous zooplankton

The herbivorous zooplankton grow with the consumption of algae and are depleted through respiration, excretion, and through carnivorous zooplankton grazing. The herbivorous zooplankton can be modelled with Equation 2.52 (Chapra, 2008).

$$\frac{dz_h}{dt} = a_{ca}\varepsilon_h k_{gh}(T, a, z_h)a - k_{rh}(T)z_h - k_{gc}(T, z_h, z_c)z_h \qquad \text{Equation 2.52}$$

Where

a_{ca}	=	ratio of carbon to chlorophyll *a* in phytoplankton biomass (mgC/mgChl*a*)
ε_h	=	grazing efficiency factor
$k_{rh}(T)$	=	herbivorous zooplankton respiration (and excretion) rate (day^{-1})
$k_{gc}(z_h, T, z_c)$	=	rate of mass loss due to carnivorous zooplankton grazing (day^{-1})
z_c	=	carnivorous zooplankton concentration (mgC/L)

The herbivorous zooplankton respiration rate is dependent on the temperature. The temperature dependence can be modelled with the Arrhenius relationship as in Equation 2.41 and Equation 2.50.

The mass loss rate due to carnivorous zooplankton grazing ($k_{gc}(z_h, T, z_c)$) is calculated in the same manner as the herbivorous zooplankton mass loss rate due to grazing ($k_{gh}(T, a, z_h)$). Equation 2.53 is used to determine the carnivorous zooplankton grazing rate.

$$k_{gc}(z_h, T, z_c) = \frac{z_h}{k_{sh} + z_h}\theta_{gc}^{T-20}C_{gc}z_c \qquad \text{Equation 2.53}$$

Where

k_{sh}	=	half-saturation coefficient for grazing on herbivorous zooplankton (mgC/L)
θ_{gc}	=	temperature factor for carnivorous zooplankton grazing
C_{gc}	=	carnivorous zooplankton grazing rate at 20 °C with no herbivore limitation (L/mgC/d)

2.8.2.2.2 Carnivorous zooplankton

Carnivorous zooplankton grow by grazing on herbivorous zooplankton and are depleted through respiration, excretion and higher organism grazing (mostly fish). The carnivorous zooplankton concentration can be modelled with Equation 2.54 (Chapra, 2008).

$$\frac{dz_c}{dt} = \varepsilon_c k_{gc}(T, z_h, z_c)z_h - k_{rc}(T)z_c - k_{dc}(T)z_c \qquad \text{Equation 2.54}$$

Where

ε_c = grazing efficiency factor

$k_{rc}(T)$ = carnivorous zooplankton respiration (and excretion) rate (day^{-1})

$k_{dc}(T)$ = rate of mass loss due to higher organism grazing (day^{-1})

2.8.2.3 Non-living Organic Carbon

Chapra (2008) included particulate and dissolved carbon in the water quality model. The particulate organic carbon (c_p) accumulates in the system through certain losses related to living organisms. The particulate organic carbon then eventually dissolves to form dissolved organic carbon (c_d). The dissolved organic carbon is then hydrolysed into its inorganic nutrients.

$$\frac{dc_p}{dt} = a_{ca}(1-\varepsilon_h)k_{gh}(T,a,z_h)a + (1-\varepsilon_c)k_{gc}(T,z_h,z_c)z_h + k_{dc}(T)z_c - k_p(T)c_p + v_pA_tc_{pu} - v_pA_tc_p \quad \text{Equation 2.55}$$

$$\frac{dc_d}{dt} = k_p(T)c_p - k_h(T)c_d \quad \text{Equation 2.56}$$

Where

$k_p(T)$ = rate of particulate organic carbon dilution (day^{-1})

$k_h(T)$ = rate of dissolved organic carbon hydrolysis (day^{-1})

2.8.2.4 Nutrients

Algae require nutrient to reproduce. These nutrients include any element that algae utilise to build their cell structure. As mentioned in section 2.8.2.1.1.2, algae require various macronutrient, micronutrient, and trace elements. Macronutrients include carbon, nitrogen, and phosphorus.

In order to model algal growth accurately, one must also model the changes in concentrations of the nutrients that the algae utilise for growth. However, normally one does not model the entire group of nutrients that algae require to grow. The assumption is consequently made that all the trace elements and micronutrients as well as some macronutrients, are present in such high concentrations that they do not inhibit the growth of algae. It is generally considered that the only limiting nutrients are nitrogen and phosphorus (Chapra, 2008).

2.8.2.4.1 Phosphorus

In nature, phosphorus is almost exclusively found in the form of phosphates. There are three major groups of phosphates that include orthophosphates, condensed phosphates (linear or ring structures containing multiple phosphate molecules) and organically bound phosphates (Clesceri, et al., 1998).

Algae have a preference for phosphorus that is soluble and readily available. Phosphorus in this form is classified as soluble reactive phosphorus (SRP) (Chapra, 2008). SRP largely

consists of orthophosphate but it may contain a small fraction of condensed phosphates (Clesceri, et al., 1998).

The SRP concentration is therefore the only form of phosphorus of interest when modelling algae growth. The SRP concentration increases through the respiration of algae and zooplankton, and the hydrolysis of organic carbon. The growth of algae reduces the SRP concentration due to phosphorus assimilation. Equation 2.57 describes these gains and losses in the SRP concentration mathematically (Chapra, 2008).

$$\frac{dp}{dt} = -a_{pa}k_{ga}(T,N,I)a + a_{pa}k_{rea}(T)a + a_{pc}k_{rh}(T)z_h + a_{pc}k_{rc}(T)z_c + a_{pc}k_h(T)c_d \qquad \text{Equation 2.57}$$

Where

p = concentration of SRP (mgP/L)

a_{pa} = ratio of phosphorus to algae (mgP/mgChl$a$)

$k_h(T)$ = hydrolysis rate as a function of temperature (day^{-1})

c_d = dissolved organic carbon concentration (day^{-1})

a_{pc} = ratio of phosphorus to organic carbon (mgP/mgC)

2.8.2.4.2 Nitrogen

Algae utilise nitrogen that is in the form of ammonium, nitrate, and nitrite to form new biomass. Although all these forms are utilised by the algae, there is a preference for ammonium (Cole & Wells, 2013). It is therefore necessary to model the ammonium and nitrate/nitrite concentrations separately.

The ammonium concentration in a water body decreases through nitrification and the assimilation into algal biomass. The ammonium concentration increases through the respiration of algae and zooplankton, as well as through the hydrolysis of organic carbon. Equation 2.58 is a mathematical expression of these processes and can be used to model the ammonium concentration in a water body (Chapra, 2008).

$$\frac{dn_a}{dt} = -a_{na}F_{am}k_{ga}(T,N,I)a + a_{na}k_{ra}(T)a + a_{nc}k_{rh}(T)z_h + a_{nc}k_{rc}(T)z_c + a_{nc}k_h(T)c_d - k_n(T)n_a \qquad \text{Equation 2.58}$$

Where

n_a = ammonium-N concentration (mgN/L)

a_{na} = ratio of nitrogen to chlorophyll a in algal biomass (mgN/mgChl$a$)

F_{am} = ammonium preference factor

a_{nc} = ratio of nitrogen to organic carbon (mgN/mgC)

$k_n(T)$ = nitrification rate as a function of temperature (day^{-1})

The ammonium preference factor (F_{am}) represents the preference that the algae have for ammonium over nitrate/nitrite. The ammonium preference factor can by calculated with Equation 2.59 (Cole & Wells, 2013).

$$F_{am} = n_a \frac{n_i}{(K_{sam} + n_a)(K_{sam} + n_i)} + n_a \frac{K_{sam}}{(n_a + n_i)(K_{sam} + n_i)} \quad \text{Equation 2.59}$$

Where

n_i = nitrate-N/nitrite-N concentration (mgN/L)

k_{sam} = half-saturation constant for ammonium preference (mgN/L)

The nitrate/nitrite concentration increases through nitrification and decreases with assimilation in algal biomass. Equation 2.60 is a mathematical expression that represents these processes (Chapra, 2008).

$$\frac{dn_i}{dt} = k_n(T)n_a - a_{na}(1 - F_{am})k_{ga}(T, N, I)a \quad \text{Equation 2.60}$$

2.8.3 Alternative Models

Various alternative models exist that incorporate similar kinetics to the activated sludge model and the algal water quality model of Bowie et al. (1985). An example of such a model is the CE-QUAL-W2 model of Cole and Wells (2013). The CE-QUAL-W2 model is an expansive surface water quality model that includes most of the state variable of the deterministic HRAP model developed in section 3.2. The CE-QUAL-W2 model is therefore a viable alternative for modelling the biological processes within an HRAP pond. However, the activated sludge model and the algal water quality model (Bowie, et al., 1985; Chapra, 2008) discussed above, has the advantage of being accompanies by well-researched kinetic rates and stoichiometric constants (Ekama & Wentzel, 2008a; Ekama & Wentzel, 2008b; Tchobanoglous, et al., 2003; Bowie, et al., 1985). Since the CE-QUAL-W2 model is a surface water quality model, it also does not include all the kinetics involved with OHOs and ANOs in a wastewater treatment environment (Cole & Wells, 2013). The activated sludge model explained in section 2.8.1 and the algal water quality model explained in section 2.8.2 was therefore deemed as an appropriate basis for the development of a deterministic HRAP model.

3 METHODOLOGY

Chapter 1 discussed the experimental part as well as the modelling part that the thesis consists of. This section discusses the methodology of these two parts.

3.1 Experimental Setup

A scale model of an HRAP was built in the water laboratory at the Department Civil Engineering at Stellenbosch University. The purpose of the laboratory experiment was to measure the water treatment capabilities, nutrient removal in particular, of the HRAP and thereby obtain data for the calibration of the deterministic model.

Various parameters had to be defined for the setup. These parameters included, but were not limited to, the pond dimensions, the pond depth, the hydraulic residence time, the available light, the characteristics of the influent water and the mixing. A photograph of the complete experimental setup is shown in Figure 3.1.

Figure 3.1 - Experimental scale model of HRAP

3.1.1 Influent characteristics

The influent concentrations were chosen to simulate a possible effluent from a wastewater treatment plant. A synthetic wastewater was developed that represents the effluent concentrations, given in Table 2.1, for a WWTP that operates under general authorisation.

Table 3.1 gives the composition of the synthetic wastewater. It indicates the substances used to represent specific compliance parameters of Table 2.1. Since the compliance parameters are only measured in terms of the weight of the parameter itself, the concentrations had to be adjusted to represent the mass of the entire representative substance as shown in Table 3.1.

Tap water was used for the mixing of the synthetic wastewater. The tap water was a source of various other micronutrients in the synthetic wastewater. The measurements of the influent were done after the tap water dilution, to include the effect that the tap water might have on the nutrients of concern. The chlorine in tap water dissipates generally quickly when exposed to the atmosphere. An assumption was made that the chlorine in the tap water did not influence the algal growth. This assumption was supported by exposing the tap water to the atmosphere for a period of time (50 to 100 minutes) before adding it to the pond to ensure some dissipation of the chlorine.

Table 3.1 – Synthetic wastewater composition

Compliance parameter	**Compliance limit**	**Representative substance**	**Formula**	**Concentration of representative substance (mg/L)**
Chemical Oxygen Demand	75 mgCOD/L	Glucose	$C_6H_{12}O_6$	70.3
Ammonia (ionised and un-ionised)	6 mgN/L	Ammonium chloride	NH_4Cl	22.9
Nitrate/Nitrite	15 mgN/L	Potassium Nitrate	KNO_3	108.2
Ortho-phosphate	10 mgP/L	Dipotassium phosphate	K_2HPO_4	56.1

3.1.2 Feeding system

It was important for the influent to have a constant composition to accurately measure the nutrient and COD removal in the HRAP. The volume and hydraulic retention time of the pond required a large volume of synthetic wastewater (between 90 and 250 litres) to be pumped through the system daily. The synthetic wastewater was fed into the pond with two peristaltic pumps. A peristaltic pump with a high flow rate was used to feed tap water into the pond. A small peristaltic pump with a low flow rate was used to feed a concentrated mixture of the synthetic wastewater into the system. The combination of the pumps gave an influent with the desired flow rate and composition. The concentrate of synthetic wastewater was kept below 4 °C to avoid premature biological activity. Figure 3.2 is a schematic representation of the feeding system.

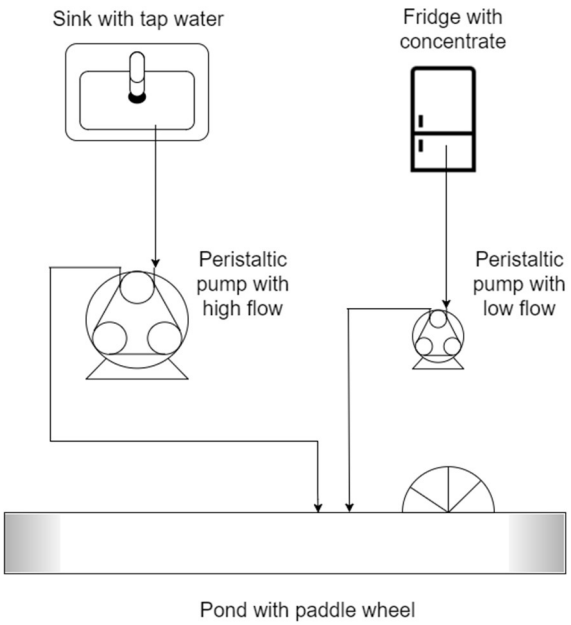

Figure 3.2 - Synthetic wastewater feeding system

This type of feeding system was developed to avoid premature biological activity in the concentrate and to allow the system to run on its own for a required period of time. The synthetic wastewater concentrate was mixed in a 20-litre bucket. A high dilution ratio allowed this concentrate to last for between 7 and 15 days before it had to be refilled. The large retention time of the refrigerated concentrate allowed the system to run unattended for a relatively long period.

3.1.3 Peristaltic pumps

Two peristaltic pumps, one with a high flow rate and one with a low flow rate, were used in the feeding system. Each peristaltic pump was driven by a 12V DC motor. The larger peristaltic pump had a flow rate of approximately 500 ml/min and the smaller pump had a flow rate of approximately 15 ml/min.

These pumps were connected to a programmable Arduino® microcontroller. The microcontroller was programmed to run the peristaltic pumps in short sequences according to the desired flow rate, as well as the required dilution for the concentrate. A sequence consisted of an interval during which the larger pump was running, an interval for the small pump and intervals during which both pumps were off. The length of a sequence depended on the desired hydraulic retention time but was typically less than 10 minutes. These sequences were very short when compared to the hydraulic retention time of multiple days. These short flow sequences were assumed to represent a continuous flow.

3.1.4 HRAP dimensions

A site visit was undertaken to the pilot scale HRAP operated as part of an Integrated Algal Ponding System by the Environmental Biotechnology Group at Rhodes University (EBRU) (Rose, et al., 2002). It was decided to base the dimensions of the laboratory scale HRAP on the length and width ratio of the HRAP at Rhodes University.

The laboratory scale pond was designed with a length of 4800 mm and a width of 700 mm. The ends of the pond are curved to improve the hydraulic flow within the pond. The pond had two channels with a width of 350 mm each and the channels were separated by a thin baffle wall. These dimensions gave the pond a surface area of 3.24 m^2. Figure 3.3 is a schematic of the laboratory scale HRAP. All the dimensions shown in Figure 3.3 are in millimetre.

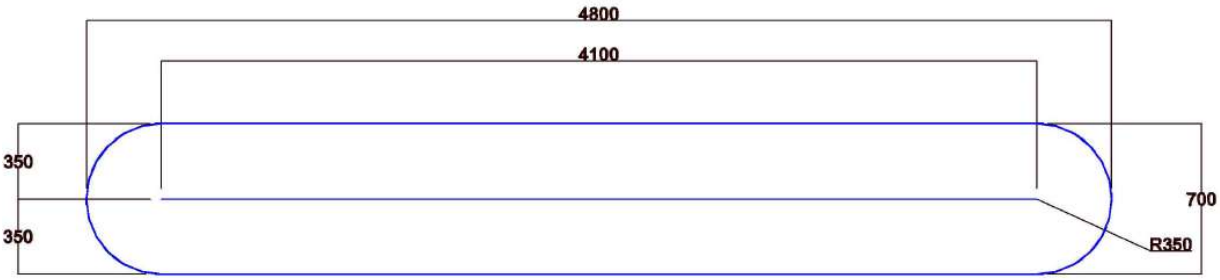

Figure 3.3 - Plan view of HRAP

3.1.5 HRAP depth

The pond was designed to have a depth of 300 mm, but due to construction inaccuracies, the measured pond depth was 288 mm. The design depth was recommended in the literature as well as by the researchers from the Rhodes HRAP (Craggs, 2005b; Render, 2015). The depth is a very important parameter in algal kinetic and especially affects the light penetration. Since the algae and light could not be scaled down, the depth was not scaled down either.

The outflow pipe was placed vertically inside the HRAP with the open end at the top of the pipe. The pond depth was consequently determined by the height of the outflow pipe. The depth of the pond could be adjusted to the desired value by shortening or lengthening the outflow pipe.

3.1.6 Hydraulic residence time

The peristaltic pumps setup allowed for the hydraulic retention time to be adjusted. The feeding system was capable of supplying large enough flow for a hydraulic residence time of approximately 1.5 days and longer. The experimental setup was first run with an HRT of 4 days, then an HRT of 10 days and finally as a batch test with no in- and outflow.

3.1.7 Lighting

Artificial lighting was provided because the HRAP model was indoors. The lighting was provided with fluorescent tubes. *Osram Biolux* tubes/lamps were used because their wavelength distribution is comparable to sunlight (Osram, 2016). Eight 58W *Biolux* tubes were mounted above the pond. The characteristics of interest of the *Biolux* lamps are summarised in Table 3.2.

Table 3.2 - Characteristics of pond lighting (Osram, 2016)

Type of fluorescent lamps	Osram Biolux
Rated wattage per lamp	58 Watt
Rated luminous flux per lamp	3700 lm
Rated lamp efficacy	64 lm/W
Colour Temperature	6500 K

The fluorescent light fixtures were mounted under an aluminium canopy. The purpose of the aluminium was to reduce losses by reflecting the light towards the pond. All the fluorescent light fixtures were connected to a mechanical timer. The timer automatically switched the lights on and off according to a programmable schedule. The mechanical timer was programmed to turn the light on at 06:00 in the morning and switch the light off at 22:00 in the evening.

3.1.8 Paddle wheel

The main purpose of the paddle wheel was to mix the water within the pond. A photograph of the paddle wheel setup is shown in Figure 3.4. The paddle wheel was driven by a 25-Watt motor that had a speed of 20 RPM. The speed of the motor was reduced with a sprocket and chain combination, as shown in Figure 3.4, to rotate the paddle wheel at approximately 7.5 RPM. At this rotation speed, the paddle wheel induced a mean water velocity of roughly 13 cm/s over the depth of the pond. This velocity was very close to the minimum mean velocity of 15 cm/s suggested in section 2.6.3 but was not sufficient to ensure the suspension of large solids. The pond was therefore also manually stirred when settling was observed.

Figure 3.4 – Paddle wheel setup

Another purpose of the paddle wheel was to serve as a partial barrier between the inflow and the outflow. The inflow discharged right in front of the paddle wheel and the outflow pipe was located just behind the paddle wheel. This was assumed to reduce short-circuiting, since the influent had to do at least one full circulation around the pond before it reached the outflow pipe. In order for the paddle to be an effective barrier, the dimensions of the paddle wheel were chosen to match the width and depth of the pond closely. The paddle wheel was also designed with eight paddles to ensure that at least one paddle was always fully submerged within the pond. Figure 3.5 contains schematics of the paddle wheel with all the dimensions in millimetre.

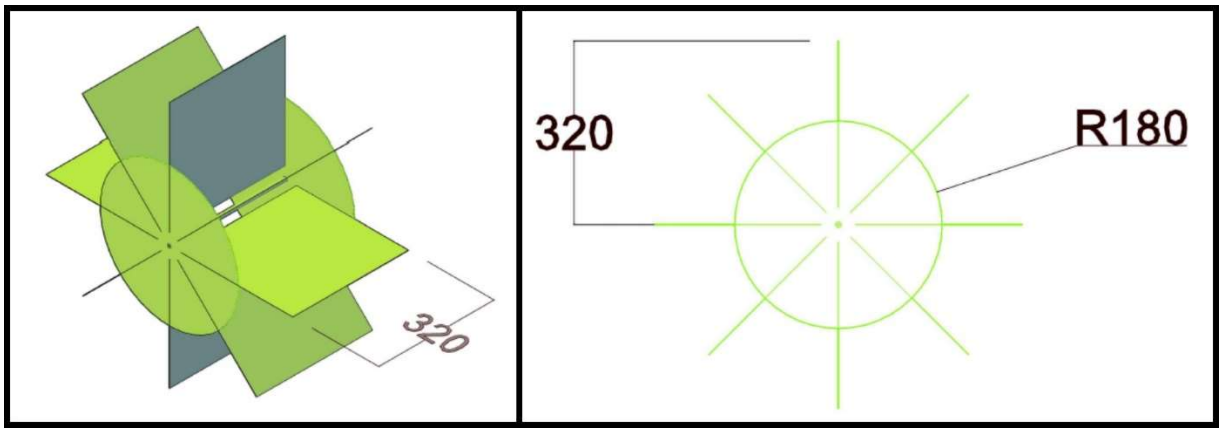

Figure 3.5 – Schematic diagrams of paddle wheel with dimensions

3.1.9 Temperature regulation

The pond was fitted with a 500 W and a 200 W aquarium heater. The purpose of the heaters was to reduce large temperature fluctuations. The heater also compensated for the lack of solar heating due to the pond being indoors.

3.1.10 Algal Seeding

A substantial algal population was required in the HRAP before the experimentation could begin. The initial algal concentration was cultivated from a water sample collected from a farm dam that showed signs of eutrophication near Stellenbosch University. The initial water sample was intentionally collected from a local water body to ensure that the cultivated algal culture was already adjusted to local conditions.

The initial 2-litre water sample that was collected on 16 March 2016 was not visibly green at the time as shown in Figure 3.6. Approximately 0.8 litres of the initial sample were then split between two glass beakers, and the nutrients discussed in section 3.1.1 were added to the samples. The samples were left for two days until 18 March 2016 after which one sample was visibly green as illustrated in Figure 3.6. A small volume of the green sample was added to the other sample to ensure that the sample was seeded with algae. The remaining volume of the green sample was then diluted with tap water to fill the beaker as illustrated in the third image of Figure 3.6. The samples were then alternated on a magnetic stirrer over the next 3 days. On 21 March 2016 both samples showed dense algal cultures. The samples were again diluted with tap water on 22 March 2016 to form a larger sample volume and more nutrients were added. One day after the dilution both samples became visibly greener as illustrated in the sixth photo of Figure 3.6. On 24 March 2016 the algal culture was further diluted in the white bucket illustrated in Figure 3.6. After a dark green colour was observed in all the containers, the algal culture was transferred to the HRAP. The algal culture was then given 2 days to grow and then the volume of the algal culture was doubled through the addition of tap water. This process was repeated until the pond was full. More nutrients were also added with each addition of tap water.

Figure 3.6 - Algal Seeding Process

3.1.11 Water quality measurement

In order to monitor and evaluate the experimental setup, various water quality parameters were measured and monitored throughout the experiment. These parameters include the pH, temperature and the concentrations of COD, ammonia, nitrate, nitrite, soluble reactive phosphorus (SRP), dissolved oxygen, dissolved carbon dioxide, chlorophyll *a* and volatile suspended solids (VSS). In this section, the equipment that was used to measure these parameters is discussed and a brief summary of the procedures that were followed are given.

3.1.11.1 Temperature, pH and dissolved oxygen

The temperature, pH, and dissolved oxygen were measured using the *HQ440d Benchtop Multi-Parameter Meter* manufactured by Hach®. This device is a water quality meter that uses probes to measure various water parameters directly. The *IntelliCAL™ PHC281 probe* was used to measure the pH. The *IntelliCAL™ LDO101* probe was used to do in situ measurements of the dissolved oxygen concentration. Both these probes can measure the temperature as well.

3.1.11.2 Dissolved carbon dioxide

The dissolved carbon dioxide concentration was measured with the use of the *CA-23 Carbon Dioxide Test Kit* supplied by Hach. This kit contains all the equipment and reagents to measure the carbon dioxide concentration through titration.

The *CA-23 Carbon Dioxide Test Kit* can measure the carbon dioxide concentration in the following ranges: 1.25-25 mg/L, 2-40 mg/L and 5-100 mg/L. The method of measurement involves adding a drop of *Phenolphthalein Indicator Solution to* a predefined sample volume. The sample volume varies depending on the desired range. Thereafter, *0.01N Sodium Hydroxide Standard Solution* is added to the sample until the colour of the mixture turns light pink. The number of *0.01N Sodium Hydroxide Standard Solution* drops required for the colour change, are then multiplied by the drop interval value (varies depending on range) to obtain the carbon dioxide concentration in the solution.

3.1.11.3 COD concentration

The COD concentration of the influent and the effluent were measured colorimetrically with Hach's *DR3900 Benchtop Spectrophotometer*, the *DRB200 Digital Reactor* and the *TNTplus™ 821/822* test kits. The *TNTplus™ 821* test kits have a range of 3 to 150 mgCOD/L and the *TNTplus™ 822* test kits have a range of 20 to 1500 mgCOD/L.

Influent samples were measured directly and effluent samples were filtered through a 0.45 µm syringe filter before measurement. Influent samples were measured directly since it contained no suspended solids. A pipet was then used to add 2 mL of the sample into the *TNTplus™ 821/822* test vial. The test vial was inverted until completely mixed and then inserted into the *DRB200 Digital Reactor* (also manufactured by Hach). The sample was digested at 150 °C for two hours. After the reactor cooled down to less than 120 °C, the sample was removed,

inverted to mix and left to cool down to room temperature. The sample was then analysed in the *DR3900 Benchtop Spectrophotometer* where a reading of the COD concentration was obtained.

3.1.11.4 Ammonia concentration

The ammonia concentrations were measured colorimetrically by using the *DR3900 Benchtop Spectrophotometer* and the *TNTplus™ 831* or *TNTplus™ 830* test kits. These kits have a range of 1 to 12 mgNH_3-N/L and 0.015 to 2 mgNH_3-N/L respectively.

The ammonia concentrations were measured for the unfiltered influent as well as for the 0.45 µm filtered effluent. The *TNTplus™ 831* test vial contains a *DosiCap™ Zip* cap. This is a two-sided cap with the test reagents located in the upper side of the cap. After 0.5 mL of the sample was pipetted into the test vial, the cap was turned over and screwed onto the test vial. The vial was then inverted until the reagents within the cap were completely mixed with the sample. The sample was given 15 minutes to react and then it was analysed colorimetrically in the *DR3900 Benchtop Spectrophotometer* to get a reading of the ammonia concentration.

The *TNTplus™ 830* test kits have exactly the same methodology as the *TNTplus™ 831* kits except that it requires a sample volume of 5 mL instead of the 0.5 mL mentioned in the previous paragraph.

3.1.11.5 Nitrate concentration

The nitrate concentrations were measured with the *DR3900 Benchtop Spectrophotometer* and the *TNTplus™ 835* test kits. These test kits are valid for nitrate concentrations between 0.23 and 13.5 mgNO_3^--N/L.

The nitrate concentrations were measured for the unfiltered influent as well as the 0.45 µm-filtered effluent. If the nitrate concentration of the sample was believed to be above the upper limit of 13.5 mgNO_3^--N/L, the sample was diluted with deionised water. A 1 mL volume of the sample and 0.2 mL of *Solution A* (included in the *TNTplus™ 835* test kit) was pipetted into the test vial. The vial was inverted to ensure complete mixture and then left for 15 minutes to react. After the reaction time, the sample was analysed colorimetrically in the *DR3900 Benchtop Spectrophotometer* to obtain the nitrate concentration of the sample.

3.1.11.6 Nitrite concentration

The nitrite concentration was measured using the *DR3900 Benchtop Spectrophotometer* and the *TNTplus™ 840* test kits. This test kit measures nitrite concentrations ranging from 0.6 to 6 mgNO_2^--N/L accurately.

Since no nitrite was added to the influent, the nitrite concentration was only measured for the 0.45 µm-filtered effluent. The *TNTplus™ 840* test vials also contain a *DosiCap™ Zip* cap. After the seal for the upper part of the cap was removed, 0.2 mL of the sample was pipetted into the test vial. The cap was turned over and screwed onto the test vial. The test vial was

inverted until all the reagents were completely mixed. A period of 10 minutes was allowed for the reaction after which the sample was analysed with the *DR3900 Benchtop Spectrophotometer.* A reading representing the nitrite concentration of the sample was obtained.

3.1.11.7 SRP concentration

The soluble reactive phosphorus (SRP) for the influent and effluent was measured with the *DR3900 Benchtop Spectrophotometer* and the *TNTplus™ 845* test kits. These test kits allow for accurate measurement of samples containing SRP ranging from 2 to 20 mgPO_4^{3-}-P/L.

The SRP concentration was measured for the influent as well as the 0.45 µm-filtered effluent. A pipet was used to add 0.4 mL of the sample and 0.5 mL of *Solution B* (supplied with the test kit) into the test vial. The old cap of the vial was replaced with the grey *DosiCap™ C* (also supplied with the test kit). The test vial was inverted to ensure complete mixing. After the 10 minutes reaction time, the sample was analysed colorimetrically with the *DR3900 Benchtop Spectrophotometer.* A reading for the reactive phosphorus concentration of the sample was obtained.

3.1.11.8 Chlorophyll *a* concentration

Chlorophyll *a* is the photosynthetic pigment found in green plants. Chlorophyll *a* is commonly used to determine the concentration of algal biomass (Clesceri, et al., 1998).

The Chlorophyll *a* measurement was outsourced to the Stellenbosch Analytical Laboratory of the CSIR (Council for Scientific and Industrial Research).

3.1.11.9 VSS concentration

The volatile suspended solids (VSS) concentration provides and estimation of the amount of organic matter that is present in the solids suspended in a water media (Clesceri, et al., 1998).

The measurement of the VSS was also outsourced to the Stellenbosch Analytical Laboratory of the CSIR.

3.2 HRAP Model Development

The activated sludge and algae water quality models discussed in section 2.8 both include important biological processes that are present in an HRAP. A model for the HRAP was developed by combining the activated sludge model and the algal water quality model in a CMFR environment. This section discusses the procedures followed to combine these two models.

3.2.1 Model definition

In an HRAP system, there are several components, called state variables that influence the state of the system. A state variable is defined as a variable that describes the state of a

dynamic system. A perfect model would include all the state variables that could be associated with an HRAP. However, attempting to incorporate every conceivable state variable can make the model very complex and could likely incorporate more uncertainty.

The state variables that were selected for the HRAP model are shown in Table 3.3. All the state variables were chosen directly from the models described in section 2.8 with a few modifications. The substrate (S) of the activated sludge model and the dissolved organic carbon (c_d) of the algal water quality model represent the same component. These parameters were consequently combined to form a soluble biodegradable organics (c_s) parameter. The ammonia (n_a) and nitrate (n_i) concentrations of the two models were also combined.

Table 3.3 – State variables of the HRAP model

Parameter	**Symbol**	**Unit**
Ordinary Heterotopic Organisms	X_a	mgVSS/L
Ammonia Oxidising Organisms	X_n	mgVSS/L
Algae	a	mgChl$a$/L
Endogenous Residue	X_e	mgVSS/L
Dissolved Biodegradable Organics	c_d	mgCOD/L
Particulate Biodegradable Organics	c_p	mgCOD/L
SRP	p	mgP/L
Ammonia	n_a	mgN/L
Nitrate/Nitrite	n_i	mgN/L

It was decided to exclude substrate storage (see section 2.8.1.1 and 2.8.1.2) and zooplankton (see section 2.8.2.2) from the combined model. The exclusion of the substrate storage parameter makes the model overly responsive to rapid changes in the influent substrate concentration but should not affect the model accuracy when the model nears steady-state. The HRAP model is consequently not valid for rapidly varying influent flows and concentrations. Zooplankton were excluded from the computational model since there was no clear indication that it was present in the HRAP scale model. The assumption was made that zooplankton have negligible to no effect on the HRAP system.

Figure 3.7 depicts the biological interactions between the different state variables of the HRAP and includes the assumptions given above. Figure 3.7 shows only the relationships between the parameters that was included in the deterministic model. Various other parameters such as carbon dioxide and dissolved oxygen are also part of the biological processes shown in Figure 3.7 but were excluded from the deterministic model. These parameters were mainly excluded to maintain simplicity.

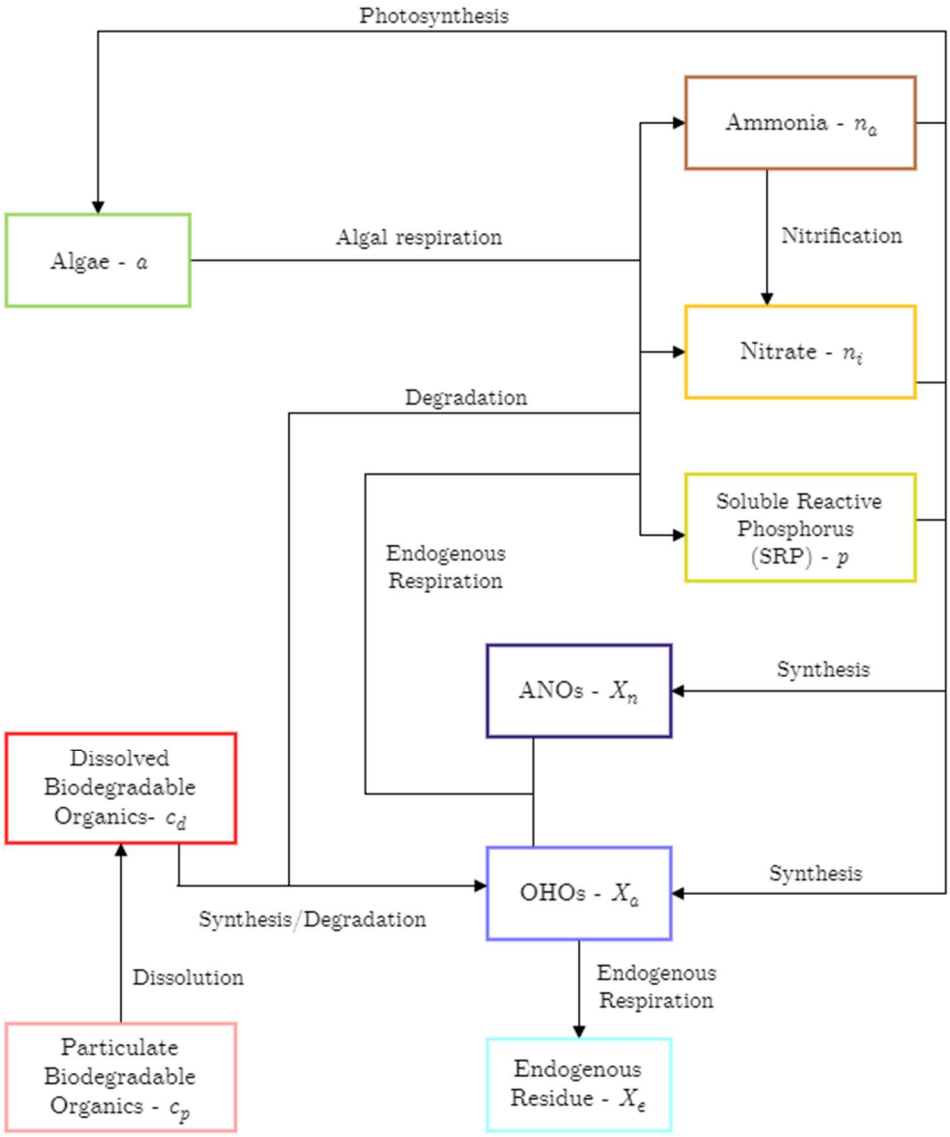

Figure 3.7 - Interactions between state variables

3.2.2 Modelling Equations

A CMFR (explained in section 2.7.2.3) approximation was used to develop the HRAP model. This section explains the combination of the biological equations of the two models of section 2.8 to develop a computational model for an HRAP. The computational model simulates the concentrations of the components in Table 3.3 over time, by solving the modelling equations developed in this section numerically through an iterative process.

Equations 3.1 to 3.9 were used through a numerical process where the concentration of a component at a certain time (t) is equal to the sum of the concentration at the end of the previous interval ($t - \Delta t$) and the change in concentration over that time interval. Equations 3.1 to 3.9 consequently assume that the concentration of a parameter changes linearly over a time interval. The smaller the time interval, the less significant this linear assumption is.

$$X_{a_t} = X_{a_{t-\Delta t}} + \Delta X_a \quad \text{Equation 3.1}$$

$$X_{n_t} = X_{n_{t-\Delta t}} + \Delta X_n \quad \text{Equation 3.2}$$

$$a_t = a_{t-\Delta t} + \Delta a \quad \text{Equation 3.3}$$

$$X_{e_t} = X_{e_{t-\Delta t}} + \Delta X_e \quad \text{Equation 3.4}$$

$$c_{d_t} = c_{d_{t-\Delta t}} + \Delta c_d \quad \text{Equation 3.5}$$

$$c_{p_t} = c_{p_{t-\Delta t}} + \Delta c_p \quad \text{Equation 3.6}$$

$$p_t = p_{t-\Delta t} + \Delta p \quad \text{Equation 3.7}$$

$$n_{a_t} = n_{a_{t-\Delta t}} + \Delta n_a \quad \text{Equation 3.8}$$

$$n_{i_t} = n_{i_{t-\Delta t}} + \Delta n_i \quad \text{Equation 3.9}$$

Each component has a mass balance equation that is used to determine the change in concentration over a time interval. The following sections look at the development of these mass balance equations from the equations in sections 2.7 and 2.8 as well as the incorporation of the mass balance equations into the computational HRAP model.

3.2.2.1 Ordinary Heterotrophic Organisms

Equation 3.10 is the mass balance equation that was used to represent the OHOs in the HRAP model. Equation 3.10 is a combination of Equation 2.16 and Equation 2.20 adjusted according to the CMFR principles of section 2.7.2.3.

$$V\frac{dX_a}{dt} = \frac{\mu_{Hm}(T)c_d}{K_S + c_d}X_a V - b_H(T)X_a V - QX_a \quad \text{Equation 3.10}$$

Where

Q = flow rate (L/d)

V = pond volume (L)

Since substrate storage was excluded from the model, the growth of the OHOs directly depends on the ambient substrate concentration. The endogenous respiration model was also preferred to the death regeneration model to represent the organism decay. This preference was due to simple nature of the endogenous respiration model with virtually no losses in model accuracy. The endogenous respiration model also has better-researched estimates of the applicable rates and constants. The last term of Equation 3.10 was also added to the account for the loss of OHO mass in the outflow. Under the CMFR assumption, the concentration in the outflow would be equal to the concentration within the reactor.

Equation 3.15 was developed to calculate the change in the OHO concentration over a time interval (ΔX_a) in the computational model. Equation 3.15 was derived from Equation 3.14 by applying the simplifications used in a numerical analysis.

$$\Delta X_a = \left[\frac{\mu_{Hm}(T)c_{d_{t-\Delta t}}}{K_S + c_{d_{t-\Delta t}}} X_{a_{t-\Delta t}} - b_H(T)X_{a_{t-\Delta t}} - \frac{Q_t}{V} X_{a_{t-\Delta t}}\right]\Delta t \qquad \text{Equation 3.11}$$

Where

ΔX_a = change in OHO concentration over the time interval (mgVSS/L)

$X_{a_{t-\Delta t}}$ = OHO concentration at the end of the previous interval (mgVSS/L)

$c_{d_{t-\Delta t}}$ = dissolved biodegradable organics concentration at the end of the previous interval (mgCOD/L)

Q_t = flow rate during the interval (L/d)

Δt = duration of the interval (days)

3.2.2.2 Ammonia Oxidising Organisms

The mass balance equation that represents the concentration of ANOs in the HRAP system is given by Equation 3.12. Equation 3.12 was developed by incorporating Equation 2.30 and Equation 2.34 into the CMFR mass balance equation (Equation 2.15).

$$V\frac{dX_n}{dt} = \frac{\mu_{Am}(T)n_a}{K_n(T) + n_a} X_n V - b_A(T)X_n V - QX_n \qquad \text{Equation 3.12}$$

Equation 3.12 includes the growth of ANOs on ammonia, the organisms' endogenous respiration as well as the mass loss due to organisms washed out from the CMFR system.

Equation 3.12 was then simplified to be functional in a computational model. Equation 3.13 is the result after all the simplifications were made.

$$\Delta X_n = \left[\frac{\mu_{Am}(T)n_{a_{t-\Delta t}}}{K_n(T) + n_{a_{t-\Delta t}}} X_{n_{t-\Delta t}} - b_A(T)X_{n_{t-\Delta t}} - \frac{Q_t}{V} X_{n_{t-\Delta t}}\right]\Delta t \qquad \text{Equation 3.13}$$

Where

ΔX_n = change in ANO concentration over the time interval (mgVSS/L)

$X_{n_{t-\Delta t}}$ = ANO concentration at the end of the previous interval (mgVSS/L)

$n_{a_{t-\Delta t}}$ = ammonia concentration at the end of the previous interval (mgN/L)

3.2.2.3 Algae

The algal mass balance equation given in Equation 2.39 was adjusted to be applicable for an HRAP system. Equation 3.14 represent the mass balance equation applicable to an HRAP system.

$$\frac{da}{dt} = k_{ga}(T, N, I)a - k_{rea}(T)a - \frac{Q}{V}a \qquad \text{Equation 3.14}$$

Equation 3.14 was developed by removing the terms for algal settling and zooplankton grazing from Equation 2.39. The settling terms were removed due of the assumption that completely mixed conditions exist in the HRAP. The term which accounts for zooplankton grazing was removed because of the exclusion of zooplankton from the model. An HRAP is also a continuous flow system. A term was therefore added to account for the changes in the algal concentration due to algal washout in the effluent.

The change in the algal concentration over a time interval (Δa) can be calculated with Equation 3.15. Equation 3.15 was derived from Equation 3.14 by applying the simplifications used in a numerical analysis.

$$\Delta a = \left[k_{ga}(T, N_{t-\Delta t}, I) - k_{rea}(T) - \frac{Q_t}{V}\right] a_{t-\Delta t} \Delta t \qquad \text{Equation 3.15}$$

Where

Δa = change in algal concentration over time interval (mgChla/L)

$a_{t-\Delta t}$ = algal concentration at the end of the previous interval (mgChl$a$/L)

$N_{t-\Delta t}$ = phosphorus, nitrogen and ammonia concentrations at the end of the previous interval (mg/L)

The algal growth rate (k_{ag}) and algal respiration rate (k_{ra}) are determined as explained in section 2.8.2.1. However, the calculation of the light extinction coefficient due to other factors than algae (k'_e) varies slightly from Equation 2.49 of section 2.8.2.1. Equation 3.16 shows how the light extinction coefficient due to non-algal suspended solids was calculated in the model. In the development of Equation 3.16, the assumption was made that apart from algae, only the OHOs, ANOs, endogenous residue and the particulate biodegradable organics contribute to the light absorption. It was also assumed that the non-volatile suspended solids concentration is negligible and would not contribute to the light extinction.

$$k'_e = k_{ew} + 0.174\left(X_{a_t} + X_{n_t} + X_{e_t} + \frac{c_{p_t}}{f_{cv}}\right) \qquad \text{Equation 3.16}$$

3.2.2.4 Endogenous Residue

The mass balance equation for the endogenous residue concentration in the HRAP system is given as Equation 3.17 and was developed from Equation 2.22. Equation 3.17 shows that the model only accounts for endogenous residue produced by the OHOs. The literature did not clearly state the quantities of endogenous residue produced by algae and ANOs. The algal models that were researched also did not incorporate endogenous residue (Chapra, 2008; Bowie, et al., 1985). It was therefore decided to only include the endogenous residue production from the OHOs which was well researched in the activated sludge models (Marais & Ekama, 1976; Ekama & Marais, 1977; Tchobanoglous, et al., 2003).

$$V\frac{dX_e}{dt} = f_H b_H(T) X_a V - QX_e \qquad \text{Equation 3.17}$$

Equation 3.18 was used to calculate the change in the endogenous residue concentration over a time step. Equation 3.18 was developed by simplifying Equation 3.17 with the purpose of incorporating it into the computational model.

$$\Delta X_e = \left[f_H b_H(T) X_{a_{t-\Delta t}} - \frac{Q_t}{V} X_{e_{t-\Delta t}} \right] \Delta t \qquad \text{Equation 3.18}$$

Where

ΔX_e = change in endogenous residue concentration during interval (mgVSS/L)

$X_{e_{t-\Delta t}}$ = endogenous residue concentration at the end of the previous interval (mgVSS/L)

3.2.2.5 Soluble Biodegradable Organics

The dissolved organic carbon parameter of the algal water quality model and the soluble substrate of the activated sludge model represent the same component, namely soluble biodegradable organics. Equation 2.56 of the algal water quality model was therefore combined with Equation 2.27 of the activated sludge model to form Equation 3.19. Equation 3.19 is the mass balance equation for the soluble biodegradable organics in the HRAP system.

$$V\frac{dc_d}{dt} = k_p c_p V - \frac{1}{Y_{Hv}} \frac{\mu_{Hm}(T) c_d}{K_S + c_d} X_a V + Q(c_{d_{in}} - c_d) \qquad \text{Equation 3.19}$$

Equation 3.19 includes terms for the dissolution of particulate biodegradable organics, the degradation of the soluble biodegradable organics by OHOs and the flow of mass in the influent and effluent.

In the development of Equation 3.19, the endogenous respiration model was applied for OHO, ANO, and algal respiration. In the endogenous respiration model, these organisms do not contribute to the soluble biodegradable organics concentration. It was assumed that all the organic carbon released during respiration is utilised by the organism for energy. Endogenous respiration can be accurately applied for OHOs and ANOs as discussed in sections 2.8.1.1.2 and 2.8.1.3.2. However, there is no evidence of the accuracy of the endogenous respiration model for algal respiration. The algal water quality model does not give a relationship between algal respiration and soluble biodegradable organics (Bowie, et al., 1985). It was consequently assumed that the endogenous respiration model can be accurately applied for algal respiration.

Equation 3.20 was then developed from Equation 3.19 by applying the simplifications necessary for a computational model. Equation 3.20 represents the change in the soluble biodegradable organic concentration over a time interval.

$$\Delta c_d = \left[k_p c_{p_{t-\Delta t}} - \frac{1}{Y_{Hv}} \frac{\mu_{Hm}(T) c_{d_{t-\Delta t}}}{K_S + c_{d_{t-\Delta t}}} X_{a_{t-\Delta t}} + \frac{Q_t}{V}(c_{d,in_t} - c_{d_{t-\Delta t}})\right] \Delta t \qquad \text{Equation 3.20}$$

Where

Δc_d = change in the soluble biodegradable organic concentration over a time interval (mgCOD/L)

$c_{d_{t-\Delta t}}$ = soluble biodegradable organic concentration at the end of the previous time step (mgCOD/L)

c_{d,in_t} = influent soluble biodegradable organic concentration during that time interval (mgCOD/L)

3.2.2.6 Particulate Biodegradable Organics

It was decided to include the particulate biodegradable organics in the computational model although the laboratory scale HRAP model did not receive any particulate organics. The kinetic regarding this variable were kept very simple. The mass balance equation, Equation 3.21, only includes mass increase due to the influent and the mass decrease due to outflow and dissolution. The dissolution process is approximated with a first order dissolution constant. Equation 3.21 was developed from Equation 2.15 and Equation 2.55.

$$V \frac{dc_p}{dt} = Q(c_{p,in} - c_p) - k_p c_p V \qquad \text{Equation 3.21}$$

As for soluble biodegradable organics, the application of the endogenous respiration model for algal, OHO and ANO respiration necessitate that the respiration of these organisms does not contribute to the particulate biodegradable organics concentration.

Equation 3.21 was rewritten in a computational form as Equation 3.22. Equation 3.22 was used to calculate the change in the concentration of the particulate biodegradable organics over a time step.

$$\Delta c_p = \left[\frac{Q_t}{V}\left(c_{p,in_t} - c_{p_{t-\Delta t}}\right) - k_p c_{p_{t-\Delta t}}\right] \Delta t \qquad \text{Equation 3.22}$$

Where

Δc_p = change in the particulate biodegradable organic concentration over a time interval (mgCOD/L)

$c_{p_{t-\Delta t}}$ = particulate biodegradable organic concentration at the end of the previous time step (mgCOD/L)

c_{p,in_t} = influent particulate biodegradable organic concentration during that time interval (mgCOD/L)

3.2.2.7 Ammonia

Equation 2.58 is the general mass balance equation for ammonia in microalgae environment as given by Chapra (2008). Ekama & Wentzel (2008b) gives Equation 2.36 for ammonia

utilisation by ANOs. Equation 2.58 and Equation 2.36 were combined into Equation 3.23 to form the mass balance equation applicable for ammonia in an HRAP system. In Equation 3.23 terms were also added for the ammonia uptake and release, due to the cell growth and respiration of OHOs and ANOs, as well as a term for ammonia release through the degradation of organics.

$$V\frac{dn_a}{dt} = a_{na}k_{ra}(T)Va - a_{na}F_{am}k_{ga}(T,N,I)Va + a_{nv}(1-f_H)b_H(T)X_aV - a_{nv}F_{am}\frac{\mu_{Hm}(T)c_d}{K_S+c_d}X_aV + a_{nv}b_A(T)X_nV - a_{nv}F_{am}\frac{\mu_{Am}(T)n_a}{K_n(T)+n_a}X_nV + f_{onc}\frac{1}{Y_{Hv}}\frac{\mu_{Hm}(T)c_d}{K_s+c_d}X_aV - \frac{1}{Y_A}\frac{\mu_{Am}(T)n_a}{K_n(T)+n_a}X_nV + Q(n_{a,in}-n_a)$$

Equation 3.23

Where

$n_{a,in}$ = ammonia concentration in the influent (mgN/L)

a_{nv} = the ratio of nitrogen to VSS in OHOs and ANOs (mgN/mgVSS)

f_{onc} = the ratio of organically bound nitrogen to COD in the influent biodegradable organics (mgN/mgCOD)

The following paragraphs explain the purpose of and the reasoning behind the different terms of Equation 3.23.

The first and second term of Equation 3.23 accounts for the ammonia release and uptake for algal respiration and growth as explained in section 2.8.2.4.2.

The third and fifth terms were added for ammonia release due to the endogenous respiration process of OHOs and ANOs. During endogenous respiration, these organisms oxidise their own mass to produce energy. For the ammonia mass balance to hold, ammonia should be released during this process in the same ratio that it was taken up in the growth process.

The fourth Equation 3.23 accounts for the accumulation of ammoniacal-N into the cell mass of the OHOs during the growth process. Between 9% and 12% of the dry mass of OHOs consist of nitrogen (Ekama & Wentzel, 2008b). Nitrogen should therefore be accumulated with the growth of OHOs. The fourth term represents the utilisation of ammonia due to the nitrogen requirements of OHO growth. The ammonia preference factor discussed in section 2.8.2.4.2 is also included in this term. It is assumed that the ammonia preference over nitrogen follows the same kinetics in OHO growth as in algal growth. The half-saturation concentration for ammonia preference is normally very low. This means that ammonia will almost exclusively be used for the nitrogen requirement until the ammonia concentration is almost zero. Thereafter nitrate will be used as the nitrogen source.

The sixth term of Equation 3.23 accounts for the ammoniacal-N accumulation during the growth of ANOs. ANOs are normally present in low concentrations due to the slow growth

rate. The literature therefore does not clearly state the cell composition of these organisms and they are normally classified with the OHOs. Due to the lack of knowledge about the cell composition of ANOs, the assumption was made that ANOs follow the same principles for ammoniacal-N accumulation as explained for OHOs in the previous paragraph.

The degradation of biodegradable organics by OHOs releases organically bound nitrogen in the form of ammonia. The seventh term of Equation 3.23 represents the release of ammonia due to the degradation of organically bound nitrogen.

The eighth term of Equation 3.23 represents the decrease of ammonia due to nitrification by ANOs. The second last and last terms account for the inflow and outflow of ammonia according to the assumptions of the CMFR.

Equation 3.23 was then modified to form Equation 3.24 which was used in the numerical calculation of the ammonia concentration in the HRAP model.

$$\begin{aligned}\Delta n_a = \Big[& a_{na} k_{ra}(T) a_{t-\Delta t} - a_{na} F_{am} k_{ag}(T, N_{t-\Delta t}, I) a_{t-\Delta t} \\ & + a_{nv}(1-f_H) b_H(T) X_{a_{t-\Delta t}} - a_{nv} F_{am} \frac{\mu_{Hm}(T) c_{d_{t-\Delta t}}}{K_S + c_{d_{t-\Delta t}}} X_{a_{t-\Delta t}} \\ & + a_{nv} b_A(T) X_{n_{t-\Delta t}} - a_{nv} F_{am} \frac{\mu_{Am}(T) n_{a_{t-\Delta t}}}{K_n(T) + n_{a_{t-\Delta t}}} X_{n_{t-\Delta t}} \\ & + f_{onc} \frac{1}{Y_{Hv}} \frac{\mu_{Hm}(T) c_{d_{t-\Delta t}}}{K_s + c_{d_{t-\Delta t}}} X_{a_{t-\Delta t}} - \frac{1}{Y_A} \frac{\mu_{Am}(T) n_{a_{t-\Delta t}}}{K_n(T) + n_{a_{t-\Delta t}}} X_{n_{t-\Delta t}} \\ & + \frac{Q_t}{V}\left(n_{a,in_t} - n_{a_{t-\Delta t}}\right) \Big] \Delta t\end{aligned} \qquad \text{Equation 3.24}$$

Where

Δn_a = change in ammonia concentration over the interval (mgN/L)

n_{a,in_t} = influent ammonia concentration during the interval (mgN/L)

$n_{a_{t-\Delta t}}$ = ammonia concentration at the end of the previous interval (mgN/L)

3.2.2.8 Nitrate

The mass balance equation for nitrate is a combination of Equation 2.6 and Equation 2.37 with terms added for the influent and effluent flux of nitrate and for the nitrate-N assimilation in OHOs and ANOs. Equation 3.25 subsequently forms the mass balance equation for nitrate applicable in an HRAP system.

$$\begin{aligned}V \frac{dn_i}{dt} = & \frac{1}{Y_A} \frac{\mu_{Am}(T) n_a}{K_n(T) + n_a} X_n V + Q\left(n_{i,in} - n_i\right) \\ & - a_{na}(1 - F_{am}) k_{ag}(T, N, I) V a \\ & - a_{nv}(1 - F_{am}) \frac{\mu_{Hm}(T) c_d}{K_S + c_d} X_a V \\ & - a_{nv}(1 - F_{am}) \frac{\mu_{Am}(T) n_a}{K_n(T) + n_a} X_n V\end{aligned} \qquad \text{Equation 3.25}$$

Where

$n_{i,in}$ = influent nitrate concentration (mgN/L)

Equation 3.26 was then derived from Equation 3.25 and used to numerically calculate the nitrate concentration in the computational HRAP model.

$$\begin{aligned}\Delta n_i = \Bigg[& \frac{1}{Y_A}\frac{\mu_{Am}(T) n_{a_{t-\Delta t}}}{K_n(T) + n_{a_{t-\Delta t}}} X_{n_{t-\Delta t}} + \frac{Q_t}{V}\left(n_{i,in_t} - n_{i_{t-\Delta t}}\right) \\ & - a_{na}(1 - F_{am}) k_{ag}(T, N_{t-\Delta t}, I) a_{t-\Delta t} \\ & - a_{nv}(1 - F_{am}) \frac{\mu_{Hm}(T) c_{d_{t-\Delta t}}}{K_S + c_{d_{t-\Delta t}}} X_{a_{t-\Delta t}} \\ & - a_{nv}(1 - F_{am}) \frac{\mu_{Am}(T) n_{a_{t-\Delta t}}}{K_n(T) + n_{a_{t-\Delta t}}} X_{n_{t-\Delta t}} \Bigg] \Delta t\end{aligned}$$

Equation 3.26

Where

Δn_i = change in nitrate concentration over the interval (mgN/L)

n_{i,in_t} = influent nitrate concentration during the interval (mgN/L)

$n_{i_{t-\Delta t}}$ = nitrate concentration at the end of the previous interval (mgN/L)

3.2.2.9 SRP

The general mass balance for SRP in the algal water quality model given in Equation 2.57 was also modified to be applicable for the HRAP system. Equation 3.27 represents the mass balance equation for SRP in the HRAP system.

$$\begin{aligned}V\frac{dp}{dt} = & a_{pa} k_{ra}(T) V a - a_{pa} k_{ag}(T, N, I) V a \\ & + a_{pv} b_H(T) X_a (1 - f_H) V - a_{pv} \frac{\mu_{Hm}(T) c_d}{K_S + c_d} X_a V \\ & + a_{pv} b_A(T) X_n V - a_{pv} \frac{\mu_{Am}(T) n_a}{K_n(T) + n_a} X_n V \\ & + f_{opc} \frac{1}{Y_{Hv}} \frac{\mu_{Hm}(T) c_d}{K_s + c_d} X_a V + Q(p_{in} - p)\end{aligned}$$

Equation 3.27

Where

p_{in} = influent SRP concentration (mgP/L)

a_{pv} = phosphorus to VSS ratio in OHOs and ANOs (mgP/mgVSS)

f_{opc} = organically bound phosphorus to COD ratio for the influent biodegradable organics (mgP/mgCOD)

Equation 3.27 is very similar to the mass balance equation for ammonia in Equation 3.23. Equation 3.27 also includes in its first six terms the SRP losses and gains due to the growth and respiration of algae, OHOs, and ANOs. These terms follow the same principles and assumptions as discussed in section 3.2.2.7 with the sole difference being the ratio in front of the terms that represents phosphorus to chlorophyll *a* and VSS instead of nitrogen. Also seen in the ammonia mass balance equation is the second to last term that represents the SRP

release due to the degradation of organically bound phosphorus, and the last term that accounts for the SRP flux in the influent and effluent.

Equation 3.28 was derived from Equation 3.27 to be applicable for the numerical calculation of the SRP concentration in the HRAP system.

$$\Delta p = \Big[a_{pa} k_{ra}(T) a_{t-\Delta t} - a_{pa} k_{ag}(T, N_{t-\Delta t}, I) a_{t-\Delta t} + a_{pv}(1 - f_H) b_H(T) X_{a_{t-\Delta t}} - a_{pv} \frac{\mu_{Hm}(T) c_{d_{t-\Delta t}}}{K_S + c_{d_{t-\Delta t}}} X_{a_{t-\Delta t}} + a_{pv} b_A(T) X_{n_{t-\Delta t}} - a_{pv} \frac{\mu_{Am}(T) n_{a_{t-\Delta t}}}{K_n(T) + n_{a_{t-\Delta t}}} X_{n_{t-\Delta t}} + f_{opc} \frac{1}{Y_{Hv}} \frac{\mu_{Hm}(T) c_{d_{t-\Delta t}}}{K_s + c_{d_{t-\Delta t}}} X_{a_{t-\Delta t}} + \frac{Q_t}{V} \left(p_{in_t} - p_{t-\Delta t} \right) \Big] \Delta t \quad \text{Equation 3.28}$$

Where

Δp = change in SRP concentration over the interval (mgP/L)

p_{in_t} = influent SRP concentration during the interval (mgP/L)

$p_{t-\Delta t}$ = SRP concentration at the end of the previous interval (mgP/L)

3.2.2.10 Volatile Suspended Solids

The Volatile Suspended Solids (VSS) was also calculated for each time interval during the simulation. The VSS concentration does not explicitly form part of the model described in Figure 3.7, but it was used to quantify the organisms included in the model into a measurable concentration.

The assumption was made that only the OHO, ANO, endogenous residue, algae, and particulate biodegradable organics concentrations would contribute to the VSS. In practice, there might be other components contributing to the VSS. However, the bulk of the VSS should always consist of the parameters given above.

The VSS concentration for each time interval was calculated by using Equation 3.29.

$$X_v = X_a + X_n + X_e + f_{va} a + \frac{c_p}{f_{cv}} \quad \text{Equation 3.29}$$

Where

f_{va} = ratio of VSS to algal biomass (mgVSS/mgChl$a$)

3.2.3 Typical Rates and Constants

The HRAP model is dependent on multiple stoichiometric constants and kinetic rates. Table A.1 in Appendix A contains all the rates and constants that are applicable to the HRAP model. Table A.1 also contains the typical ranges for all the applicable rates and constants as found in various literature. The values in Table A.1 were incorporated into the HRAP model and were used to calibrate the model with the measured results.

3.2.4 Model Assumptions

Various assumptions were made during the model development described in the previous paragraphs. The following list is a summary of all the assumptions that were made during the development of the HRAP model:

1. **Completely mixed conditions exist within the pond**. Observations during the laboratory experiment strongly suggested that this assumption was correct. The paddle wheel mixing and the turbulent flow conditions in the experimental HRAP ensured effective mixing for soluble compounds and suspended particulates. Settling was observed for larger solids but periodic manual stirring ensured the resuspension of these solids. In practice, the resuspension of larger solids can be done through periodic increases in the rotation speed of the paddle wheel.
2. **The dissolved carbon dioxide concentration does not limit the algal growth.** During the batch experiment, the dissolved carbon dioxide concentration exceeded the measuring method's upper limit of 100 mg/L on all six occasions when the dissolved carbon dioxide concentration was measured. This high dissolved carbon dioxide concentration most likely did not limit algal growth in the batch experiment, however, some sources suggest that carbon dioxide may become limiting in very dense algal cultures (Park, et al., 2011).
3. **The dissolved oxygen concentration does not limit the growth of Ordinary Heterotrophic Organisms (OHOs) and Ammonia Oxidising Organisms (ANOs).** This should generally be correct for most HRAPs. Due to the intense algal photosynthesis in these ponds, oxygen levels are generally above the saturation level. The average dissolved oxygen concentration from 40 measurements during the batch experiment was 9.9 mg/L. This is a very high dissolved oxygen concentration as it is approximately equal to the saturation concentration for water.
4. **Ammonia volatilisation and phosphate precipitation are negligible.** The simulations with the deterministic model showed no indications of significant ammonia volatilisation during the laboratory experiments. However, it is discussed in section 4.2.5 that there were strong indications of phosphate precipitation. The assumption of negligible phosphate precipitation is unsubstantiated.
5. **The endogenous respiration model can be applied for algal and ANO respiration.** The model underestimated the effluent COD concentrations. A reason for this COD estimation may be due to the application of the endogenous respiration model to algae.
6. **Zooplankton are not present in the system.** Regular visual inspections showed no clear indications of the presence of zooplankton during the laboratory experiments. However, due to the microscopic size of certain zooplankton, this assumption could not be officially supported or negated.

7. **Evaporation losses are negligible.** Rapid evaporation was experienced during the batch operation. It was therefore required to adjust the measured concentrations for evaporation. However, in practice, evaporation losses should be less significant.
8. **There are no rapid variations in the influent.** The influent was controlled during the laboratory experiment to ensure adherence to this assumption.
9. **Only OHOs produce endogenous residue.** The model underestimated the VSS concentration. Endogenous residue contributes to the VSS concentration. The exclusion of algae and ANO endogenous residue may be a reason for the VSS underestimation.
10. **Ammonia preference is the same for algae, OHOs, and ANOs.** The computational modelling of the laboratory experiments suggested that this assumption was valid. However, due to a lack of experimental results, this assumption could not be officially supported or negated.
11. **There is always enough nitrogen and phosphorus available for OHO and ANO cell accumulation.** This assumption was necessary since the growth equations of OHOs and ANOs do not include nutrient limitations.
12. **OHOs and ANOs have the same cell compositions.** This assumption could not be supported or negated. However, due to the relatively low biomass production of ANOs, this assumption did not have a significant influence on the results obtained from the simulations.
13. **Ammonia Oxidising Organisms (ANOs), rather than Nitrite Oxidising Organisms (NNOs), are limiting in nitrification.** This assumption is required by the activated model (see section 2.8.1.3).
14. **Only algae, OHOs, ANOs, endogenous residue and the particulate biodegradable organics contribute to the light absorption.** An actual HRAP should have additional suspended solids that contribute to light absorption besides those mentioned in the assumption. However, it is believed that the algae, OHOs, ANOs, endogenous residue and particulate biodegradable organics would contribute to the bulk of the suspended solids.
15. **The temperature, maximum solar intensity and day-night period are assumed to be constant throughout the simulation period.** Although these parameters were not constant throughout the experiments, a representative average was calculated as an input parameter for the computational model as shown in section 4.2.2.

3.2.5 Model Implementation

The HRAP model described in the previous sections was implemented in Microsoft Excel (version 2013, Microsoft Corporation ©) [Computer Software] together with Microsoft Visual Basics for Applications (VBA) (version 7.1, Microsoft Corporation ©) [Computer Software].

Microsoft Excel served as the interface. The modelling equations and executing methods were programmed with VBA.

3.2.5.1 Model Interface

The model interface consists of six different sections: "Simulation Setup", "Rates and Constants", "Influent data", "Measured values", "Chart" and "Values". The "Simulation Setup", "Rates and Constants", "Influent data" and "Measured data" are used by the user to define the different parameters of the simulation, and the "Chart" and "Values" sections display the outcome of the simulation.

3.2.5.1.1 Simulation Setup

The first section, Simulation Setup, allows the user to define the physical characteristics of the HRAP, the environmental conditions of the pond, the initial conditions, and the variables that must be displayed on the chart. This section also includes the button that the user should press in order to start the simulation. The simulation setup interface is shown in Figure 3.8.

In this section, the user must also provide the required time step. The time step defines the length of a time interval during the numerical calculations. A smaller time step gives results that are more accurate but the calculation time is longer.

General Variables

Pond Volume (V)	938.6	L	Time step	20	min
Pond depth (d)	0.28	m	Time step	0.013889	days
Tempertature	18.0	°C			
I_m	70.0	W/m2			
f_{Id}	0.667				

Initial Conditions

X_{ai}	7.6	mgVSS/L	c_{pi}	0.0	mgCOD/L
X_{ni}	0.030	mgVSS/L	p_i	9.1	mgP/L
a_i	0.250	mgChl*a*/L	n_{ai}	3	
X_{ei}	0.1	mgVSS/L	n_{ii}	15	
c_{di}	60.0	mgCOD/L			

Chart Setup

☐ Ordinary Heterotrophic Organisms	☐ Measured Chlorophyll a
☐ Ammonia Oxidising Organisms	☑ Measured SCOD
☐ Algae	☑ Measured SRP
☐ Endoginous Residue	☑ Measured Ammonia
☑ Soluble BCOD	☑ Measured Nitrate
☐ Particulate BCOD	☐ Measured VSS
☑ SRP	☑ Influent SCOD
☑ Ammonia	☐ Influent SRP
☑ Nitrate	☐ Influent Ammonia
☐ VSS	☐ Influent Nitrate

Calculate Model

Figure 3.8 - Model Interface: Simulation Setup

3.2.5.1.2 Rates and Constants

The second section of the model interface is the "Rates and Constants" section. This section allows the user to define all the rates and constants required for the modelling equations of section 3.2.2. The literature recommended values of these rates and constants are given in Table A.1. The Rates and Constants section are shown in Figure 3.9.

Stoichiometric Constants					
Influnet:					
f_{onc}	0	mgN/mgCOD			
f_{opc}	0	mgN/mgCOD			
OHOs, ANOs, PBCOD:			**Algae:**		
f_{cv}	1.48	mgCOD/mgVSS	f_{va}	75	mgVSS/mgChla
a_{nv}	0.12	mgN/mgAVSS	a_{na}	15	mgN/mgChla
a_{pv}	0.03	mgP/mgAVSS	a_{pa}	1	mgP/mgChla
Ordinary Heterotrophic Organisms					
Rates			**Constants**		
$\mu_{Hm,20}$	3	/d	K_s	80	mgCOD/L
Θ_{gXa}	1.07		Y_{Hv}	0.45	mgAVSS/mgCOD
$b_{H,20}$	0.24	/d	f_H	0.2	mgVSS/mgAVSS
Θ_{rXa}	1.03		K_{sam}	0.025	mgNH4-N/L
Ammonia Oxidising Organisms					
Rates			**Constants**		
$\mu_{Am,20}$	0.2	/d	$K_{n,20}$	0.74	mgN/L
Θ_{gXn}	1.07		Θ_{Kn}	1.05	
$b_{A,20}$	0.04	/d	Y_A	0.12	mgVSS/mgN
Θ_{rXn}	1.04		K_{sam}	0.025	mgNH4-N/L
Algae					
Rates			**Constants**		
$k_{ga,20}$	2.5	/d	K_{sp}	0.03	mgP/L
Θ_{ga}	1.066		K_{sn}	0.025	mgN/L
$k_{rea,20}$	0.1	/d	K_{sam}	0.025	mgNH4-N/L
Θ_{rea}	1.08		I_s	170	W/m2
			k_{ew}	0.04	m-1
Particulate BCOD					
Rates			**Constants**		
k_p	0.1	/d			

Figure 3.9 - Model Interface: Rates and Constants

3.2.5.1.3 Influent Data

The "Influent Data" section is used to define the inflow rate and influent concentration at various times. The data is captured in a tabulated form as shown in Figure 3.10. The model uses this influent data in a stepwise manner during the calculations. This means that the flow rate and concentrations from one date are used until the next date is reached. The model stops the simulation at the last date.

Date	Q (L/day)	P (mgP/L)	N_a (mgN/L)	N_i (mgN/L)	SCOD (mgCOD/L)	PCOD (mgCOD/L)
13-04-2016 09:39	242.7	9.35	7.33	14.33	81.66	0
15-04-2016 10:38	242.7	10.91	8.04	15.41	83.11	0
19-04-2016 09:53	242.7	9.49	6.62	12.58	77.78	0
26-04-2016 09:39	242.7	10.73	8.04	15.8	86.68	0
03-05-2016 09:52	242.7	10.47	8.06	15.7	85.48	0
10-05-2016 16:10	242.7	9.1	6.89	13.24	73.28	0
11-05-2016 10:20	0.0	0	0	0	0	0

Figure 3.10 - Model Interface: Influent data

3.2.5.1.4 Measured Values

The values that were measured directly from the laboratory scale HRAP model, were captured in the Measured Values section. The values captured in this section can be plotted on the chart with the simulated values. This enables a comparison between the simulated and the measured concentrations. The measured concentrations were also captured in a tabulated format as shown in Figure 3.11.

Date	P (mgP/L)	N_a (mgN/L)	N_i (mgN/L)	Chl*a* (mgChl*a* /L)	COD (mgCOD/L)	VSS (mgVSS/L)	Nitrate (mgN/L)	Nitrite (mgN/L)
13-04-2016 09:39	9.37	3.86	13	0.085	60		13	
18-04-2016 12:15	9.01	3.02	12.9		25.5		12.9	
20-04-2016 08:44				0.089				
05-05-2016 14:40	8.75	1.32	13.3	0.103	21.8	27	13.3	
11-05-2016 09:54	8.88	1.56	13.2	0.046	18.8		13.2	

Figure 3.11 - Model Interface: Measured Values

3.2.5.1.5 Chart and Values

The last two sections display the results of the simulation to the user. The Chart section displays all the concentrations selected in the Simulation Setup on a graph. The graph is shown in Figure 3.12 but may vary depending on the concentrations that were chosen in the Simulation Setup. On Figure 3.12 one can see that a dotted line represents influent concentrations, a square marker represents a measured concentration and a solid line represents the simulated concentration.

The Values section contains all the values that were calculated during the simulation. These values are then used to plot the graph in the Chart section.

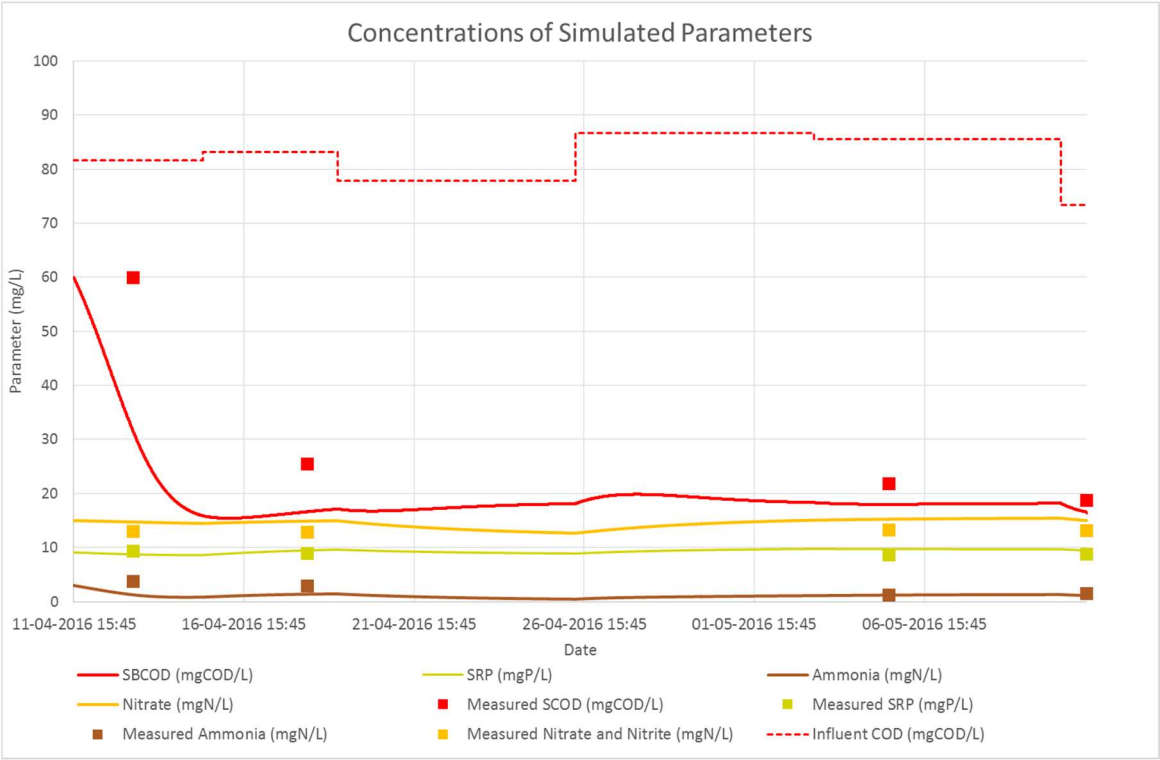

Figure 3.12 - Model Interface: Chart

3.2.5.2 Model Coding

The equations of section 3.2.2 were programmed in VBA with the use of repetitive structures. The full VBA code is given in Appendix H. A simplified extraction of the code is shown below. This extraction illustrates the repetitive structure, called a for-loop, which was used to calculate the concentration at each time interval. For example, if the time step was set as 20 minutes and the simulation was run for 10 days, the for-loop shown below would repeat 720 times. The number of times the for-loop executes, depends on the simulation time and the time step.

It is illustrated in the first part of the code extraction above how Equations 3.1 to 3.9 was implemented into the model. For example, Equation 3.1 is represented by the following line of code:

```
"Xa = Xa + Dynamic.ohoChange(Xaj, csj, currentRow)"
```

The second part of the code extraction stores the calculated concentrations in the "Values" section of the model interface.

```
For i = 1 To steps

        ***

        Xa = Xa + Dynamic.ohoChange(Xaj, csj, currentRow)
        Xn = Xn + Dynamic.anoChange(Xnj, amj, currentRow)
        a = a + Dynamic.algalChange(aj, Xaj, Xnj, Xerj, cpj, pj, amj + nij,
                                    currentRow)
        Xer = Xer + Dynamic.erChange(Xaj, Xerj, currentRow)
        cs = cs + Dynamic.sbCODchange(Xaj, csj, cpj, currentRow)
        cp = cp + Dynamic.pbCODchange(cpj, currentRow)
        p = p + Dynamic.srpChange(aj, pj, amj, nij, Xaj, Xnj, Xerj, cpj, csj,
                                  currentRow)
        am = am + Dynamic.ammoniaChange(aj, pj, amj, nij, Xaj, Xnj, Xerj, cpj,
                                        csj, currentRow)
        ni = ni + Dynamic.nitrateChange(aj, Xaj, Xnj, Xerj, pj, amj, nij, csj,
                                        cpj, currentRow)

        ***

        Sheet3.Cells(i + 2, 1).Value = ti + timeStep * i
        Sheet3.Cells(i + 2, 2).Value = Xa
        Sheet3.Cells(i + 2, 3).Value = Xn
        Sheet3.Cells(i + 2, 4).Value = a
        Sheet3.Cells(i + 2, 5).Value = Xer
        Sheet3.Cells(i + 2, 6).Value = cs
        Sheet3.Cells(i + 2, 7).Value = cp
        Sheet3.Cells(i + 2, 8).Value = p
        Sheet3.Cells(i + 2, 9).Value = am
        Sheet3.Cells(i + 2, 10).Value = ni
        Sheet3.Cells(i + 2, 11).Value = getVSS(Xa, Xn, Xer, a, cp)

Next i
```

*** - indicate that a portion of the code has been removed at that location

The first part of the code extraction above uses different methods to calculate the change in the concentration over each time interval. These methods incorporate the computational equations developed in section 3.2.2. For example, the "`Dynamic.ohoChange`" method is used to calculate the change in the OHO concentration over a time interval. This method is shown in the code extraction below. Equation 3.11 is represented in the code extraction below by the following line:

```
ohoChange = (Xa * kgx - Xa * krx - Q / V * Xa) * dt
```

Also shown in the code extraction below is that some calculations were broken down into further methods to make the code more efficient. For example, the calculation of the Monod growth limiting factor of Equation 3.11 was done in a separate method called "`ohoGrowthRate`". Each of the parameters included in the HRAP model has a similar method in which the change in concentration over a time interval is calculated.

```
Function ohoChange(Xa, cs, row) As Double

    Dim Q, V, dt, kgx, krx As Double

    dt = Sheet5.Range("t").Value
    Q = Dynamic.getFlow(row)
    V = Sheet5.Range("V").Value

    kgx = ohoGrowthRate(cs)
    krx = ohoRespirationRate()

    ohoChange = (Xa * kgx - Xa * krx - Q / V * Xa) * dt

End Function
```

3.2.5.3 Model instability

The computational model developed above is susceptible to instabilities and inaccuracies as with most numerical models. It was noted that modelling errors occurred as soon as a state variable approaches zero. If the time interval, over which the mass balance equations are solved, is too large, the variable approaching zero might adopt a negative value. If a negative value is calculated for one of the variables, all the remaining calculations will be incorrect. This instability in the model can be corrected by decreasing the duration of the time interval over which the mass balance equations are solved. The optimum time interval is dependent on numerous different input parameters and each simulation should be assessed individually. The model coding also tries to prevent negative values this by forcing the value of a variable to zero if a negative value is calculated. Although this results in better results, the recommended and most accurate method to eliminate the model instability is to reduce the duration of the time interval.

4 RESULTS AND DISCUSSIONS

The results obtained from the experimental HRAP were analysed and are discussed in the first part of this section. These results were then used to calibrate the computational HRAP model and this process is discussed in the second part of the section. In the last part of this section, the calibrated computational model was used to investigate the use of HRAPs for eutrophication prevention.

4.1 Experimental Results

Two different types of experiments were done on the laboratory scale HRAP, namely continuous experiments and batch experiments. During the continuous operation, the pond was fed with a constant influent in terms of flow and concentration, while the batch experiments had no inflow or outflow. The results obtained from these two types of experiments are discussed in this section.

4.1.1 Continuous Operation

The HRAP was first operated continuously with a hydraulic retention time (HRT) of 4 days for a duration of 28 days after which the HRT was increased to 10 days for a further duration of 34 days. The influent and effluent concentrations of each of these experiments were analysed in terms of nutrient and COD removal. Results were compared to gain insight into the differences in nutrient removal between short and long retention times.

4.1.1.1 Influent Concentrations

The system was set up to approximate the influent characteristics given in section 3.1.1. Table B.1 in Appendix B represents the measured influent concentrations for this experiment. Influent measurements were done each time the mixture of the synthetic wastewater was replaced. The values in Table B.1 were assumed to be reasonably accurate. The possibility exists that there were variations in the influent due to the inaccuracies of the peristaltic pump system, as well as possible premature biological activity in the refrigerated concentrate (see section 3.1.2 and 3.1.3).

4.1.1.2 Effluent Concentrations

Table B.2 in Appendix B shows concentrations that were periodically measured for the 0.45 µm filtered effluent. The samples were taken directly from the pond. It was initially assumed that the nitrite concentration would be negligible. Periodic nitrite measurements were planned to ensure the validity of this assumption. The first nitrite measurement on 26 March 2016 confirmed the assumption, but a subsequent nitrite measurement on 24 May 2016 contradicted it. It was then decided to measure the nitrite concentration in all of the subsequent samples as indicated in Table B.2.

4.1.1.3 Data Refining

Table B.1 and Table B.2 show measurements that are marked with an asterisk. These measurements were outside the recommended range of the applicable measurement method. To use this data for further calculations, the accuracy of these data points were analysed and the required adjustments were made. These adjustments are displayed in the following sections.

4.1.1.3.1 Nitrate Concentrations

The nitrate method discussed in section 3.1.11.5 had a recommended upper limit of 13.5 mgN/L. Dilution of the samples was therefore required if the nitrate concentration in the sample was deemed to be more than 13.5 mg/L. In four instances, indicated in Table 4.1, it was incorrectly assumed that dilution was not required. These measured nitrate concentrations were thus over the 13.5 mgN/L limit. The *DR3900 Benchtop Spectrophotometer* used in the experiments still gave a reading for the nitrate concentration but it also issued a warning indicating a larger margin of error for these readings.

In order to avoid inflated results, it was decided to adjust these values conservatively. It is known that the nitrate concentrations of these samples are larger than 13.5 mgN/L, but the extent of this exceedance is unknown. A conservative approach would consequently require the reduction of influent concentrations to 13.5 mgN/L, and keeping the effluent concentrations at the larger values as read by the *DR3900 Benchtop Spectrophotometer*. This approach ensured that the removal efficiencies (the difference between the influent and effluent concentrations) calculated in section 4.1.1.4.4, were not inflated. Table 4.1 indicates the adjustments that were made to the applicable nitrate concentrations.

Table 4.1 - Refinements made to nitrate measurements

Date Measured	**HRT**	**Influent/ Effluent**	**NO_3-N Concentration (mgN/L)**	
			Measured	**Adjusted**
15-04-2016	4	Influent	15.4*	**13.5**
26-04-2016	4	Influent	15.8*	**13.5**
03-05-2016	4	Influent	15.7*	**13.5**
18-05-2016	10	Effluent	14.9*	**14.9**

4.1.1.3.2 Ammonia Concentration

Table 4.2 illustrates the initial and adjusted ammonia measurements for samples that yielded ammonia concentrations below the recommended lower limit of 1 mgN/L for the *TNTplus™ 831* test kits described in section 3.1.11.4. Since all these measurements were done on the effluent, the conservative approach would entail changing all these concentrations to

1 mgN/L. However, in section 4.1.1.4.1 it is indicated that nitrification was present for the 10-day HRT. Measured ammonia concentrations were as low as 1.3 mgN/L (see Table B.2) for an HRT of 4 days with no evidence of nitrification. Changing the ammonia concentrations to 1 mgN/L in this case, would be too conservative and an inaccurate representation of the actual removal efficiencies would be obtained. It was therefore decided to keep the concentrations as read by the *DR3900 Benchtop Spectrophotometer* as illustrated in Table 4.2.

Table 4.2 - Refinements made to ammonia measurements

Date	**HRT (days)**	**Influent/ Effluent**	**NH4-N Concentration (mg/L)**	
			Initial	**Adjusted**
18-05-2016	10	Effluent	0.09*	**0.09**
24-05-2016	10	Effluent	0.1*	**0.1**
30-05-2016	10	Effluent	0.08*	**0.08**
03-06-2016	10	Effluent	0.15*	**0.15**
09-06-2016	10	Effluent	0.19*	**0.19**

4.1.1.4 Performance evaluation

4.1.1.4.1 Nitrification

Nitrification is the biological process in which ammonia is converted to nitrite and then nitrate. Nitrification is an important biological process of ammonia removal. Nitrification in the HRAP system can be detected by a decrease in the ammonia concentration coupled with an increase in the nitrate (or nitrite) concentration. Figure 4.1 is a graph of the influent and effluent ammonia, nitrate and nitrite concentrations for the HRAP operated with a 4-day HRT. The graph indicates a decrease in the ammonia concentration but no prominent increase in the nitrate concentrations. The single nitrite measurement in Figure 4.1 was done to confirm that the nitrite concentration in the system was negligible. It can therefore be concluded that there was no clear indication that nitrification was present in the experiment with a 4-day HRT. Instead, ammonia may have been removed through volatilisation or algae assimilation.

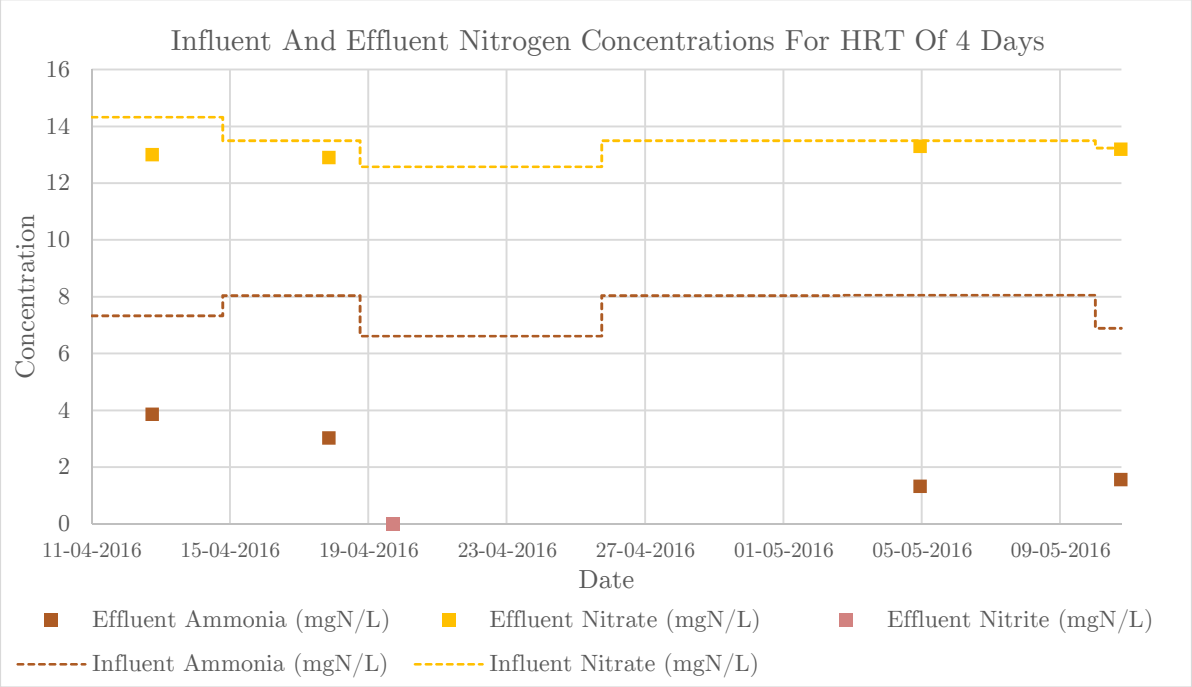

Figure 4.1 - Chart of influent and effluent nitrogen concentrations for HRT of 4 days

This, however, was not the case for the experiment with a 10-day HRT. Figure 4.2 contains a graph of the influent and effluent ammonia, nitrate and nitrite concentrations measured for the 10-day HRT. The large decrease in the influent ammonia concentration coupled with the increase in the nitrate and nitrite concentrations that can be seen in Figure 4.2, is a clear indication of nitrification. One can therefore safely conclude that nitrification was present in the HRAP for the operation with a 10-day HRT.

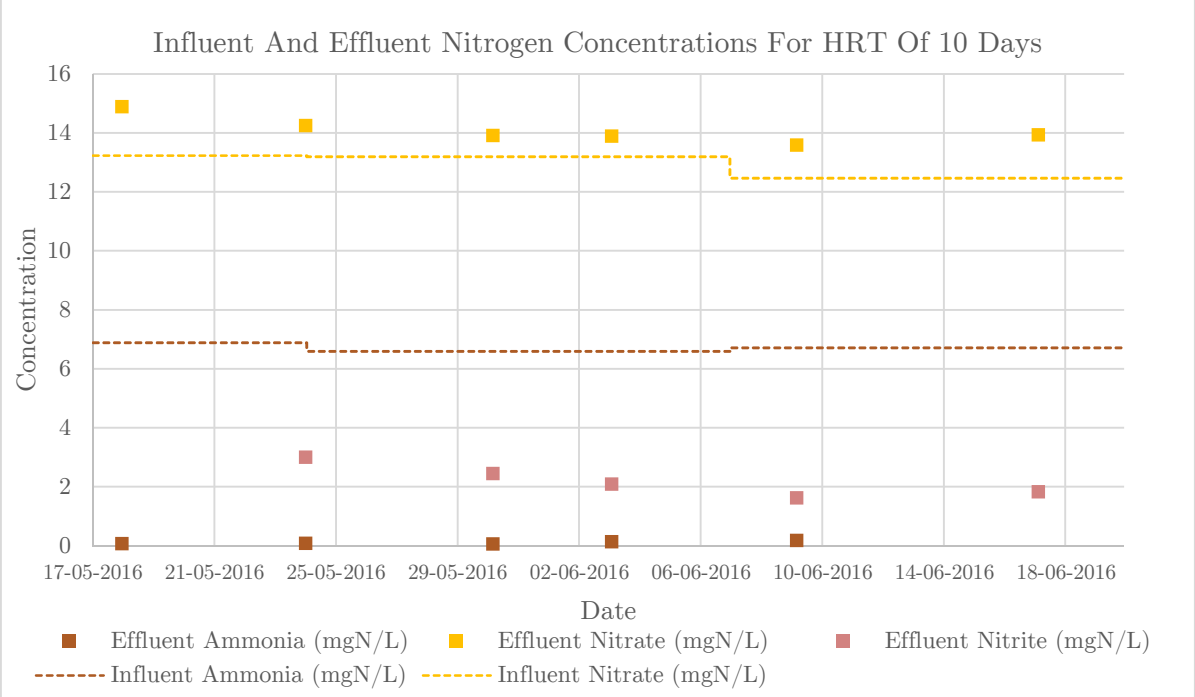

Figure 4.2 - Chart of influent and effluent nitrogen concentrations for HRT of 10 days

4.1.1.4.2 Nutrient Removal

The nutrient removal of the HRAP was evaluated by examining the influent and effluent concentrations of the SRP, ammonia and the Total Inorganic Nitrogen. Due to nitrification, it would not make sense to look at the nitrate and nitrite concentrations alone. The ammonia, nitrate, and nitrite concentrations were consequently summed to form a collective term called the Total Inorganic Nitrogen, which was used to determine the nitrogen removal.

The graph in Figure 4.3 shows the influent and effluent SRP, ammonia and Total Inorganic Nitrogen concentrations for the 4-day HRT. The graph shows that substantive ammonia removal was achieved. Phosphate removal was insignificant. The reduction in the Total Inorganic Nitrogen concentration was mostly due to the decrease in the ammonia concentration since almost no nitrate removal can be seen in Figure 4.1. Since no nitrification occurred, the decrease in the ammonia concentration was mostly due to assimilation into algal biomass and possibly through volatilisation. Ammonia was also assimilated into OHO biomass but the growth of these organisms is generally limited by a biodegradable carbon source. It is therefore believed that the ammonia assimilation by OHOs was insignificant compared to the assimilation by algae.

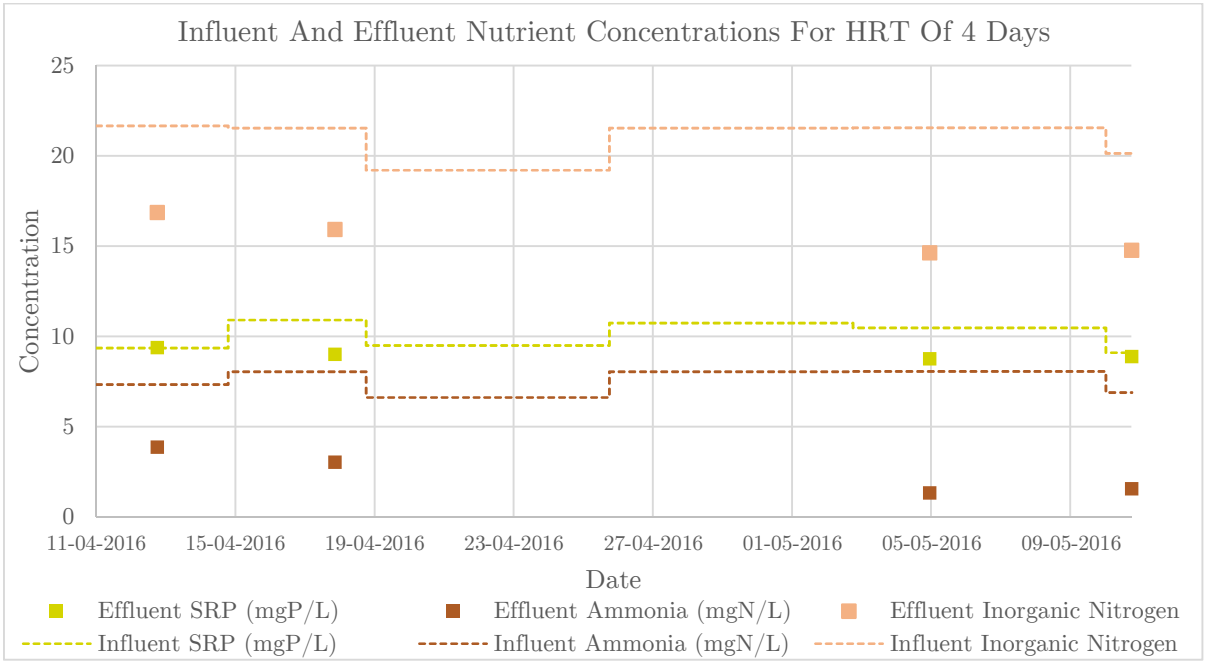

Figure 4.3 - Chart of influent and effluent nutrient concentrations (HRT = 4 days)

Figure 4.4 contains a graph of the influent and effluent nutrient concentrations for the HRAP operated with a 10-day HRT. The longer HRT should theoretically have much lower effluent concentrations since the algae would have more time to assimilate nutrients. This was the case for ammonia with effluent concentrations close to zero as shown in Figure 4.4. This ammonia decrease was due to a combination of nitrification and assimilation. In the case of SRP and the Total Inorganic Nitrogen, the effluent concentrations for the 10-day HRT seem very similar and possibly higher than for a 4-day HRT. This is investigated further in section 4.1.1.4.4.

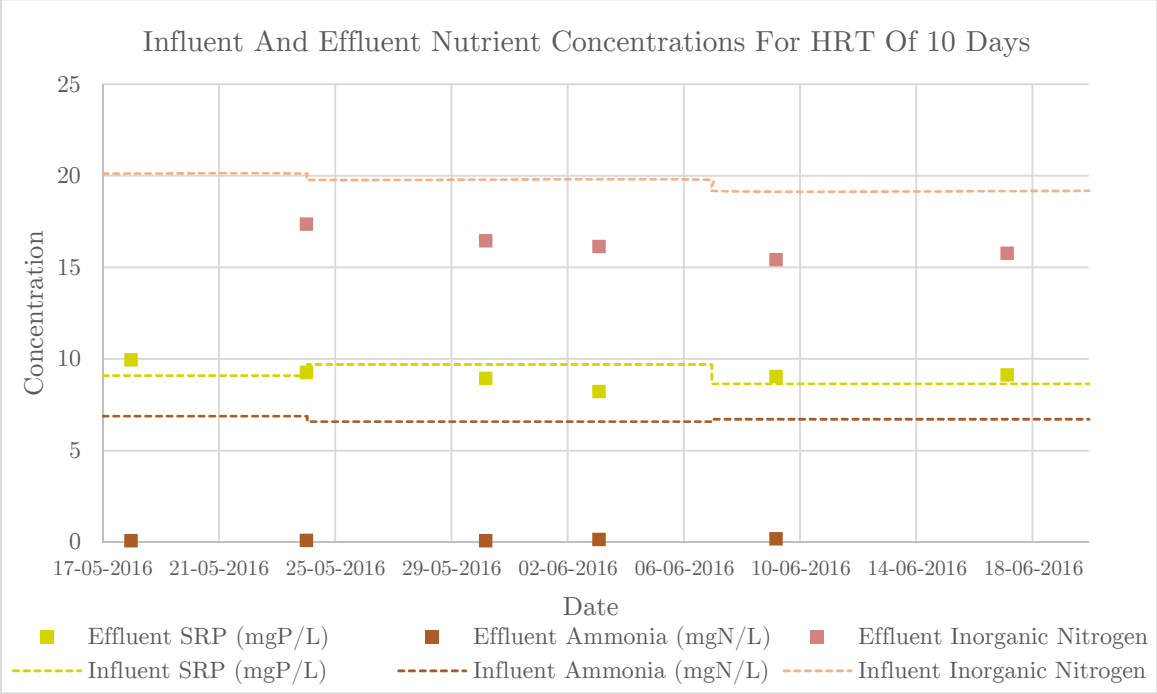

Figure 4.4 - Chart of influent and effluent nutrient concentrations (HRT = 10 days)

4.1.1.4.3 COD Removal

Figure 4.5 and Figure 4.6 show the influent and effluent COD concentrations for the HRAP operated with a 4-day HRT and a 10-day HRT. The charts show similar effluent concentrations for both HRTs with the exception of the high effluent COD concentration (60 mgCOD/L) measured on 13 April 2016 (shown in Figure 4.5 and Table B.1). This measurement was done before the OHO concentration reached steady-state. The OHO concentration was therefore relatively low, which resulted in a higher effluent COD concentration.

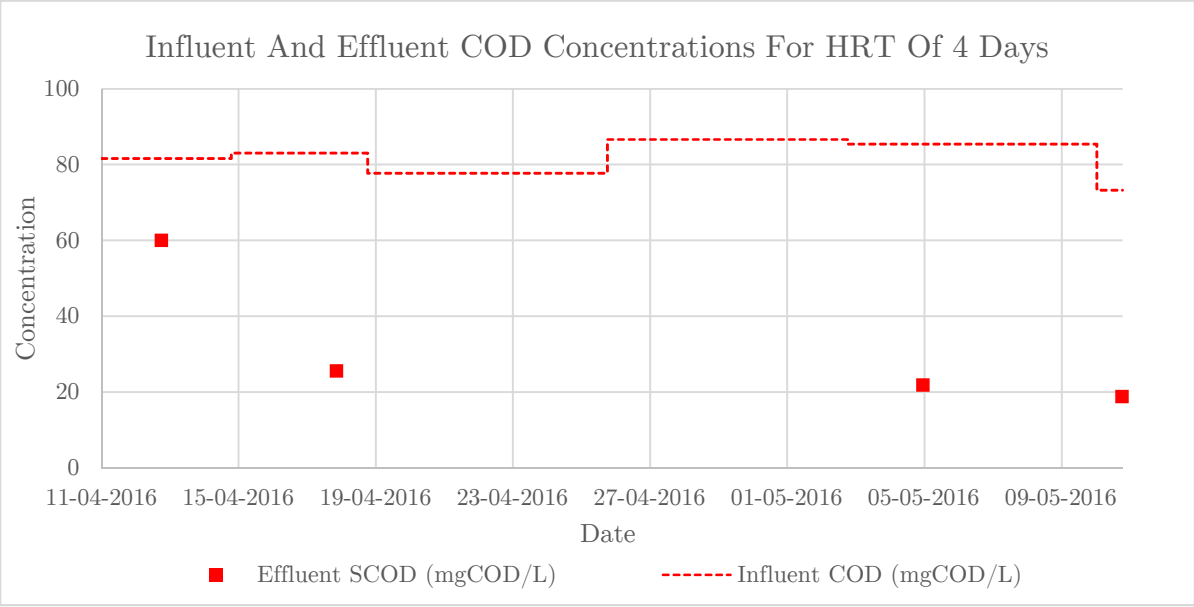

Figure 4.5 - Chart of influent and effluent COD concentrations for a 4-day HRT

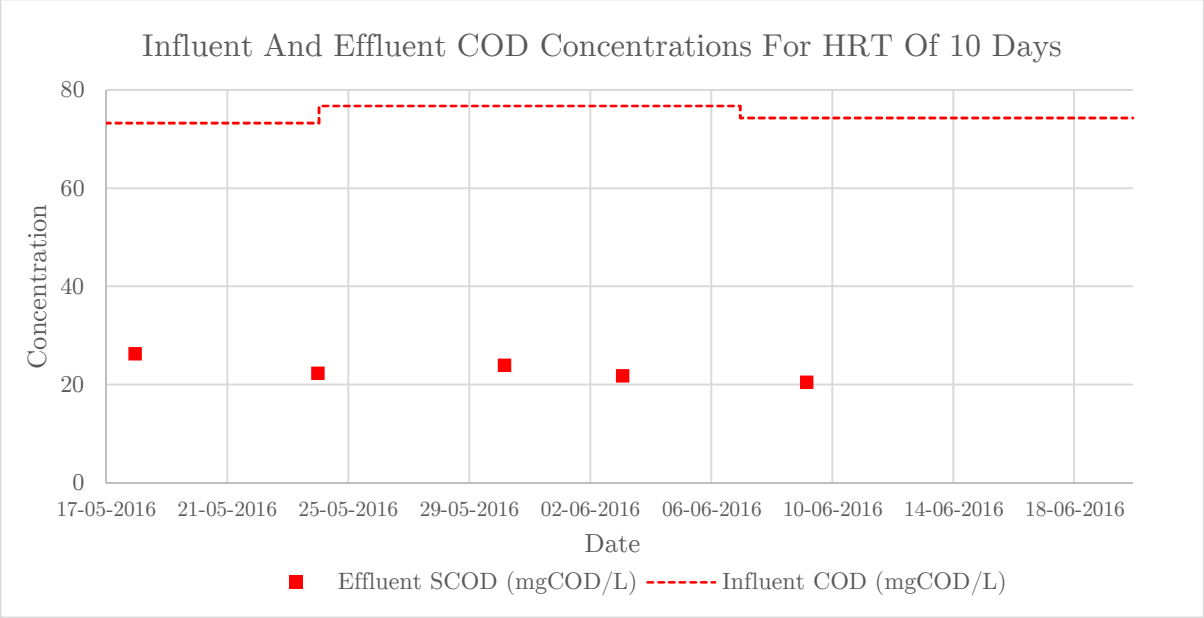

Figure 4.6 - Chart of influent and effluent COD concentrations for a 10-day HRT

4.1.1.4.4 Removal Efficiencies

The measured concentrations shown in Table B.1 and Table B.2 together with the adjustments of Table 4.1 and Table 4.2 were used to determine the average percentage nutrient and COD removal achieved in the HRAP for a 4-day and a for a 10-day HRT. These removal efficiencies are illustrated in Figure 4.7. The removal efficiencies were calculated as the percentage difference between a weighted average of the measured influent and effluent concentrations. The weighted averages were calculated by weighing each measured influent and effluent concentration with a representative portion of the operational period.

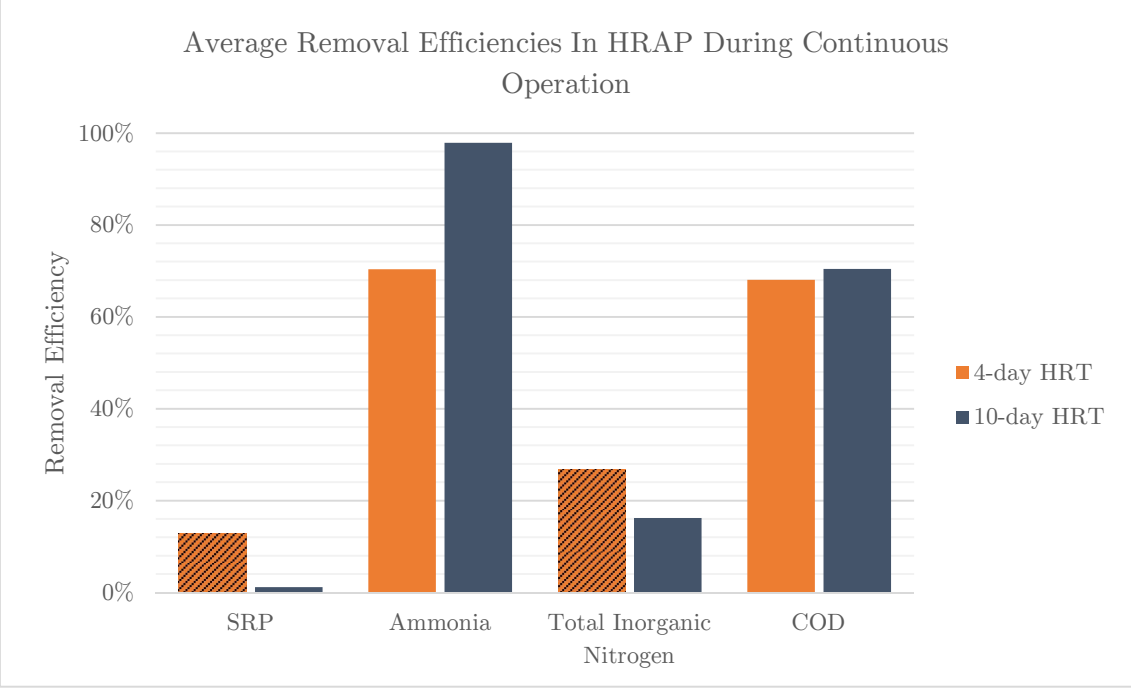

Figure 4.7 - Average removal efficiencies in the HRAP during continuous operation

The following paragraphs discuss each of the parameters shown in Figure 4.7 separately.

SRP:

As mentioned previously, one would expect better nutrient removal capabilities with a longer HRT. This was not the case for the SRP removal. However, the results obtained from the experiment may be misleading due to the reasons discussed below.

The peristaltic pumps used for the 4-day HRT had a much higher flow variation than the pumps used for the 10-day HRT. This difference in pump accuracy between the two experiments may have contributed to the unexpected results.

Periodic pH measurements were done during the experiment. During the 4-day HRT operation period, unusually low pH measurements were observed. The initial justification was that the rapid algal respiration during the night initialised a pH drop to below a self-recoverable level. Sodium hydroxide was added in an attempt to correct this pH "crash". However, upon further investigation, it was discovered that the pH meter was faulty and that the pond's pH was in fact normal (approximately 7). The addition of sodium hydroxide consequently caused a sharp rise in the pond's pH. This elevated pH may have caused the phosphate to precipitate as a solid compound. The higher phosphate removal observed during the 4-day HRT operation was therefore possibly due to phosphate precipitation caused by sodium hydroxide addition. The phosphate removal observed during the 10-day HRT is a better indication of the phosphate removal due to algal assimilation. This increase in SRP removal due to precipitation gives an indication of the effectiveness of SRP removal due to this mechanism. The assumption in the computational model that SRP precipitation is negligible, may consequently cause the model to underestimate the SRP removal.

Ammonia:

In the case of ammonia removal, the longer HRT obtained a better removal efficiency. This was mostly due to the presence of nitrification at a 10-day HRT. Figure 4.7 also shows that the HRAP was very effective in ammonia removal even with a relatively short retention time. As mentioned earlier, the ammonia removal processes were nitrification and assimilation. It was accepted that most of the ammonia assimilation was due to algal growth since the growth of OHOs was presumably limited by a biodegradable carbon source.

Total Inorganic Nitrogen:

The Total Inorganic Nitrogen removal observed for a 4-day HRT was higher than for a 10-day HRT. However, despite the difference in the accuracy of the peristaltic pumps mentioned earlier, there are two more points to consider when comparing these removal efficiencies.

The Total Inorganic Nitrogen removal calculated in Figure 4.7 for the HRT of 4 days is possibly an overestimation, since only one nitrite measurement was done. The notable reduction in the effluent ammonia concentration shown in Figure 4.3 could be an indication that partial nitrification occurred towards the end of the 4-day HRT operation period. This

however could not be confirmed due to the lack of nitrite measurements. It is therefore possible that the actual effluent Total Inorganic Nitrogen concentrations for a 4-day HRT might have been higher than Figure 4.3 suggests.

Another point to consider is that the 4-day HRT (weighted average of 7.6 mgN/L) had a higher influent ammonia concentration than the 10-day HRT (weighted average of 6.7 mgN/L). It was previously concluded that the HRAP is effective in terms of ammonia removal. The higher influent ammonia concentration, as well as the absence of nitrification, meant that more ammonia was available for assimilation during the 4-day HRT. Since ammonia was removed more effectively than nitrate or nitrite, a higher influent ammonia concentration could possibly suggest a higher Total Inorganic Nitrogen removal despite the shorter HRT.

Consequently, the Total Inorganic Nitrogen removal of Figure 4.7 is most likely misleading, due to the absence of nitrite measurements and due to the difference in the influent ammonia concentrations. However, it can be concluded that there is a clear indication in Figure 4.1, Figure 4.2 and Figure 4.7 that the algae strongly favour ammonia over nitrate and nitrite.

COD:

Figure 4.7 also indicated that both retention times had very similar COD removal efficiencies. This was expected since OHOs are fast growing organisms. The HRTs of 4 days and 10 days used in this experiment, should be more than sufficient to allow the complete depletion of the biologically available COD concentrations under normal operating conditions.

4.1.2 Batch Operation

The continuous experiment was followed by a batch experiment that was operated for a duration of 38 days. The aim of the batch experiment was to eliminate the inaccuracies in the flow rates produced by the peristaltic pump system. The resultant data were used to accurately determine the nutrient assimilation capabilities of the algae. In this section, the data obtained from the batch experiment are discussed and analysed.

4.1.2.1 Evaporation Correction

Since there was no inflow during the batch experiment, the water level continuously lowered due to evaporation. The pond had an unusually high average evaporation rate due to the artificial lighting and the heaters. The evaporation rate was approximately 3.9 mm/day. Tap water was periodically added to compensate for the evaporation losses. The evaporation was monitored through regular measurement of the water level. The changes in the pond water level due to evaporation can be seen in Figure 4.8. A water level of 288 mm represents a full pond with zero evaporation losses. The periodic additions of tap water can also be seen in Figure 4.8 with rapid rises in the water level. Note the scale of the chart in Figure 4.8 otherwise the evaporation losses might seem much higher than it was.

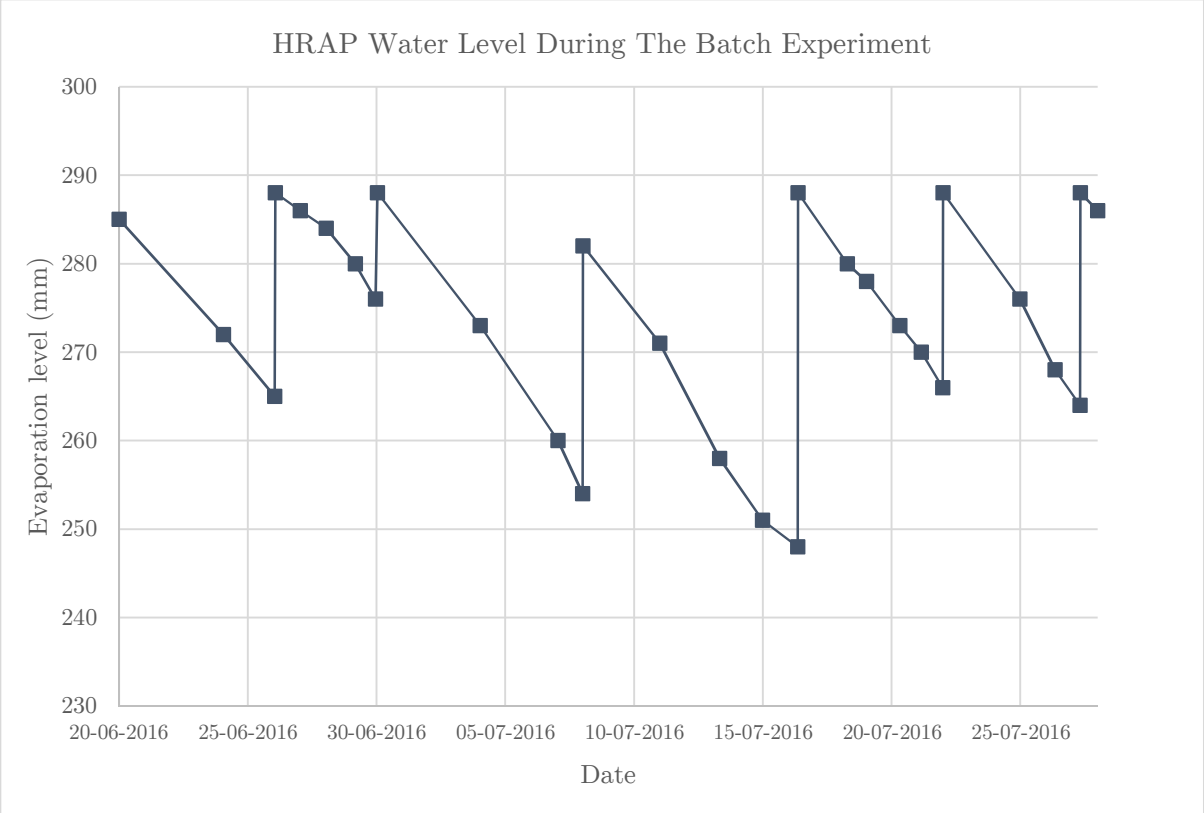

Figure 4.8 - HRAP water level during the batch experiment

The evaporation of water also meant that all the substances and organisms in the HRAP became more concentrated as the water level dropped. A lower water level meant that a substance was dissolved in a smaller volume of water which resulted in an increased concentration. The evaporation data of Figure 4.8 was used to apply corrections to the measured concentration for evaporation losses. These corrections were necessary to compensate for the effect of the unusually high evaporation rate. Since the area of the HRAP was constant over the depth, the measured concentrations were corrected by only using the water levels as shown in Equation 4.1.

$$c_{adjusted} = c_m \cdot \frac{WL_m}{WL_{full}} \qquad \text{Equation 4.1}$$

Where

$c_{adjusted}$	=	concentration of substance after evaporation correction was applied (mg/L)
c_m	=	concentration of substance as measured (mg/L)
WL_m	=	water level when the sample was taken for measurement (mm)
WL_{full}	=	water level when the HRAP is full (288 mm)

4.1.2.2 Measured Concentrations

Frequent measurements were done on the parameters of concern during the batch experiment. All of these measurements were done on 0.45 µm filtered samples. The samples were filtered

to remove the suspended solids. The measurement therefore only included the soluble concentrations. The COD and nutrients captured in solids were considered to be removed since the solids can be removed from the system through settling. The concentrations shown in this section are already corrected for evaporation. Table C.1 and Table C.2 in Appendix C contain measured and evaporation corrected concentrations.

4.1.2.2.1 Soluble Reactive Phosphorus (SRP)

The chart in Figure 4.9 contains the measured SRP concentrations for the batch experiment. It clearly shows a decrease in the SRP concentration over the duration of the experiment. A total of 22.7% SRP removal was achieved during the experiment. This SRP reduction was achieved over a period of 38 days with an average SRP removal rate of 63.9 µg/day. The SRP removal achieved during the operation was considered to be poor, especially if one takes the long operation period into account. However, the algal growth in this experiment may have been limited due to a lack of high-intensity sunlight. The SRP removal capabilities could conceivably improve for a pond in direct sunlight.

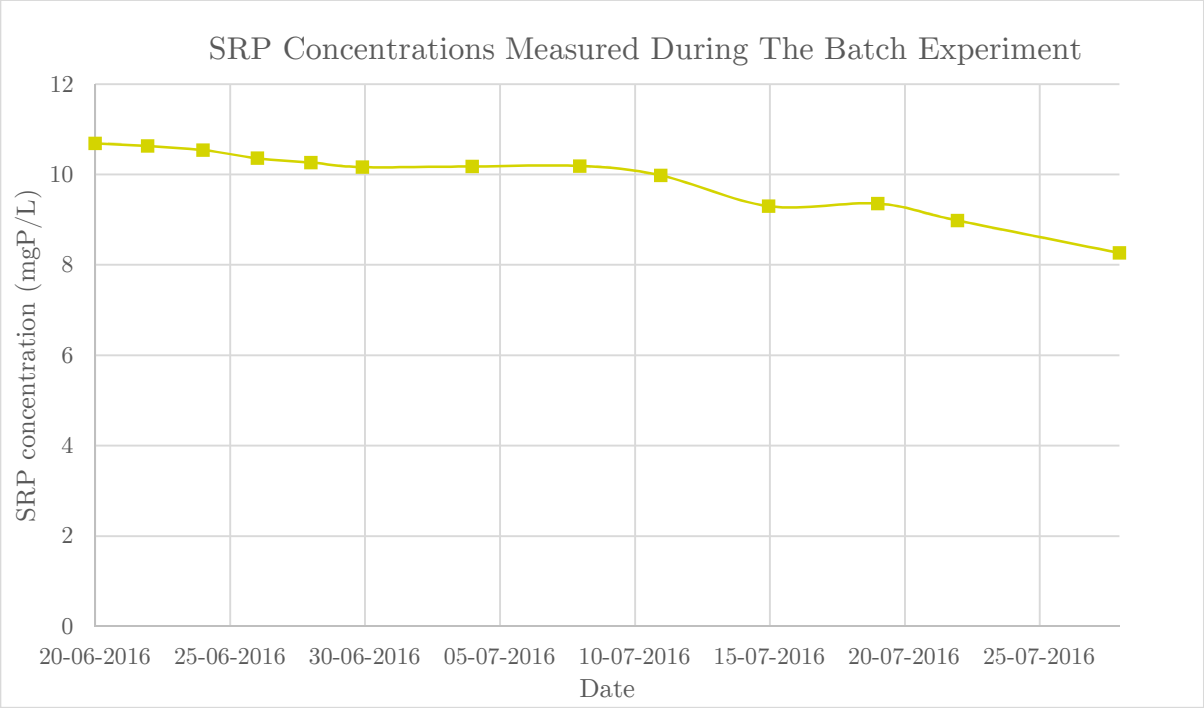

Figure 4.9 - Chart of SRP concentrations measured during the batch experiment

4.1.2.2.2 Nitrogen

The chart in Figure 4.10 shows the concentrations that were measured for ammonia, nitrate, nitrite and Total Inorganic Nitrogen during the batch experiment. There was a 99.7% reduction in the ammonia concentration and a 19.8% reduction in the Total Inorganic Nitrogen concentration during this experiment. The decrease in the Total Inorganic Nitrogen concentration was believed to be mainly due to nitrogen assimilation into algal biomass. As

with the SRP removal, the Total Inorganic Nitrogen removal over the duration of the experiment was modest. The average nitrogen removal rate was 122.4 µN/L.

The chart in Figure 4.10 also shows that nitrification of ammonia occurred during the experiment. The initial increase in the nitrite concentration reveals that the ammonia was not fully nitrified for the first part of the experiment. However, between 11 and 15 July, there was a sudden reduction in the nitrite concentration and a subsequent increase in the nitrate concentration. At this stage, an unknown catalyst possibly caused a rapid growth in the nitrite oxidising organisms (NNOs) mentioned in section 2.8.1.3. The NNOs then oxidised all the nitrite into nitrate.

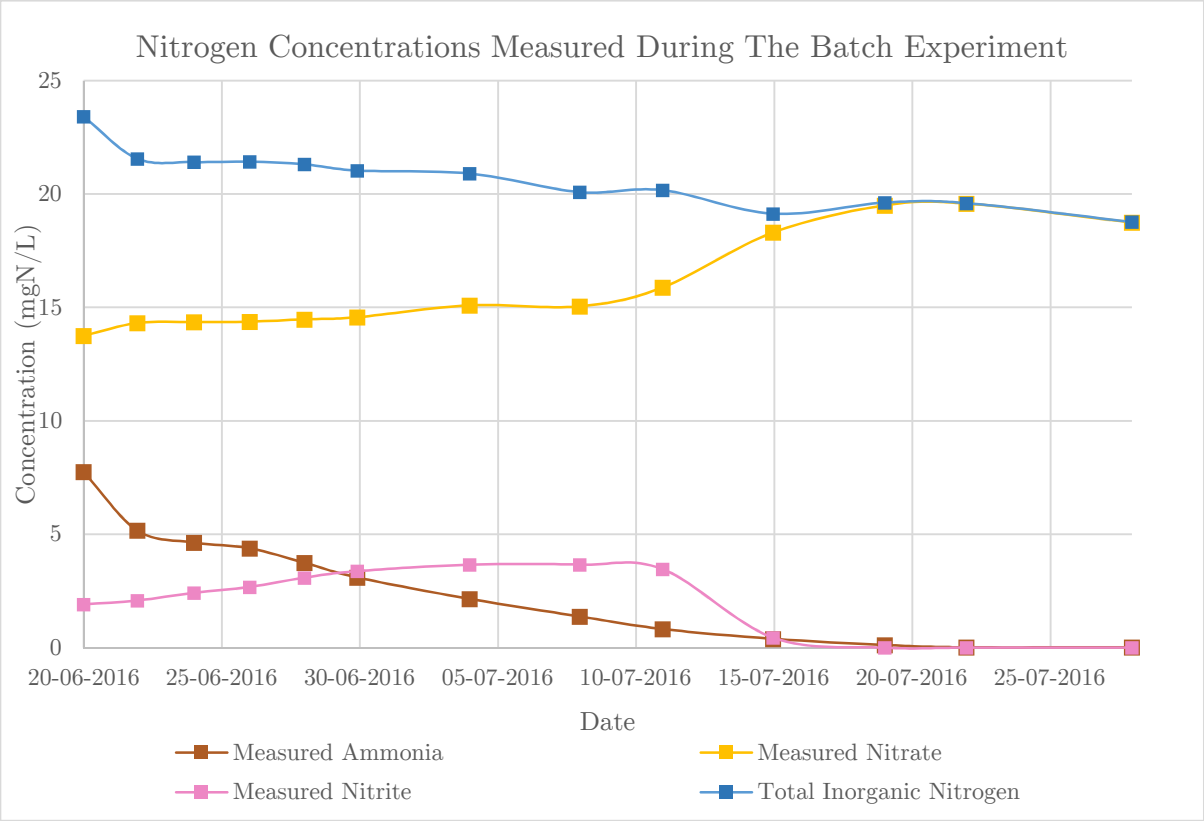

Figure 4.10 - Chart of nitrogen concentrations measured during the batch experiment

4.1.2.2.3 COD

Figure 4.11 contains the COD concentrations measured during the batch experiment. The batch experiment achieved approximately 60% COD removal in the first couple of days after which the COD concentration stayed roughly constant. This rapid reduction in the initial COD concentration was accepted to be due to the fast growth rate of OHOs.

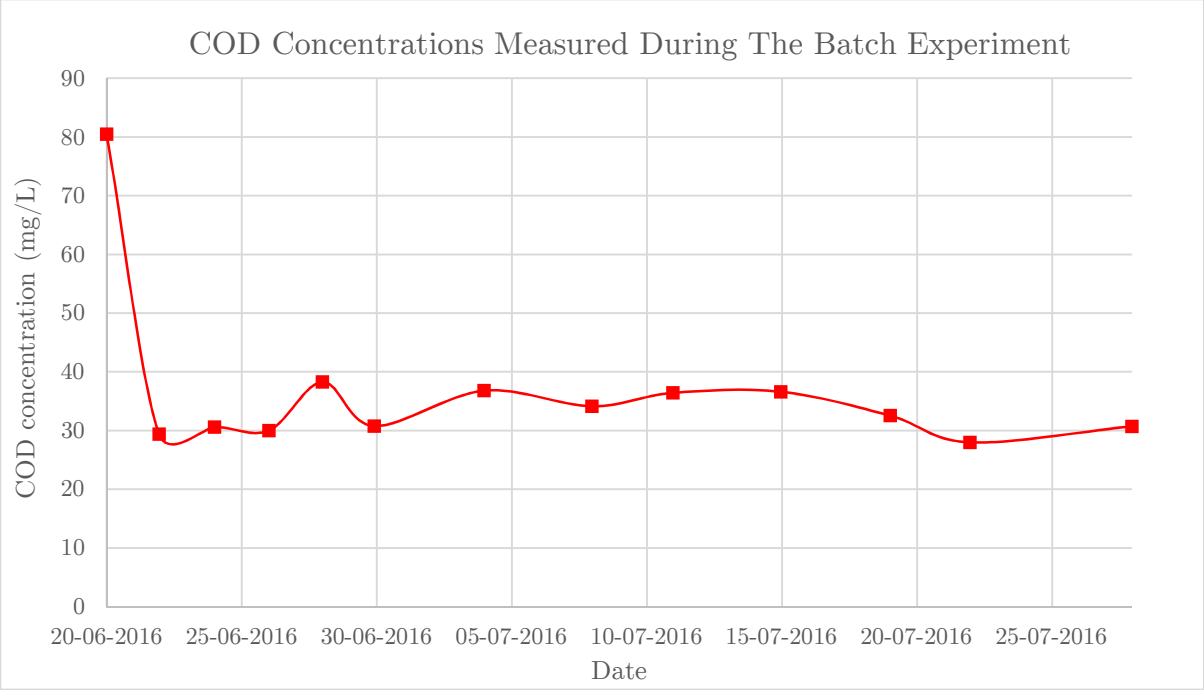

Figure 4.11 - Chart of COD concentrations measured during the batch experiment

4.1.3 Conclusion

The nutrient removal achieved during the continuous and batch experiments was considered modest. However, it should be noted that the algal growth was possibly limited by the light availability during these experiments. Since the pond was indoors and had no exposure to direct sunlight, the light required for photosynthesis was provided with artificial lighting (see section 3.1.7). However, the intensity of the artificial lighting was much lower than that of sunlight. The algal growth rate was presumably inhibited during the experiments due to a lack of high-intensity sunlight. A pond exposed to direct sunlight, may therefore have a better nutrient removal capacity than that which was obtained in the experiments.

The effluent COD concentrations obtained in the experiments are also quite high. The theoretical effluent COD concentration of an activated sludge system is typically negligible (Ekama & Wentzel, 2008a; Tchobanoglous, et al., 2003). The relatively high effluent COD measured in these experiments may be an indication of a biological process in the HRAP that was a source of soluble carbon. This process was most likely the algal respiration, excretion, and mortality processes. The algae convert carbon dioxide into organic carbon during photosynthesis. The organic carbon is then possibly released into the HRAP as non-living soluble or particulate organic carbon during these processes.

The continuous experiments had external variables that may have influenced the results. These external variables included the inaccuracy of the peristaltic pump system and premature biological activity in the refrigerated concentrate. The batch experiment was done to eliminate these variables. The results obtained from the batch experiment were therefore used to

calibrate the computational model. However, the continuous experiment did indicate that ammonia is strongly favoured over nitrate in an HRAP system and that nitrification occurs in an HRAP with a high retention time (10 days). The misguided addition of sodium hydroxide during the 4-day HRT experiment also showed the possible effectiveness of SRP precipitation.

4.2 Computational HRAP Model Calibration

In this section, the results of the computational model calibration are presented.

4.2.1 Nitrite Incorporation

It was discussed in section 4.1 that ammonia was only partly nitrified during the batch experiment and an increase in the nitrite concentration was observed. The computational model makes the assumption that all the nitrite is immediately nitrified to nitrate (see section 2.8.1.3 and 3.2). It was therefore required to incorporate the nitrite into the computational model as fully nitrified nitrate. The nitrate concentration used in the computational model therefore includes the nitrite. During the later stages of the batch experiment, all the nitrite was rapidly nitrified to nitrate after which the nitrite concentration was zero.

4.2.2 General Variables of the Batch Experiment

Certain general variables are required by the computational model. These variables include the pond volume, the pond depth, temperature, maximum light intensity, photoperiod and the time step. Some of these varied over the operation period and a representative average was determined. Table 4.3 is a summary of the general variables that was used in the computational model of the batch experiment.

Table 4.3 - General Variables applicable to the batch experiment

Variable	**Value**	**Unit**
Pond Depth	0.274	m
Pond Volume	887	L
Temperature	19.3	°C
Maximum Light Intensity	72.1	W/m^2
Photoperiod	0.67	-
Time Step	20	min

4.2.2.1 Pond Depth

The depth of the HRAP varied over the duration of the batch experiment due to the evaporation losses. The chart in Figure 4.12 shows the variation in the water level as well as the average water level for the batch experiment. The average water level was calculated as

the line (or water level) on Figure 4.12 below which the area would be the same as the area below the graph of the actual water level. The average water level was calculated as 273.7 mm.

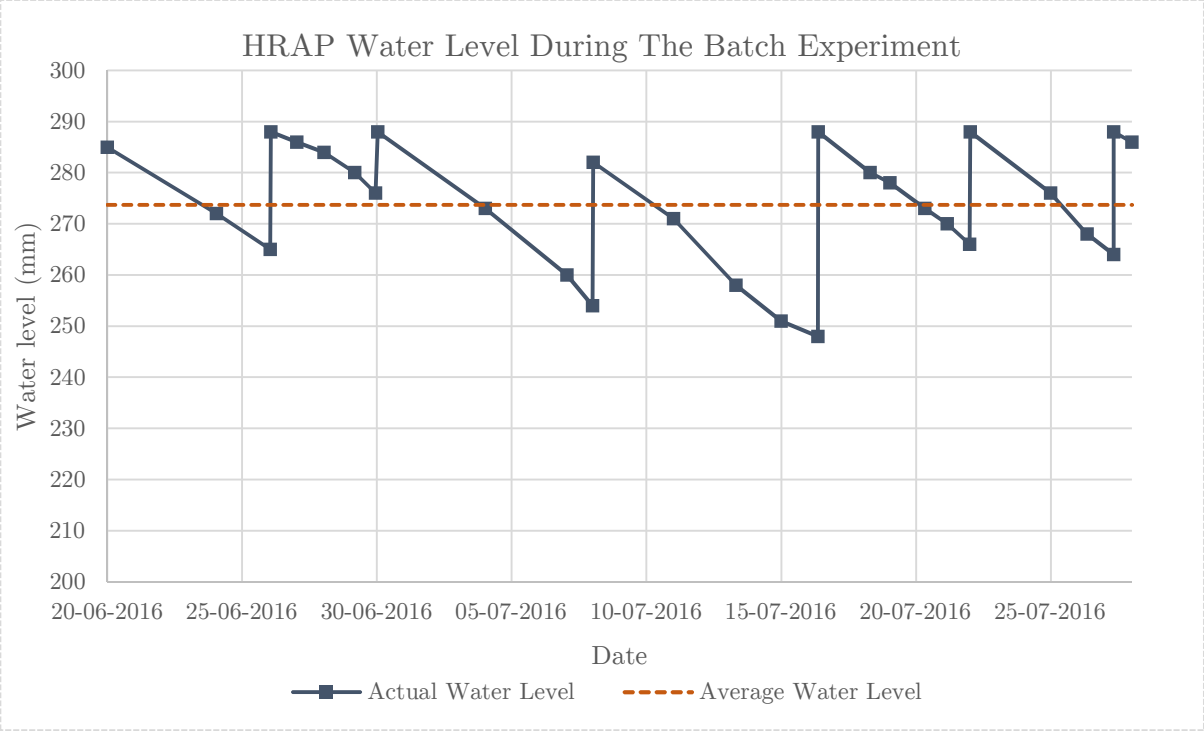

Figure 4.12 - Average water level during batch experiment

4.2.2.2 Pond Volume

The surface area of the HRAP was given in section 3.1.4 as 3.24 m^2. The average volume of the HRAP for the batch test was determined by using the average water level calculated in section 4.2.2.1. With a surface area of 3.24 m^2 and an average depth of 273.7 mm, the average volume of the HRAP was calculated as 887 litres.

4.2.2.3 Temperature

The temperature of the water in the HRAP fluctuated over the duration of the batch experiment. The chart in Figure 4.13 shows the actual water temperatures as measured during the batch experiment, as well as the average water temperature for the entire experiment. The average temperature was calculated in the same manner as the average pond depth in section 4.2.2.1. The average pond temperature for the batch experiment was 19.3 °C.

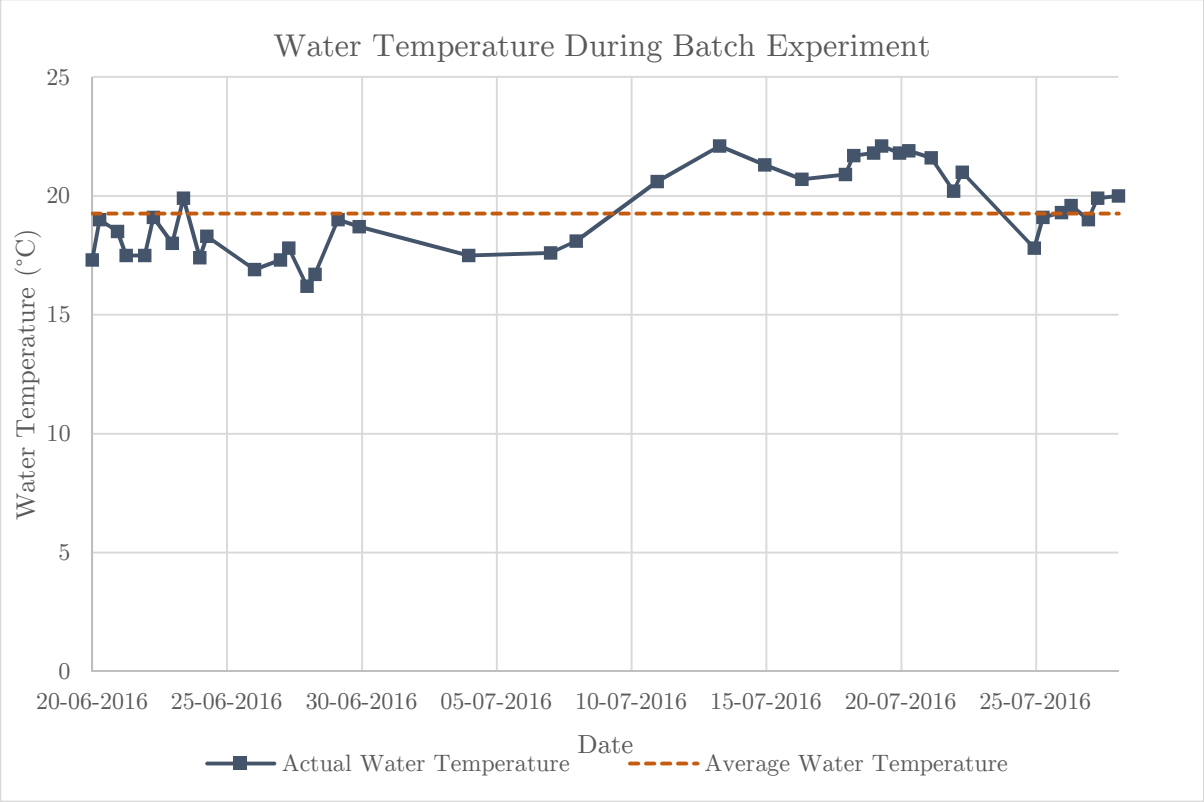

Figure 4.13 - Water Temperature During Batch Experiment

4.2.2.4 Maximum Light Intensity

The light intensity was indirectly measured through illuminance. The illuminance was measured in lux. Lux is a measuring unit for illuminance and gives the number of lumens (lm) in a square meter. The fluorescent tubes had a rated lamp efficacy of 64 lm/W. The values measured for the illuminance divided by the lamp efficacy give an estimation of the light intensity in W/m^2.

The light intensity was not constant over the pond's surface. The illuminance measurements were therefore taken by floating a light meter for one circulation around the HRAP on the pond surface. The light meter then gave a maximum, minimum and average illuminance for each circulation. The illuminance was measured on 12 different occasions during the operation of the HRAP. Figure 4.14 shows the results obtained from these measurements. Figure 4.14 illustrates the minimum, maximum and average illuminance for each measurement as well as the combined average for all the circulations.

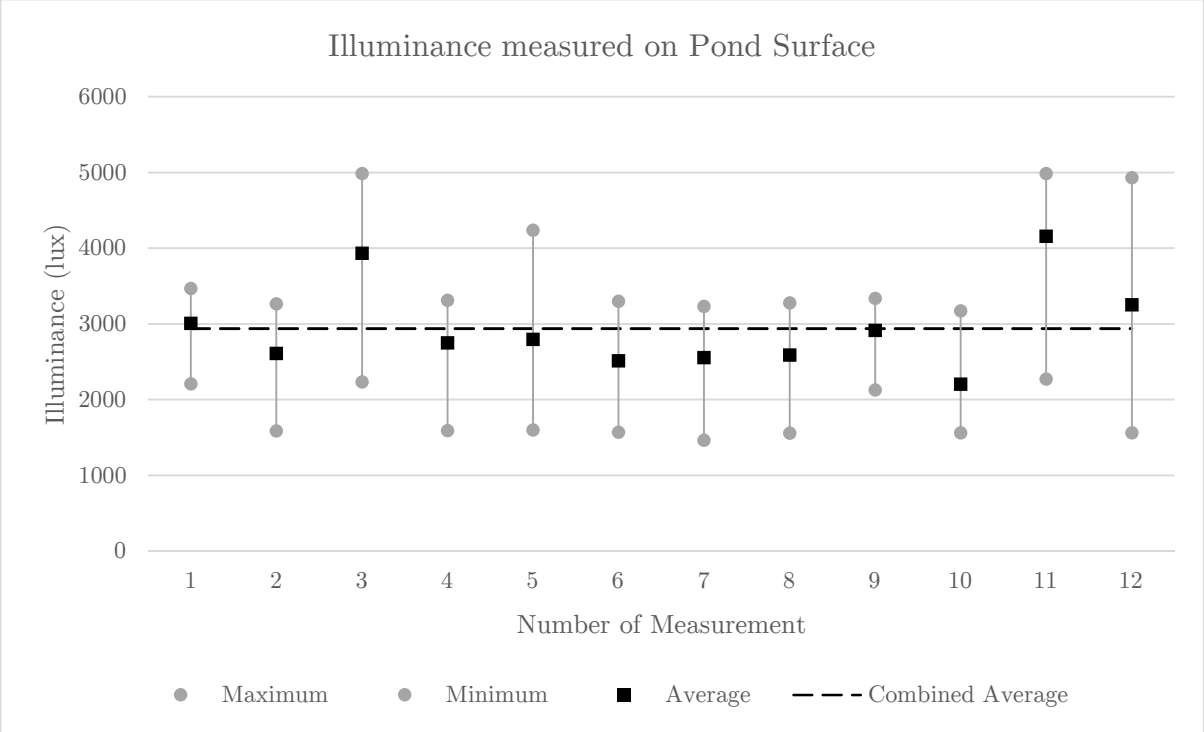

Figure 4.14 - Illuminance on HRAP surface

The combined average illuminance shown in Figure 4.14 was calculated as 2940 lm/m^2. This was converted to a light intensity of 45.9 W/m^2 through division by the efficacy of the fluorescent tubes. However, the light intensity of 45.9 W/m^2 was constant throughout the light period. The computational model requires a maximum light intensity as an input and distributes that light intensity over the photoperiod according to a half-sinusoid approximation as shown in Figure 4.15. With Figure 4.15 in mind, Equation 2.47 was used to convert the constant light intensity of 45.7 W/m^2 to a maximum light intensity of 72.1 W/m^2.

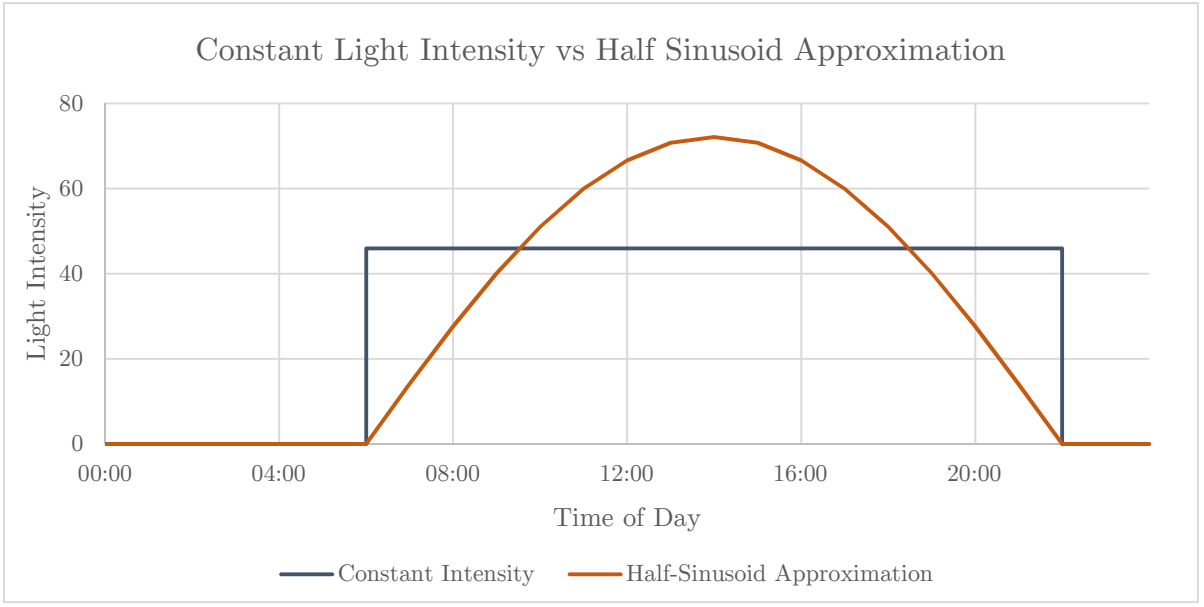

Figure 4.15 - Constant light intensity vs Half Sinusoid Approximation

4.2.2.5 Photoperiod

It was already mentioned in section 3.1.7 that a mechanical time was used to switch the light on and off. The mechanical was programmed to switch the lights on at 06:00 each morning and then to switch the lights off at 22:00 each night. The lights were on for 16 hours and off for 8 hours a day. The photoperiod was therefore 0.67.

4.2.2.6 Time Step

The time step defines the resolution of the computational model as described in section 3.2. A short time step would give better results, but the model would take longer to calculate. A 20-minute time step was chosen for these simulations. This time step was deemed to be small enough to give reasonably accurate results and still have a relatively short calculation time.

4.2.3 Initial Concentrations

The computational model requires the initial concentrations of the various state variables. During a dynamic simulation, these initial concentrations would not be of too much importance since the model will always converge to the same steady state concentrations. However, in a batch simulation, it is important to know the initial concentrations in order to achieve a good correlation between the measured and simulated concentrations.

Table 4.4 shows the initial conditions that were measured for the batch experiment. These concentrations were used during the batch test calibration.

Table 4.4 - Initial Condition for batch experiment

Parameter	**Symbol**	**Initial Concentration**	**Unit**
Ordinary Heterotopic Organisms	X_a	Unknown	mgVSS/L
Ammonia Oxidising Organisms	X_n	Unknown	mgVSS/L
Algae	a	0.052	mgChl$a$/L
Endogenous Residue	X_e	Unknown	mgVSS/L
Dissolved Biodegradable Organics	c_d	80.5	mgCOD/L
Particulate Biodegradable Organics	c_p	0*	mgCOD/L
SRP	p	10.69	mgP/L
Ammonia	n_a	7.75	mgN/L
Nitrate/Nitrite	n_i	15.67	mgN/L
*assumed			

The OHO, ANO, and endogenous residue concentrations were unknown and were estimated during the model calibration process. The particulate biodegradable organics concentration was assumed to be zero.

4.2.4 Calibration of Rates and Constants

It was not possible to determine all the rates and constants through analytical measurements. The rates and constants were therefore estimated through a model calibration process. This process involved choosing the values of the rates and constants in the model as the values that gave the most accurate simulation of the measured results. The typical ranges of these rates and constants, given in Table A.1 in Appendix A, served as the basis of the calibration process.

The computational model was expanded to allow for the estimation of the rates of constants. This enabled a range to be applied to the rates and constants. The computational model would then calculate for a set number of iterations. A random value within the predefined range for each of the selected rates and constants was chosen for each iteration. A similarity between the measured and simulated results was determined after the execution of each iteration. After all the iterations were executed, the computational model would give the values for the particular combination of rates and constants that gave the best similarity between the simulated and measured results. The reasoning behind this method was that an optimal or near-optimal combination of rates and constants should be found if the computational model does enough iterations with the random rates and constants.

Since the main focus of this thesis is nutrient removal, the SRP, ammonia and nitrate/nitrite concentrations were used to calculate the similarity between the measured and simulated concentrations. These similarities were calculated as the summation of the absolute difference between each of the measured SRP, ammonia and nitrate/nitrite concentrations and its equivalent simulated concentration. A smaller similarity value consequently represented a better simulation of the measured concentrations. The similarities were calculated according to Equation 4.2.

$$Similarity = \sum |p_{m,i} - p_{s,i}| + \sum \left|n_{a_{m,i}} - n_{a_{s,i}}\right| + \sum \left|n_{i_{m,i}} - n_{i_{s,i}}\right| \qquad \text{Equation 4.2}$$

Where

p_m = measured SRP concentration at date i (mgP/L)
p_s = simulated SRP concentration at date i (mgP/L)
n_{a_m} = measured ammonia concentration at date i (mgN/L)
n_{a_s} = simulated ammonia concentration at date i (mgN/L)
n_{i_m} = measured nitrate/nitrite concentration at date i (mgN/L)
n_{i_s} = simulated nitrate/nitrite concentration at date i (mgN/L)

The rates and constants of the computational model were calibrated within their typical ranges as given in Table A.1. This increased the probability that the calibrated rates and constants were an accurate representation of the actual kinetics in the HRAP. Table D.1 in Appendix D contains the rates and constants that were selected for the model calibration. The

recommended values or the middle of the ranges were chosen for the rest of the rates and constants.

The model calibration was done through a number of calibration rounds. In the first calibration round, the program was executed for 30 000 iterations. After an inspection of the results, the ranges were refined. The program was then executed for a further 10 000 iterations. The results were analysed and the ranges were refined further. After another 5000 iterations, an acceptable similarity between the simulated and measured concentrations was obtained. Figure 4.16 shows the graph that was obtained for the final model calibration. The different ranges used during the three calibration rounds are shown in Table D.1 in Appendix D. Table D.2, also in Appendix D, contains the calibrated values of the rates and constants for the solution shown in Figure 4.16. The assumption was made that the combination of rate and constants in Table D.2 is a fair representation of the kinetics in the system.

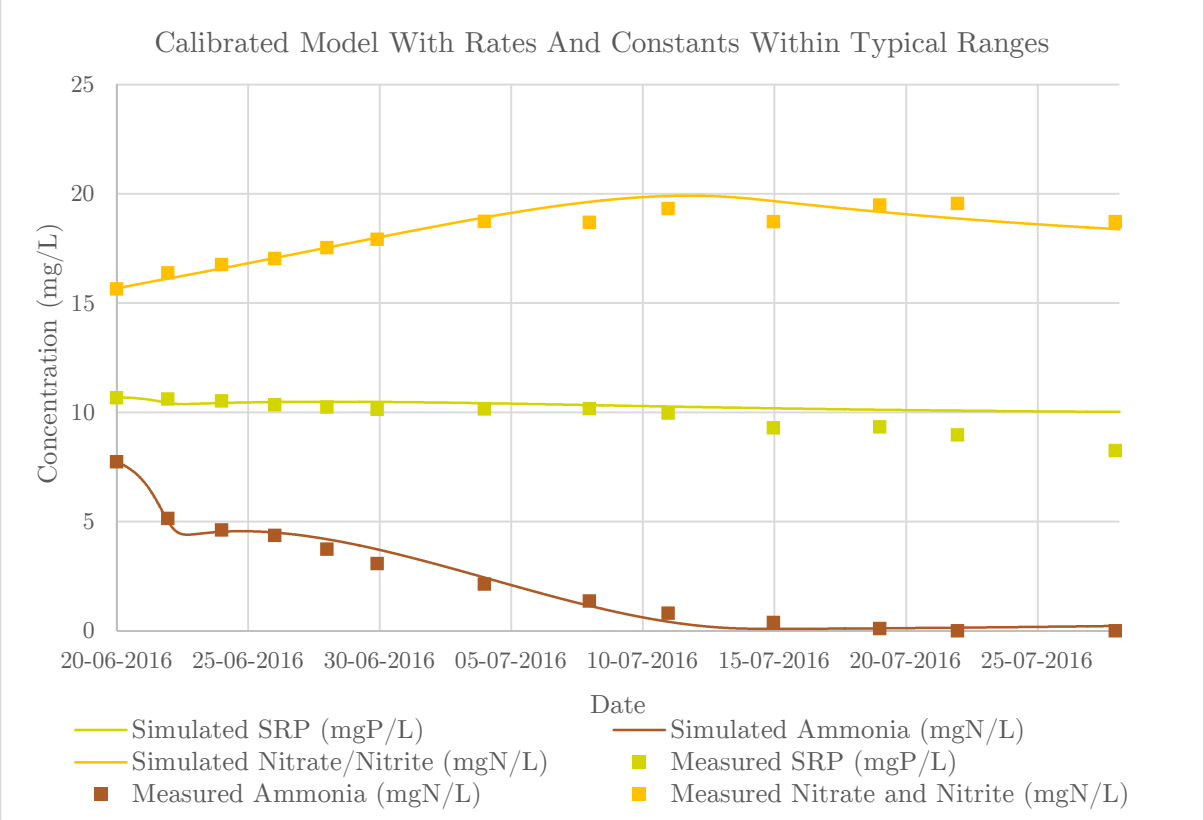

Figure 4.16 - Chart of calibrated model with rates and constants within the typical ranges

4.2.5 Accuracy of Calibrated Model

Periodic measurements of the SRP, ammonia, nitrate, nitrite, Chlorophyll *a* and VSS were taken through the duration of the batch experiment. These measured concentrations were corrected for evaporation as explained in section 4.1.2.1 and are given in Appendix C. These measured concentrations were compared with simulated concentrations to determine the accuracy of the model.

The coefficient of determination (R^2) was deemed as an appropriate measure to estimate the accuracy of the calibrated model. Equation 4.3 was used to calculate the coefficient of determination between the measured and simulated concentrations for each parameter (Montgomery & Runger, 2007).

$$R^2 = 1 - \frac{SS_E}{SS_T} = 1 - \frac{\sum_i (c_{m_i} - c_{s_i})^2}{\sum_i (c_{m_i} - \overline{c_m})^2} \qquad \text{Equation 4.3}$$

Where

c_{m_i} = measured concentration of parameter at date i (mg/L)

c_{s_i} = simulated concentration of parameter at date i (mg/L)

$\overline{c_m}$ = mean of measured concentrations of parameter (mg/L)

It can be seen in Equation 4.4 illustrates that the coefficient of determination compares the fit of the measured and simulated data with the fit between the measured data and its mean. A value of 1 indicates a perfect correlation between the measured and simulated concentrations. A value of 0 indicates that the simulated data fits the measured data just as poorly as the horizontal line of the measured mean. It is possible for the coefficient of determination to be negative. A negative coefficient of determination indicates that the simulated data is a worse representation of the measured data than the measured mean. Figure 4.17 shows the coefficient of determination between the measured and simulated SRP, ammonia, nitrate/nitrite and chlorophyll *a* concentrations for the calibrated model. The VSS and COD correlations are not shown in Figure 4.17 since negative coefficient of determination values were obtained for these parameters.

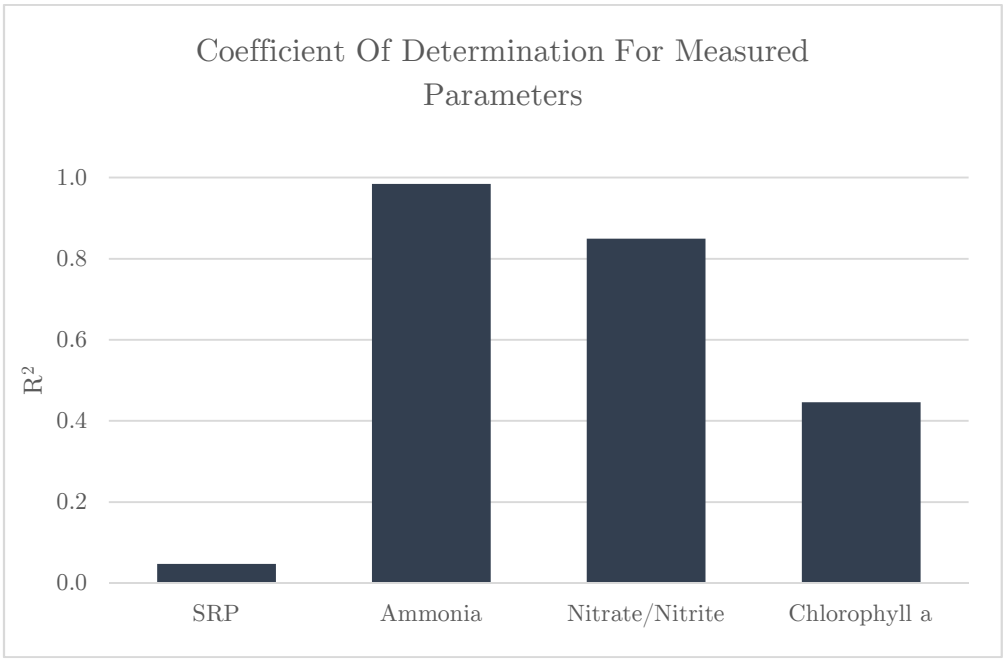

Figure 4.17 - Coefficient of determination for measured parameter

An estimate of the simulation error for each parameter was additionally determined. This was done by calculating the mean absolute error (MAE) for each set of measured and simulated concentrations. The MAE was divided by the mean of the scaled measured concentrations. The scaling was done by subtracting the minimum value in a set of measured and simulated concentrations from each of the measured concentrations. The measured concentrations were scaled to ensure that a representative base was used for the calculation. The resultant value was the MAE as a percentage of the scaled mean of the measured concentrations and was termed the average percentage error. The average percentage error was calculated for each parameter by using Equation 4.4.

$$APE = 1 - \frac{\sum|c_{m_i} - c_{s_i}|}{\sum\left(c_{m_i} - \min(c_m, c_s)\right)} \qquad \text{Equation 4.4}$$

Where

APE = average percentage error (%)

c_m = represent all the measured concentrations of parameter (mg/L)

c_s = represent all the simulated concentrations of parameter (mg/L)

Figure 4.18 shows the average percentage error that was estimated between simulated and measured concentrations for each of the measured parameters.

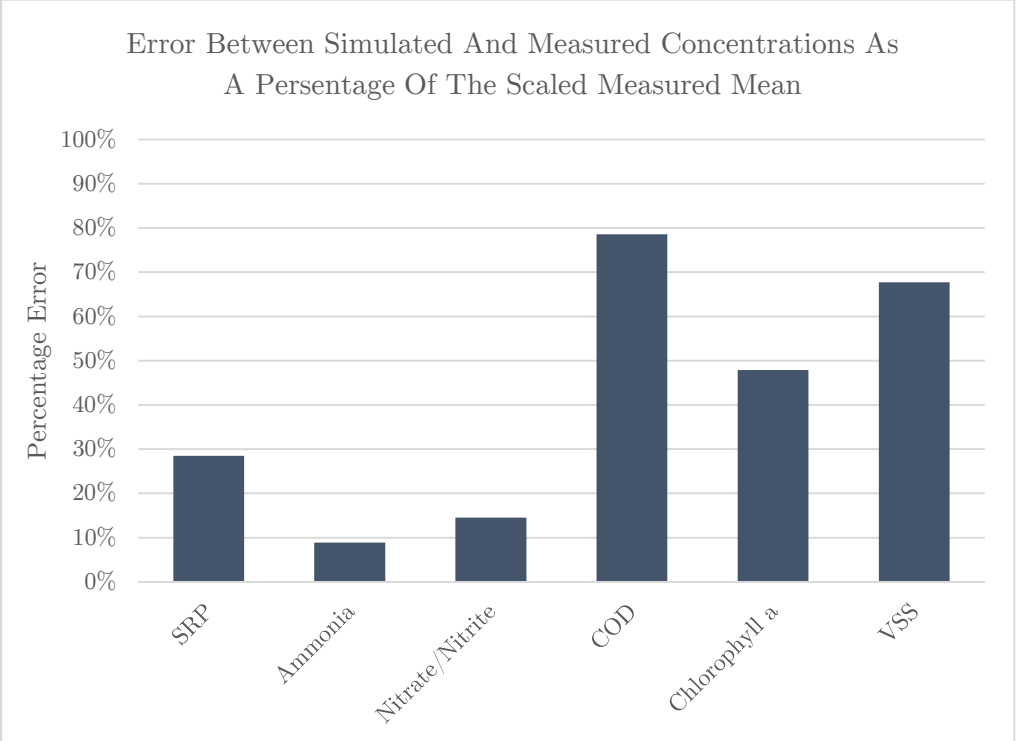

Figure 4.18 - Average percentage error between simulated and measured concentrations in calibrated model

The accuracy of the calibrated model for each of the measured parameters is discussed below with reference to the data shown in Figure 4.17 and Figure 4.18.

4.2.5.1 Soluble Reactive Phosphorus

The coefficient of determination for the SRP was 0.05 and the estimated average percentage error of simulated SRP concentrations was 29%. The correlation between the measured and simulated concentrations was poor with a relatively high estimated percentage error. However, the coefficient of determination value represents a much worse correlation than the average percentage error suggests. This was due to the scaling issues with the SRP concentrations. The calculation for average percentage error did not incorporate such a representative scale as the calculation of the coefficient of determination. The coefficient of determination value is therefore a more accurate representation of the correlation between the measured and simulated SRP concentrations.

The SRP predictions from the computational model were very inaccurate. Figure 4.19 gives a detailed comparison between the measured and simulated concentrations. The poor correlation between the measured and simulated SRP concentrations are evident in Figure 4.19. Possible reasons for this poor correlation are discussed in section 4.2.6.1.

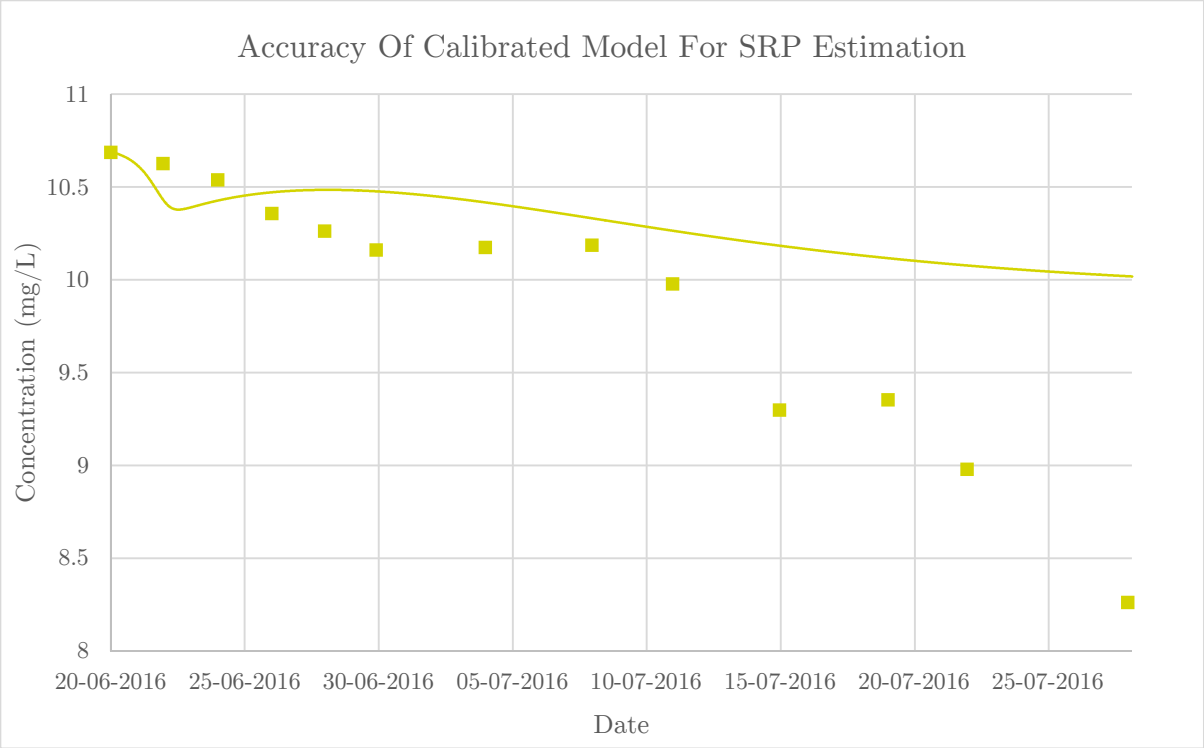

Figure 4.19 - Accuracy of calibrated model for SRP estimation

4.2.5.2 Ammonia

The correlation between the measured and simulated ammonia concentration was 0.98. The estimated average percentage error was only 9%. These values indicate that the computational model was adequate in predicting the ammonia concentrations. The model's accuracy in predicting the ammonia concentration is illustrated in Figure 4.20.

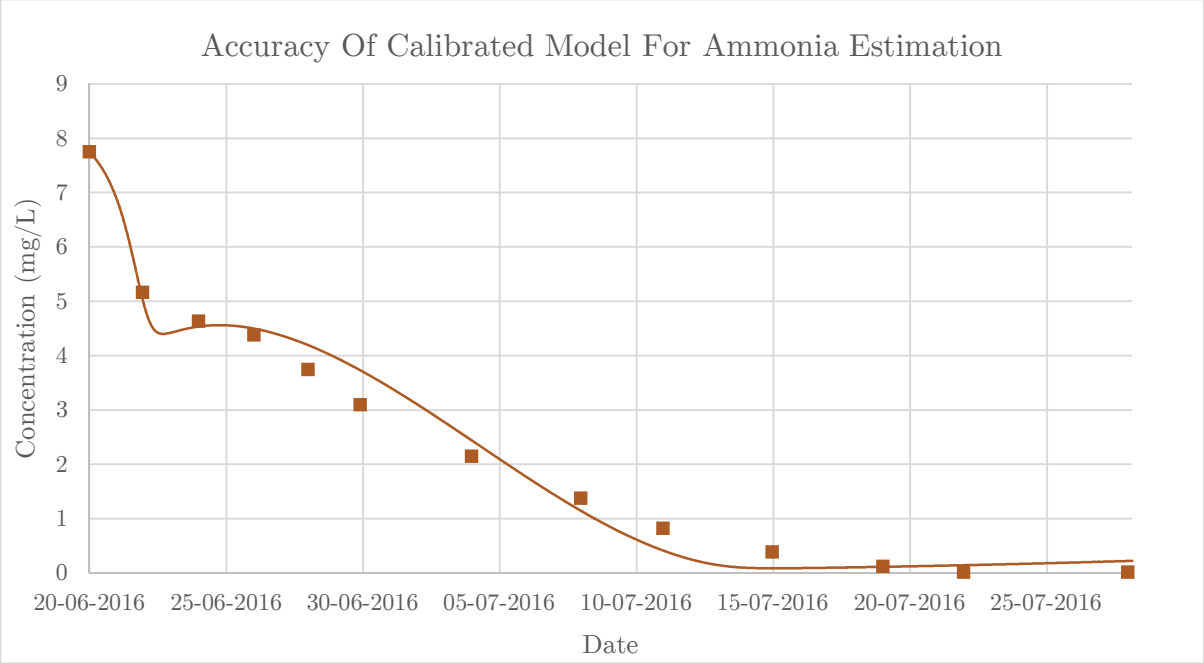

Figure 4.20 - Accuracy of calibrated model for ammonia estimation

4.2.5.3 Nitrate/Nitrite

The calibrated computational model had a satisfactory coefficient of determination value of 0.85 for predicting the nitrate/nitrite concentration. The estimated average percentage error was also relatively low at 14.6%. The correlation between the measured and simulated nitrate/nitrite concentrations is shown in Figure 4.21. It is clear that the model is sufficient in predicting the nitrate/nitrite concentration.

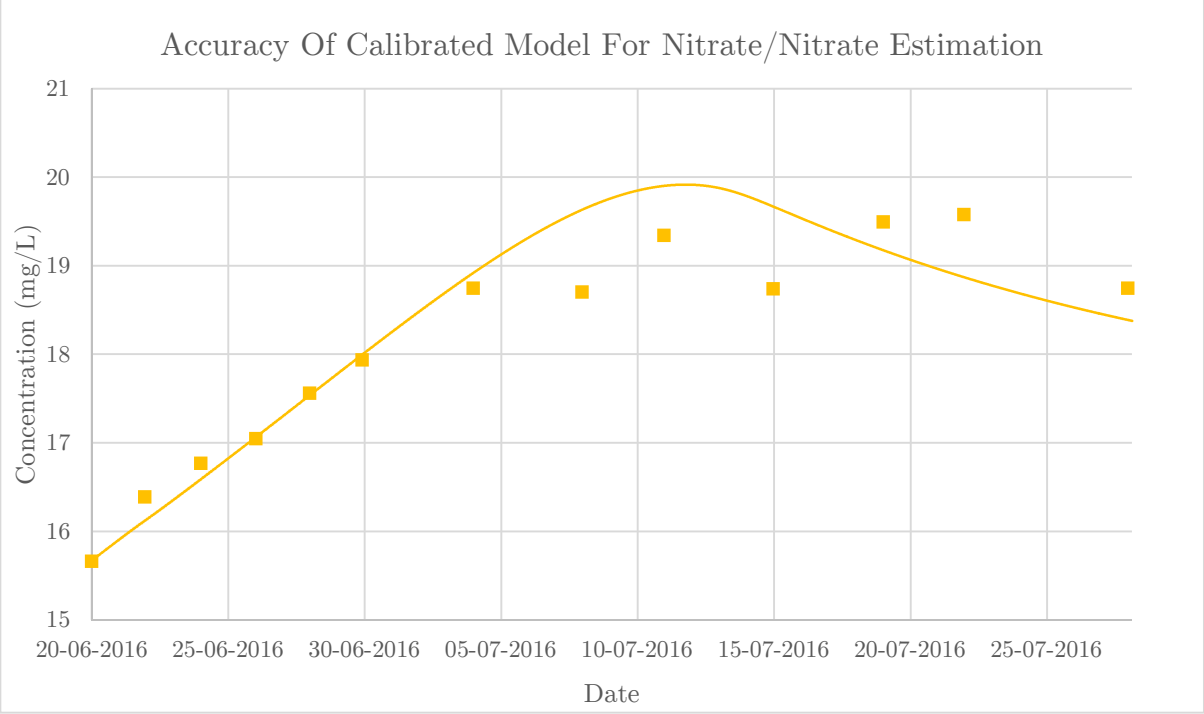

Figure 4.21 - Accuracy of calibrated model for nitrate/nitrite estimation

4.2.5.4 COD

In predicting the COD concentration, the computational model had an estimated average percentage error of 79% and a negative value for the coefficient of determination. The computational model is clearly very inaccurate in estimating the COD concentration. Figure 4.22 shows that the computational model severely over-predicted the COD removal observed in the batch test. Possible reasons for this poor correlation are discussed in section 4.2.6.2.

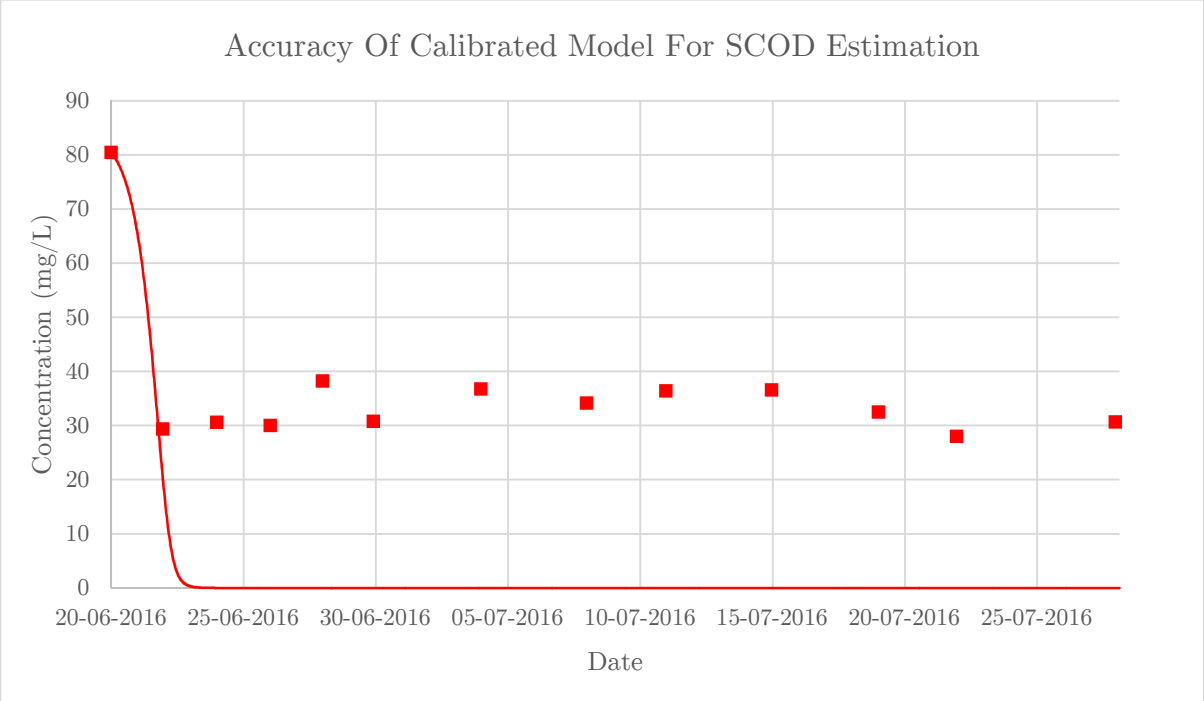

Figure 4.22 - Accuracy of calibrated model for SCOD estimation

4.2.5.5 Chlorophyll *a*

A 0.45 correlation between the simulated and measured chlorophyll *a* concentrations was obtained for the calibrated computational model. The estimated average percentage error was 48%. These values indicate that the calibrated computational model did not accurately predict the chlorophyll *a* concentration. However, the comparison between the measured and simulated concentrations shown in Figure 4.23, indicates that these correlation values might be misleading. The correlation with the measured concentrations is very good until the last measurement on 28 July 2016. The correlation increases to an admirable 0.97 if the last chlorophyll *a* measurement is disregarded. The nutrient concentrations did not show any indication of a rapid increase in the chlorophyll *a* concentration. The rapid increase observed between the last two measured chlorophyll *a* concentrations in Figure 4.23 should be coupled with a corresponding decrease in the nutrient concentrations. It is therefore possible that the last measurement is erroneous but since only four chlorophyll *a* measurements were done during the batch experiment, one cannot draw too many conclusions from the chlorophyll *a* correlations.

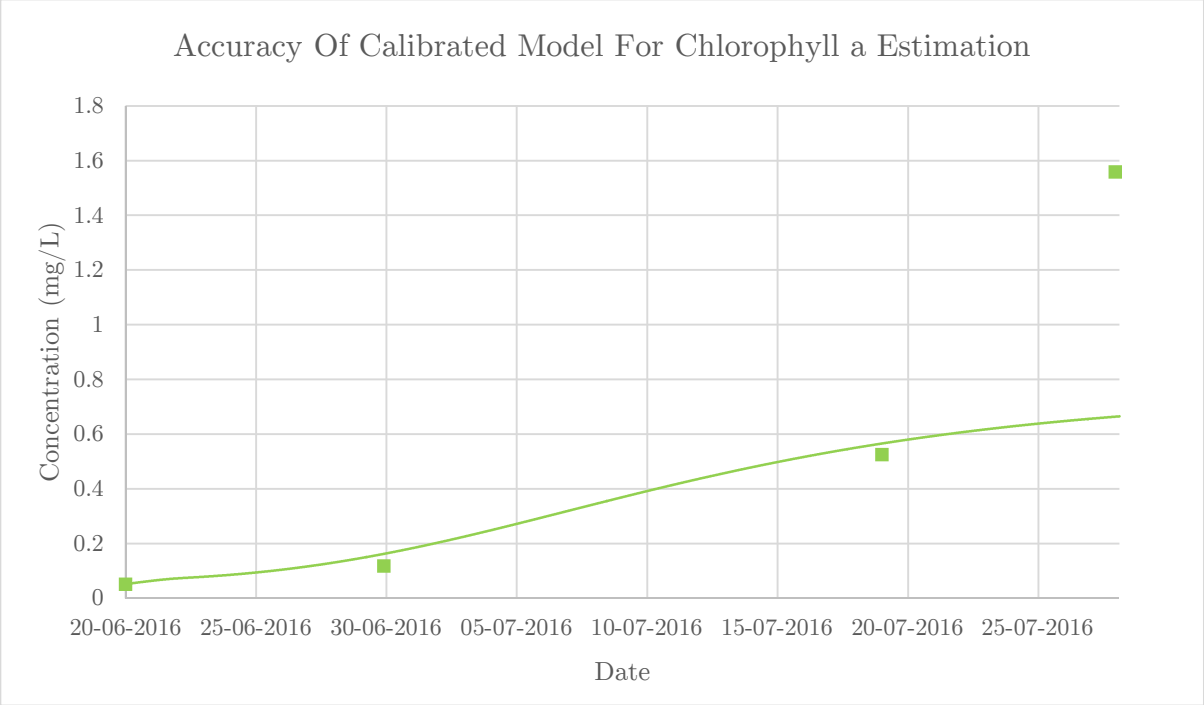

Figure 4.23 - Accuracy of calibrated model for Chlorophyll *a* estimation

4.2.5.6 VSS

Figure 4.18 and Figure 4.24 show that the calibrated model had a very poor correlation with the measured concentrations. A negative coefficient of determination value was obtained and the estimated average percentage error was 68%. Possible reasons for this poor correlation are discussed in section 4.2.6.3.

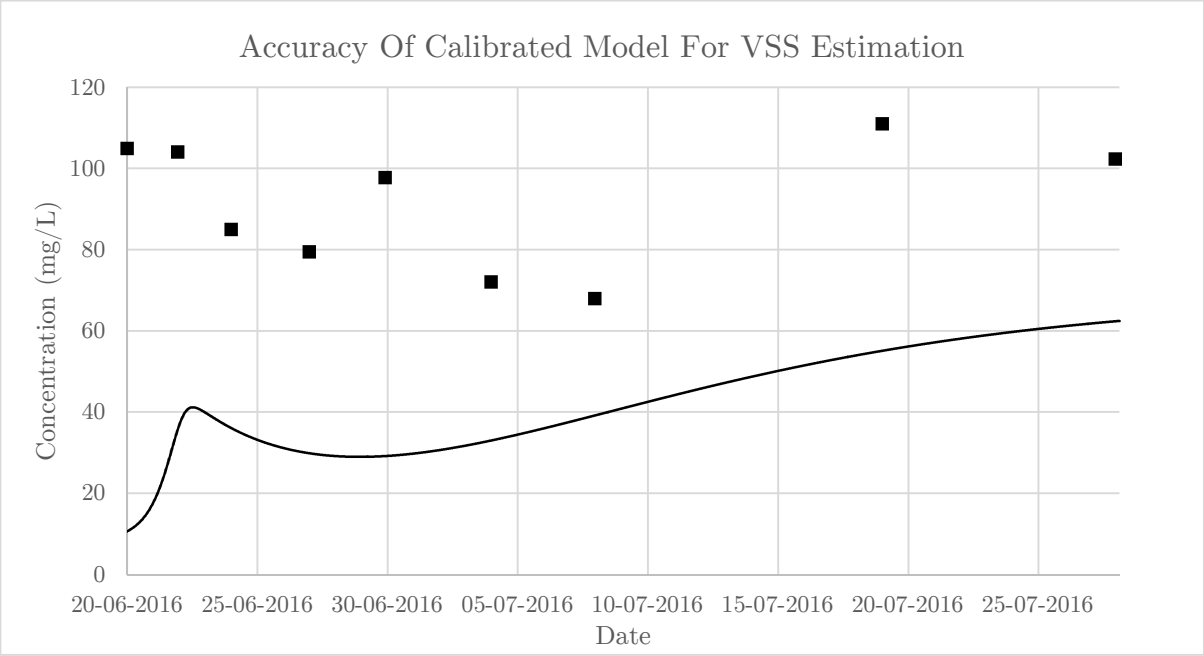

Figure 4.24 - Accuracy of calibrated model for VSS estimation

4.2.6 Possible Sources of Error

It is illustrated in the previous section that the calibrated computational model was inaccurate in predicting the SRP, COD and VSS concentrations. This section considers possible sources that contributed to the calibrated model's inaccuracy in predicting these concentrations.

4.2.6.1 SRP

The inaccuracy of the computational model in predicting the SRP concentration indicates that there was an additional mechanism of SRP removal in the scale model HRAP that the model did not take into account. It is believed that this mechanism was SRP precipitation. The calibrated model only gives an estimate of the SRP assimilated by algae. It was mentioned in section 2.4.1.1.2 that SRP assimilation is often accompanied by SRP precipitation in HRAPs.

The calibrated computational model only accounted for 28% of the total SRP removal that was measured during the batch test. This means that 72% of the SRP removal measured in the batch test was possibly due to SRP precipitation. The pH is a highly important parameter in phosphate precipitation. Phosphate precipitation can account for up to 80% of the SRP removal in waste stabilisation ponds with a pH above 8.2 (Craggs, 2005a). In the batch test, the measured pH was below 8.2. Initially the pH in the HRAP was quite low (approximately between 5.5 and 6.5) due to the nitrification of ammonia. However, towards the end of the experiment after all the ammonia was nitrified, the pH started to rise to between 6.5 and 7. Figure 4.19 illustrates the measured SRP concentrations and that the rate of SRP removal increased towards the end of the batch experiment when the pH started to rise. It is therefore believed that the difference between the simulated and measured SRP concentrations was due to SRP precipitation despite the measured pH being lower than the suggested 8.2.

The computational model is flawed in estimating the SRP concentration. However, the model potentially still gives an estimate of the minimum SRP removal that can be expected through algal assimilation.

4.2.6.2 COD

There are a few of possible reasons for the model's inaccuracy in predicting the soluble biodegradable COD concentration. These reasons are explored below.

The first explanation is that the COD measurement was on the total soluble COD. The computational model only models the biodegradable fraction of the total soluble COD. A fraction of the measured COD might have been unbiodegradable COD, which contributed to the large difference between the simulated and measured results. However, it is believed that the soluble unbiodegradable COD was a small fraction of the total soluble COD.

It was already mentioned in section 4.1.3 that the algal respiration, excretion, and mortality processes might have been a source of soluble organic carbon. The results obtained from experiments indicate that a significant amount of non-living organic carbon is present in the

system. The computational model assumed that all the carbon released during the respiration processes are used for energy generation. The high COD indicates that the endogenous respiration model may have been incorrectly applied for algal respiration. The surface water quality model of Chapra (2008) that was used to develop the deterministic HRAP model, ignores the algal mortality process and combines algal excretion and respiration. Figure 2.7, developed by Cole & Wells (2013), suggests that the algal mortality and excretion processes increase the soluble and particulate organic matter. The deterministic HRAP model therefore does not account for the possible contribution of algal respiration, excretion, and mortality towards the COD concentration. This limitation of the model resulted in a severe overprediction of the COD removal potential.

4.2.6.3 VSS

The reason for the poor VSS correlation is the same as the reason for the poor COD correlation. The computational model failed to include all the processes involved with regard to the non-living soluble and particulate biodegradable organics. The actual soluble and most likely particulate biodegradable organic concentrations were much higher than in the model simulations. Since soluble and particulate organics are a substrate for OHOs, the actual OHO (and endogenous residue) concentrations were probably higher than the computational model suggested. The difference between the measured VSS concentrations and the simulated VSS concentrations is therefore likely due to non-living particulate biodegradable organics, OHOs, and endogenous residue that the model failed to consider.

It is also possible that the algal and ANO respiration processes produced a particulate unbiodegradable residue that was not included in the computational model. This particulate residue possibly contributed towards the difference between the measured and simulated VSS concentrations.

Additionally, the VSS method is a gravimetric method with large possible errors inherent in the methodology itself where small masses of substances are measured.

The inaccuracy in the model's prediction of the VSS also explains the slow algal growth rate that was obtained in section 4.2.4. The VSS contributes to the light extinction over the depth of the pond. Since the model did not accurately predict the VSS concentration, the light extinction factor was lower than it should have been. The low algal growth rate consequently compensates for the high light extinction factor. The actual algal growth rate was most likely higher, but the actual light extinction coefficient was also lower.

4.2.7 Conclusion

The computational model gave an accurate prediction of the ammonia and nitrate/nitrite concentrations. The model's prediction of the chlorophyll *a* was also satisfactory, especially if the last measurement is disregarded. The evaluation of the model's accuracy for SRP

estimation indicated that an estimate of the minimum SRP removal that can be expected from assimilation, is potentially predicted by the calibrated model.

Since nutrient removal is of main concern in the next section, the assumption was made that the model's inaccuracy in terms of COD and VSS did not invalidate the nutrient removal results obtained from the model. There are only two interactions where the model's inaccuracy in COD and VSS can influence the nutrient concentrations. The first interaction is the underestimation of the light extinction coefficient due to the inaccurate VSS concentration. This interaction is compensated for by the low algal growth rate that was obtained in the model calibration. The second interaction is the nutrient assimilation by OHOs. Since the OHO concentration was underestimated, the nutrient assimilation by these organisms was also underestimated. However, when compared to algal nutrient assimilation, the nutrient assimilation in OHO biomass is normally insignificant. The underestimation of the nutrient assimilation by OHO biomass should not have a significant effect on the nutrient removal and would only make the model's estimations more conservative.

It was accepted that the model could be applied to investigate the nutrient removal potential of HRAPs located in different climates within South Africa, on the condition that cognisance is taken of the model's shortcomings.

4.3 Eutrophication Prevention Potential of an HRAP

This section uses the calibrated model of section 4.2 to estimate the eutrophication prevention potential of HRAPs in South Africa. Three major cities in South Africa have been selected for the investigation. These cities are Cape Town, Durban, and Johannesburg. Climate data for these cities were incorporated into the calibrated HRAP computational model to estimate nutrient removal capabilities.

4.3.1 Environmental Conditions

The average temperature, maximum solar intensity, and photoperiod had to be determined for each city. Table 4.5 is a summary of the applicable environmental conditions of these cities. This section discusses the determination of each of these parameters. The environmental conditions given in Table 4.5 are yearly averages. If these values are entered into the computational model, one will obtain the average performance data for the HRAP.

Table 4.5 - Environmental conditions of cities chosen for the investigation

City	Average Temperature (°C)	Average Photoperiod	Average Maximum Solar Intensity (W/m^2)
Cape Town	16.7	0.506	665.9
Johannesburg	16.0	0.506	709.4
Durban	20.8	0.506	539.1

4.3.1.1 Average Temperature

Average temperature data for each city in question were obtained (WWIS, 2014a; WWIS, 2014b; WWIS, 2014c). The temperature data contained monthly average minimum and maximum temperatures for each city. It was decided to use the average of all the monthly minimum and maximum temperatures as the temperature input for the model. An average was deemed appropriate since the model requires the water temperature as an input. Water temperatures are typically between the maximum and minimum air temperatures and have less fluctuation. The average yearly temperatures were calculated as 16.7, 16 and 20.8 for Cape Town, Johannesburg, and Durban respectively. These calculations are shown in Table E.1 in Appendix E.

4.3.1.2 Average Photoperiod

The yearly average photoperiod was calculated from day length data that were obtained for each city (timeanddate.com, 2016a; timeanddate.com, 2016b; timeanddate.com, 2016c). The average day length for each city was calculated as the average between the longest day and the shortest day of 2015. The longest day was on 22 December 2015 and the shortest day was on 21 June 2015 for all three cities in question. The photoperiod was calculated from the average day length by dividing the total minutes of daylight by the total minutes in a day. Table 4.6 illustrates the calculation of the photoperiod for each city.

Table 4.6 - Calculation of photoperiod for evaluation cities

	Cape Town	Johannesburg	Durban
Longest day	14:25	13:47	14:04
Shortest day	09:53	10:29	10:13
Average day length	12:09	12:08	12:08
Average photoperiod	0.506	0.506	0.506

4.3.1.3 Average Maximum Solar Intensity

The average maximum solar intensity for each city was determined from the global horizontal irradiation map of South Africa shown in Figure 4.25. Figure 4.25 illustrates that the average annual sum of the global horizontal irradiation is approximately 1880 $kWh/m^2/yr$,

2000 kWh/m^2/yr and 1520 kWh/m^2/yr for Cape Town, Johannesburg and Durban respectively.

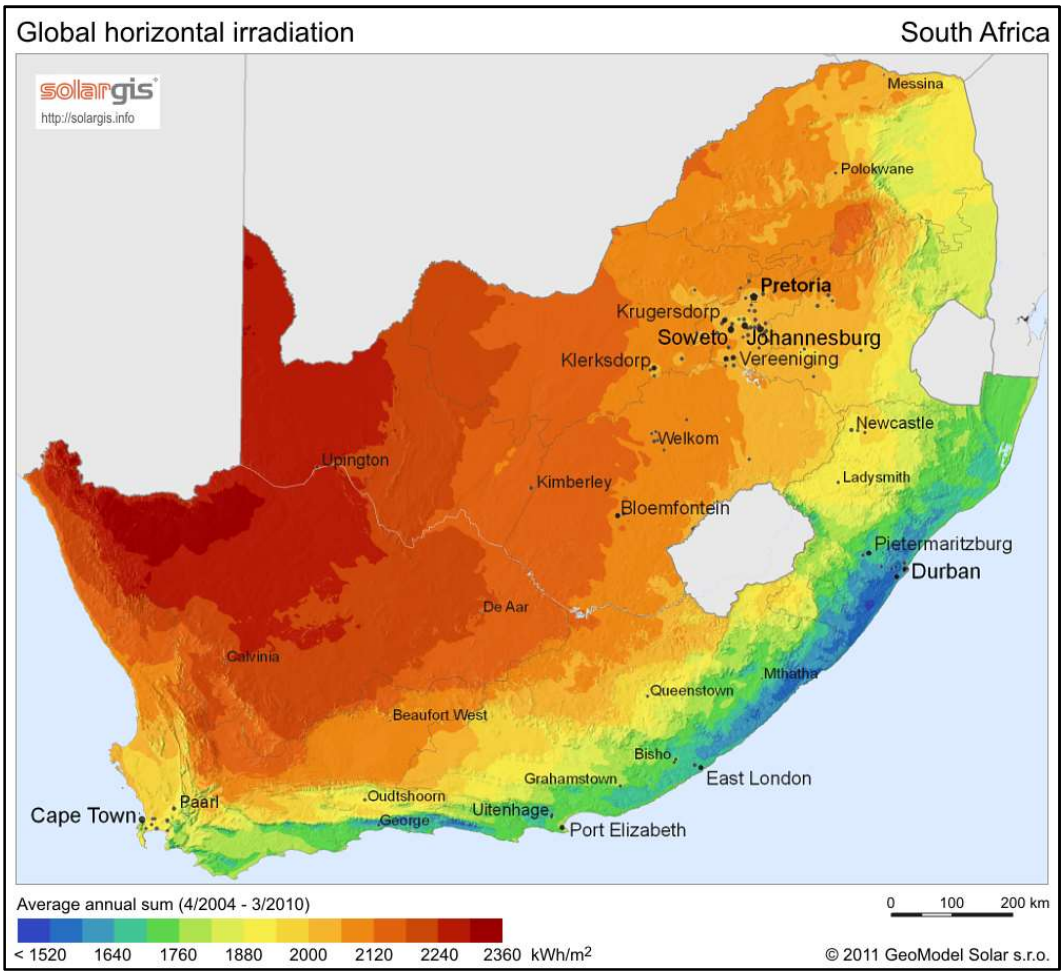

Figure 4.25 - Global Horizontal Irradiation map of South Africa (GeoSUN Africa, 2016)

The annual sum of the global horizontal irradiance is the amount of solar energy that is received by a one square meter horizontal surface over a period of a year. Since the computational model requires the maximum daily solar intensity as an input, the values obtained for the global horizontal irradiance had to be converted. The global horizontal irradiance was first converted to obtain an average solar intensity over a 24-hour day. This value was then divided by the photoperiod, since the sun only shines during the photoperiod. The value obtained was then the average solar intensity during the photoperiod. This value was then converted by using Equation 2.47 to allow for the half-sinusoid approximation used in the model (see sections 2.8.2.1.1.3 and 4.2.2.4). The value obtained from the last conversion is a yearly average of the maximum solar intensity for each day. Table 4.7 shows the steps followed in converting the average annual sum of the global horizontal irradiance to the average maximum daily solar intensity.

Table 4.7 - Calculation of average maximum solar intensity

	Cape Town	Johannesburg	Durban
Annual Global Horizontal Irradiation (kWh/m2/yr)	1880	2000	1520
Average daily solar intensity (W/m2)	214.6	228.3	173.5
Average daylight solar intensity (W/m2)	423.9	451.6	343.2
Average Maximum Daily Solar Intensity (W/m2)	**665.9**	**709.4**	**539.1**

4.3.2 Nutrient Removal Potential

The effectiveness of an HRAP for eutrophication prevention was investigated through its ability to remove soluble nitrogen and phosphorus from wastewater effluents. Nitrogen and phosphorus are the main nutrients of concern for eutrophication. This section investigates the nutrient removal potential of an HRAP for wastewaters with characteristics as described in section 3.1.1.

The environmental data from each city were put into the calibrated computational model. The steady-state SRP, ammonia, and Total Inorganic Nitrogen removal percentages were determined from model simulations for each of the cities for various HRT and pond depth combinations. It was mentioned in section 2.6.1 that the typical depths of an HRAP are between 0.2 and 1 meter. Section 2.6.2 states that typical HRTs of an HRAP are between 2 and 8 days. These ranges were used as a guideline for the different HRT and depth combinations for which the nutrient removal was determined. The computational model was executed for each HRT and depth combination until steady-state conditions were achieved. These steady-state concentrations were then used to determine the steady-state nutrient removal potential for the applicable HRT and depth combination.

4.3.2.1 Cape Town

4.3.2.1.1 Total Inorganic Nitrogen Removal

The potential Total Inorganic Nitrogen removal percentages obtained for Cape Town are shown as a function of HRT and depth on the graph in Figure 4.26.

Figure 4.26 shows that HRAPs could potentially be very effective in terms of Total Inorganic Nitrogen removal. Close to 100% Total Inorganic Nitrogen removal can theoretically be achieved. However, to achieve this Total Inorganic Nitrogen removal, the pond should be shallow and have a long retention time. A long HRT and shallow pond depth lead to large surface area requirements by the pond.

An examination of the HRTs in Figure 4.26 shows that at least a 3-day HRT was required to sustain algal growth. The flat line at the bottom of the chart for a 2-day HRT represents the

nutrient removal due to the fast growing OHOs. Nutrient removal percentages above these flat lines were due to algal assimilation.

Figure 4.26 shows that a depth of 0.1 m and an HRT of 6 days should be sufficient to obtain close to 100% Total Inorganic Nitrogen removal. The minimum recommended depth for an HRAP was suggested as 0.2 m in sections 2.5.4 and 2.6.1. At this depth, the highest Total Inorganic Nitrogen removal that was obtained was 72% for a 10-day HRT.

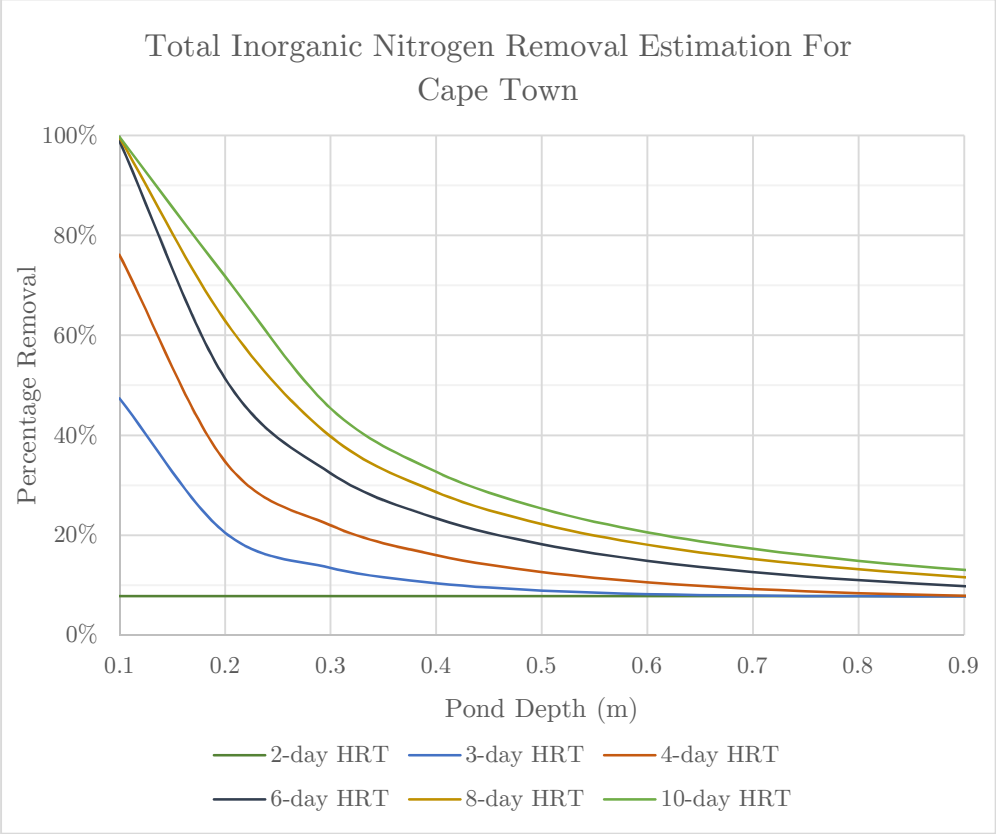

Figure 4.26 - Estimation of Total Inorganic Nitrogen removal for an HRAP in Cape Town

4.3.2.1.2 Ammonia Removal

The potential ammonia removal percentages obtained for Cape Town are shown as a function of HRT and depth on the chart in Figure 4.27. A comparison of the charts in Figure 4.27 with those in Figure 4.26 confirms that ammoniacal-N is much easier removed than nitrogen in the form of nitrate or nitrite.

Figure 4.27 shows that high ammonia removal can be achieved in a relatively deep pond with a short retention time. It is evident that ammonia removal would not have such high surface area requirements as Total Inorganic Nitrogen removal. Explanations for this lower surface area requirement include that algae assimilate ammoniacal-N first, due to its ammonia preference, and that nitrifying bacteria are not influenced by the pond's surface area.

Close to 100% ammonia removal was estimated for a relatively short retention time of 3 days at a depth of 0.1 m. At the minimum recommended depth of 0.2 m, an estimated HRT of between 4 and 6 days was required for approximately 100% ammonia removal.

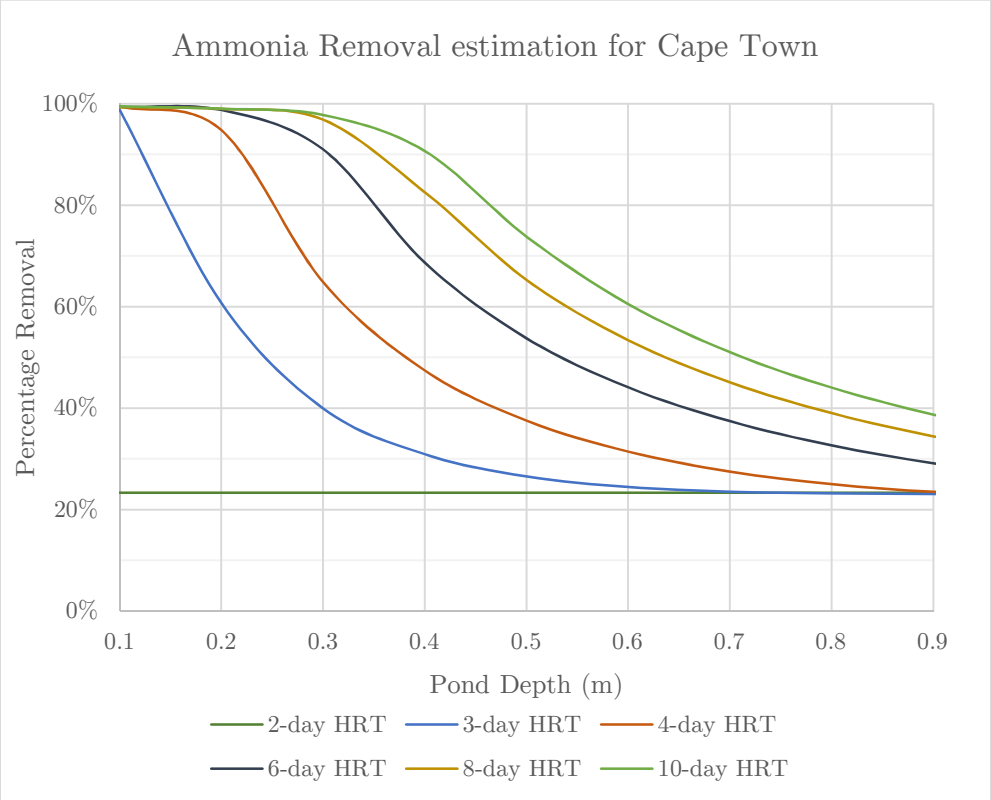

Figure 4.27 - Estimation of ammonia removal for an HRAP in Cape Town

4.3.2.1.3 SRP Removal

Figure 4.28 shows the minimum SRP removal that can be expected for various HRT and depth combinations for an HRAP in Cape Town. The removal percentages in Figure 4.28 are relatively low with a maximum removal of 31%. This indicates that an HRAP is possibly not effective in SRP removal. However, these removal percentages only include the SRP removal through assimilation into algal biomass. It was discussed in section 4.2.6.1 that phosphate precipitation is another effective mechanism of SRP removal in HRAPs that the computational model does not consider. Phosphate precipitation can account for up to 80% of the SRP removal in waste stabilisation ponds (Craggs, 2005a). It was estimated that approximately 72% of the measured SRP removal in the batch test was due to phosphate precipitation.

Figure 4.28 also shows that the SRP assimilation was limited by the available nitrogen concentrations. The nitrogen to phosphorus ratio in algal biomass was 7:1 in the computational model. The influent conditions, specified in Table 3.1, had a nitrogen to phosphorus ratio of 2.1:1. The SRP assimilation was therefore limited by the depletion of nitrogen. A higher influent nitrogen concentration would consequently mean that a higher SRP assimilation percentage could be achieved.

It was concluded that for the influent conditions in Table 3.1, SRP removal in HRAPs through algal assimilation in Cape Town are very modest and have larger surface area requirements. However, there are strong indications that the SRP removal can significantly increase if phosphate precipitation is considered.

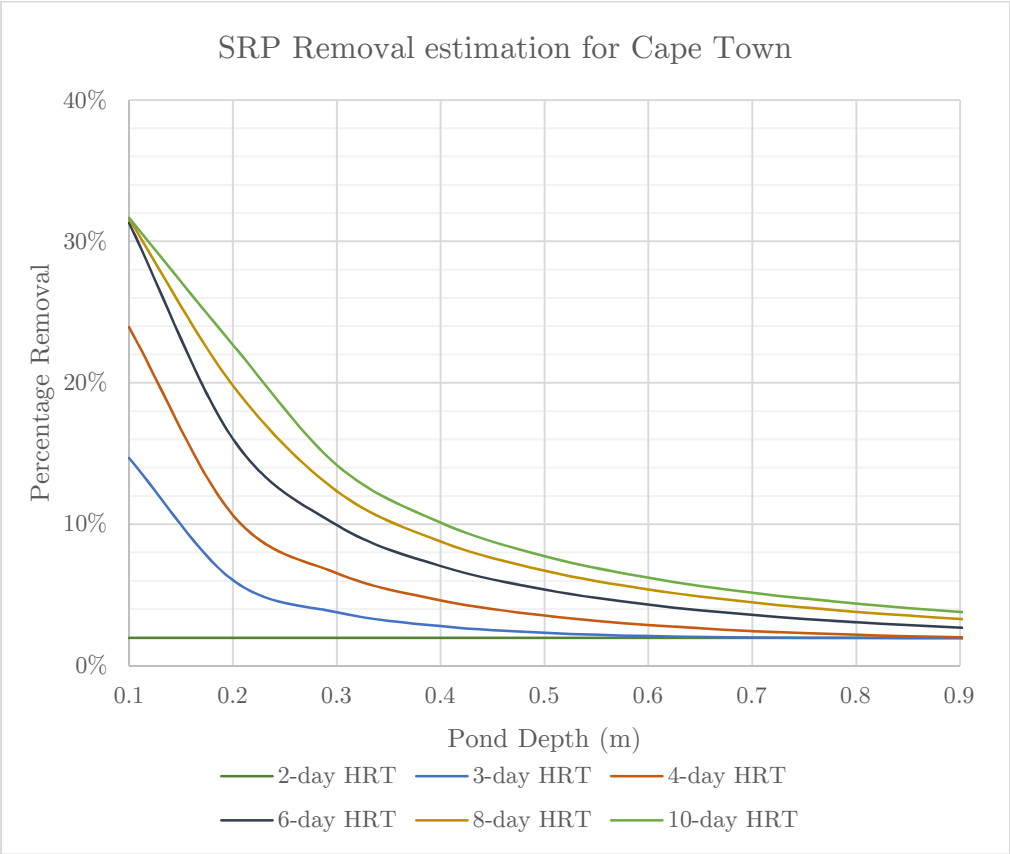

Figure 4.28 - Estimation of SRP removal for an HRAP in Cape Town

4.3.2.2 Johannesburg and Durban

The nutrient removal graphs for Durban and Johannesburg have the same trends as those for Cape Town, with only slightly different nutrient removal percentages. These graphs are therefore not discussed individually but are included in Appendix F.

A comparison of these nutrient removal charts with those of Cape Town shows that the nutrient removal percentages are generally slightly lower for Johannesburg and higher for Durban. The environmental conditions of Durban are also able to sustain algal growth at a 2-day HRT. Johannesburg as well as Cape Town, requires at least a 3-day HRT to sustain algal growth.

The nutrient removal charts of the three cities indicate that the warmer condition of Durban is more favourable for algal growth, despite the relatively low solar intensity at this location. It was concluded from these nutrient removal charts that an HRAP favours a warm region with a lower solar intensity over a relatively cold region with a higher solar intensity.

4.3.3 Area Requirements

One of the major disadvantages of HRAPs is their large surface area requirement. Figure 4.29 shows the area that an HRAP requires to treat 1 m^3 of daily flow for the HRT and depth combinations of section 4.3.2. The nutrient removal charts indicate that for a pond to achieve a nutrient removal in excess of 95%, the depth should be in the region of 0.1 m and the HRT should be larger than 6 days. Figure 4.29 specifies that the area requirements for a pond with these characteristics are more than 60 m^2 per cubic meter of daily flow. These area requirements are very large even for the small wastewater treatment plants in South Africa that have design flows of up to 2000 m^3/day.

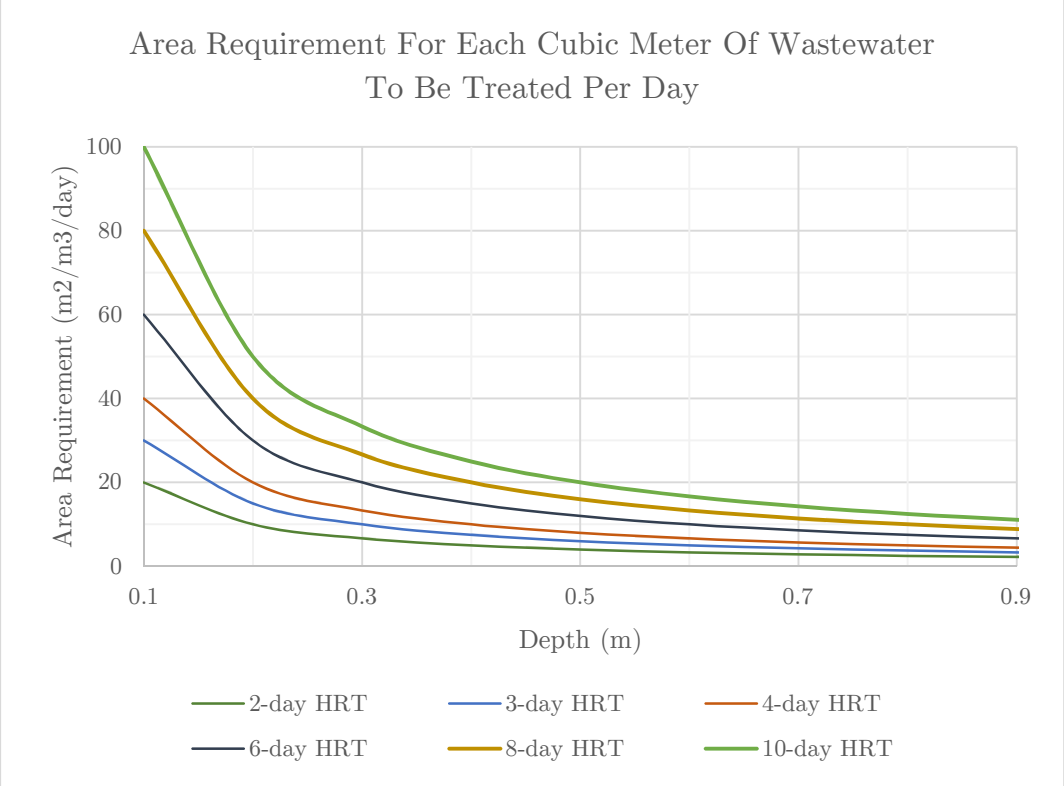

Figure 4.29 - Surface area requirement of an HRAP

The area requirements were determined for each of the nutrient removal percentages calculated in section 4.3.2. The data from all three cities were included in the analysis. The calculated areas were then plotted against the nutrient removal percentages as shown on the charts in Appendix G. The graphs in Appendix G show that the smallest estimated area requirement for approximately 100% Total Inorganic Nitrogen removal is 60 m^2/m^3/day. This area requirement is also applicable for the maximum SRP removal through assimilation of 31%. The estimated area requirement to achieve approximately 100% ammonia removal is only 20 m^2/m^3/day.

Figure 4.30 is a scaled down version of the chart in Figure G.1 in Appendix G. This chart has been capped at an area requirement of 30 m^2/m^3/day since this value was deemed as a more

practically attainable surface area for an HRAP. Figure 4.30 shows that between 36% and 68% Total Inorganic Nitrogen removal can be expected with an area requirement as large as 30 m^2/m^3/day. A more realistic surface area requirement of 15 m^2/m^3/day has a corresponding Total Inorganic nitrogen removal of between 18% and 31%.

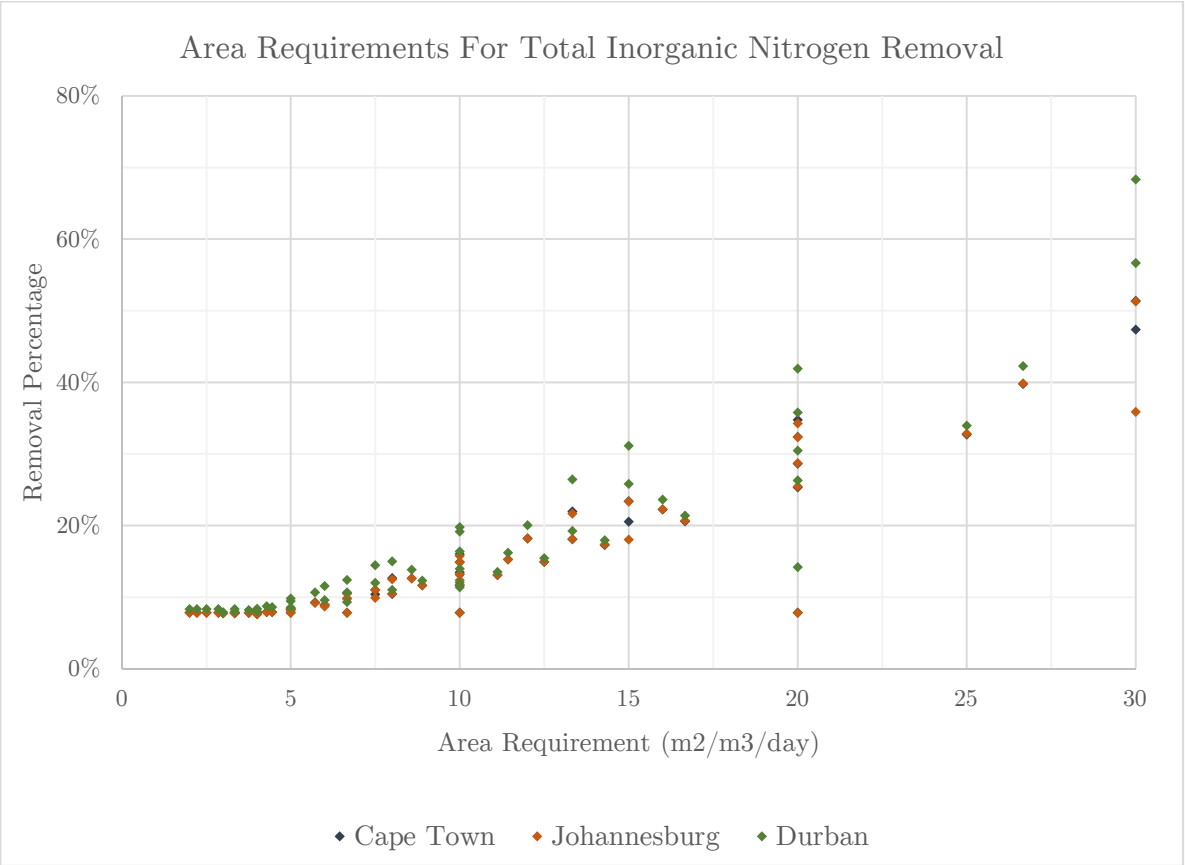

Figure 4.30 - Partial chart of surface area requirements for Total Inorganic Nitrogen removal

Figure 4.31 is the capped version of the chart shown in Figure G.2. Figure 4.31 shows the area requirements for ammonia removal and is also capped at 30 m^2/m^3/day. Figure 4.31 shows that up to 98% ammonia removal can theoretically be obtained with a relatively low surface area requirement of 20 m^2/m^3/day. For a surface area requirement of 15 m^2/m^3/day, one would be able to theoretically remove between 53% and 89% of the total ammonia.

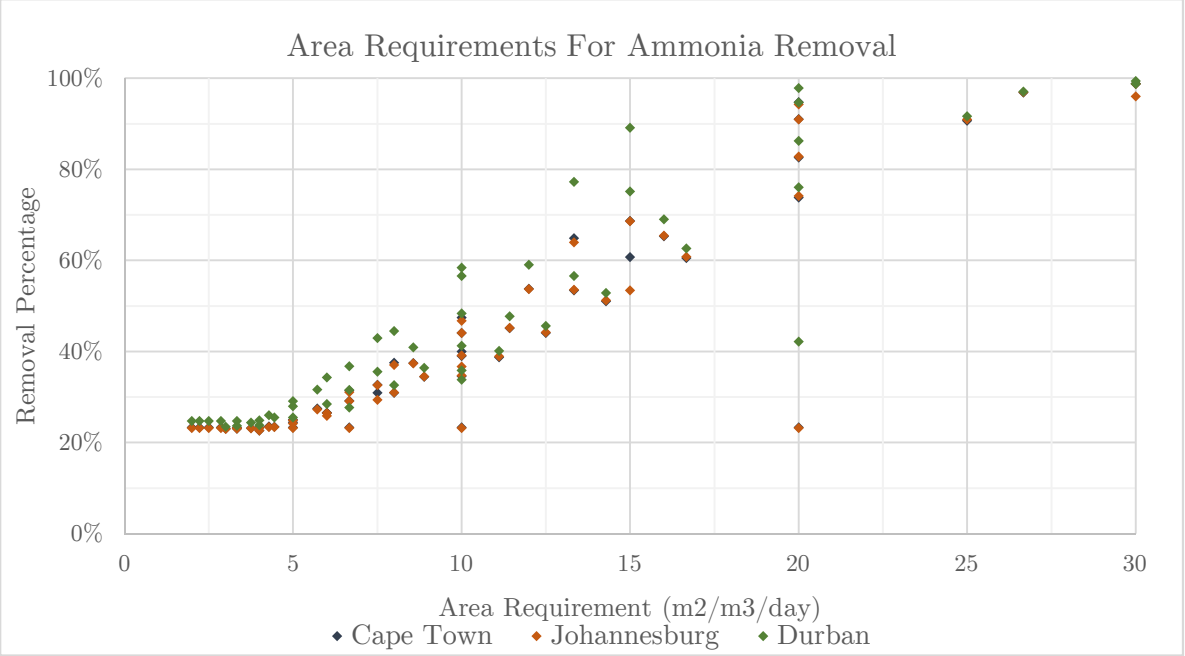

Figure 4.31 - Partial chart of surface area requirements for ammonia removal

Figure 4.32 is the capped version of the chart shown in Figure G.3. Figure 4.32 shows the surface area requirements for SRP removal and is capped at a maximum surface area requirement of 30 m^2/m^3/day. Figure 4.32 shows that an SRP removal between 11% and 21% can theoretically be achieved through SRP assimilation with a surface area requirement of 30 m^2/m^3/day. A surface area requirement of 15 m^2/m^3/day would result in an SRP removal of between 5% and 9% through assimilation according to the calibrated computational model. There are indications that these SRP removal percentages can significantly increase if phosphate precipitation is considered.

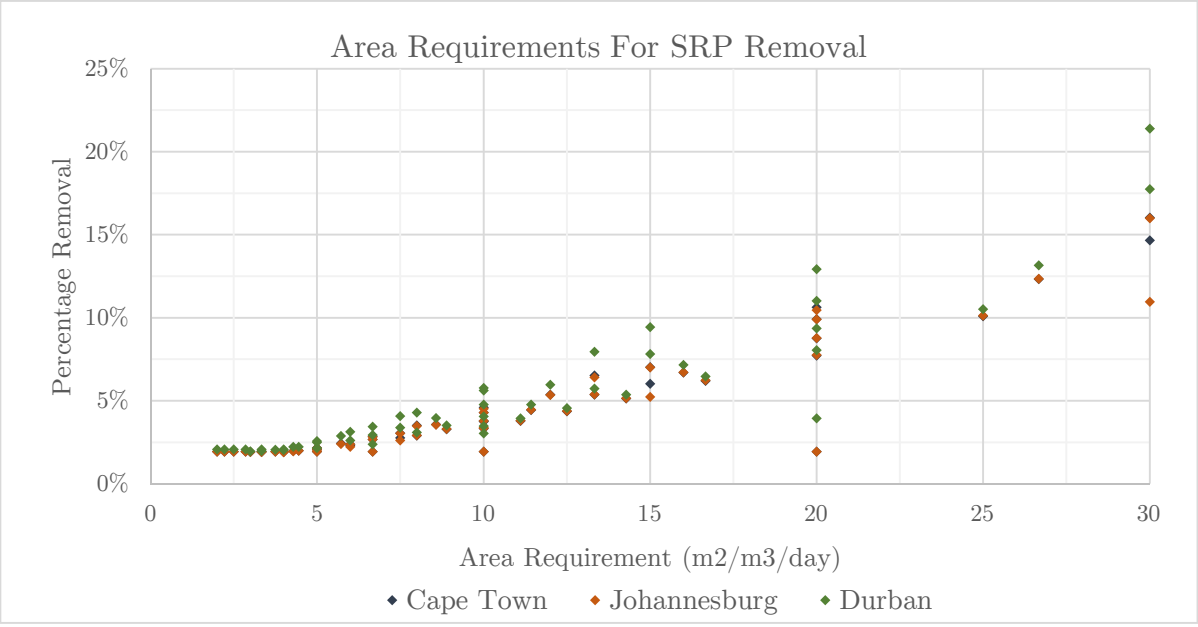

Figure 4.32 - Partial chart of surface area requirements for SRP removal

4.3.4 Conclusion

The HRAP can be very effective for nutrient removal with close to 100% nitrogen removal, and the prospect of high SRP removal according to the theoretical calculations of the calibrated computational model. However, achieving these high levels of nutrient removal with an HRAP is not necessarily practically feasible. The first issue is the unpractically large surface area requirements to achieve these high levels of nutrient removal. Another issue is that these high nutrient removals occur at pond depths in the region of 0.1 m. Computational simulations suggest that the algal culture in shallow ponds might be very unstable. The reason for this instability is that algae require depth to enable it to adjust its vertical position according to the light intensity it requires (Mara, 2004). The computational simulations suggested that shallow HRAPs with depths in the region of 0.1 m need a very high initial algal concentration to avoid algal washout. In these shallow ponds, the algae shade itself from the high-intensity sunlight. If the initial algal concentration is not high enough, insufficient shading is provided and the algae die-off. A shallow pond therefore will possibly not be able to recover its algal culture from a low concentration. A deeper pond provides enough shading through its depth that algal cultures can generally recover or grow from very low concentration. This is also confirmed in the literature with a minimum depth of 0.2 m that is recommended for HRAPs (Craggs, 2005b; Oswald, 1978).

The nutrient removal from HRAPs with practical surface area requirements and more stable depth, is still notable but might not be worth the capital and land investments that these ponds require.

5 CONCLUSION

5.1 Summary of Findings

The HRAP was investigated as a possible option for effluent polishing in South Africa through a laboratory model and the development of a deterministic design model. The thesis statement that was defined in section 1.3, was largely supported by the results obtained from the research. However, as explained below, effluent polishing with an HRAP may not always be practically attainable.

The nutrient removal that was measured from the HRAP during the laboratory experiments was modest. The algal growth was limited in these experiments due to a lack of high-intensity sunlight. This was an early indication of the importance of sufficient sunlight for an HRAP to be effective. The laboratory experiments also confirmed that algae have a strong preference for ammonia over nitrate/nitrite.

The calibrated computational model accurately predicted the ammonia and nitrate/nitrite concentrations. It was unsatisfactory in predicting the soluble reactive phosphorus (SRP) concentration, since it did not account for the phosphorus that was removed through precipitation. The model only gave an estimate of the SRP assimilated by algae. The COD and VSS estimations were also very inaccurate, presumably due to the model's deficiency in accounting for the increase in soluble and particulate organics, caused by the algal respiration, excretion and mortality processes.

The calibrated HRAP model indicated that an HRAP could be very effective in Total Inorganic Nitrogen and ammonia removal in South Africa. The HRAP also has the prospect of effective SRP removal when SRP precipitation is considered in conjunction with assimilation. It was established that shallow ponds with long retention times are required to achieve these levels of nutrient removal. These conditions led to a large surface area requirement by the HRAP. It was estimated that an area of 60 m^2 per cubic meter of daily flow is required for complete Total Inorganic Nitrogen removal. A smaller area requirement of approximately 20 $m^2/m^3/day$ was estimated for complete ammonia removal.

The HRAP can theoretically serve as an effective method for eutrophication prevention. However, the large surface areas required to achieve satisfactory nutrient removals, may diminish the feasibility of these ponds. These area requirements are too large for the HRAP to be feasible in and around cities. It can potentially be an effective eutrophication prevention solution for small towns where land is inexpensive and widely available.

5.2 Contributions

The computational HRAP model developed in this thesis has its shortcomings and further development is required before it can be implemented in the HRAP design and operation

phases. However, the potential improvement that a fully developed deterministic HRAP model can bring to the design and operation phases is evident. It can potentially enable an accurate prediction of the nutrient and organics removal, as well as the potential biomass production. A representative deterministic model can also greatly improve the design and operation of other types of waste stabilisation ponds.

This research revealed that an HRAP is theoretically very effective in nutrient removal, granted that the suspended solids can be removed effectively. However, due to the sunlight requirements of algae and the light absorption in deep ponds, very large surface areas are required for an HRAP to be effective.

5.3 Limitations and Future Research

This research had various limitations due to restrictions on the scope, time and funding of the project. This section explores these limitations and gives recommendations for the rectification of these limitations in future research projects.

The first major limitation of the research was that the data from only one laboratory experiment was used for the calibration of the computational HRAP model. It was therefore not possible to determine the accuracy of the model's response to changing environmental conditions. It is recommended that batch experiments with different environmental conditions should be done to determine whether the calibrated model still applicable to varying environmental conditions.

All the laboratory experiments were conducted at the same pond depth. Supplementary research is required to determine if the model accurately responds to variations in the pond depth.

The computational model was limited by the kinetics of only two deterministic models. The HRAP model needs to be developed further to incorporate processes such as phosphate precipitation, and algal respiration, excretion, and mortality. The computational model can possibly be expanded to include these processes by incorporating some of the kinetics in existing surface water quality models such as the CE-QUAL-W2 model by Cole and Wells (2013).

The computational model did not include the carbon dioxide concentration as a possible limitation in the algal growth. Although the dissolved carbon dioxide concentrations were not limiting during the batch experiment, Craggs (2005b) suggested that carbon dioxide might become limiting at high pH. More research is required on the dynamics of carbon dioxide in an HRAP and its limitation of algal growth.

The research did not include an investigation into the removal of the suspended solids from the HRAP effluent. The implementation of an HRAP would generally require the removal of

the solids before the HRAP effluent could be discharged. Algal settling ponds have successfully been used to remove the suspended solids from HRAP effluent (Rose, et al., 2002; Oswald, 1978). However, more research is required to determine the most effective and economical method of solids removal.

Other less significant research limitations include the indoors nature of the experiments and the synthetic wastewater used in the experiments. It is possible that the sunlight and actual wastewater effluent may have a different effect on the HRAP kinetics than the artificial lights and the synthetic wastewater. More research is required to determine the interchangeability between sunlight and the artificial lights, and between synthetic wastewater and the actual effluent from an underperforming WWTWs.

6 RECOMMENDATIONS

This section gives recommendations on the use of the computational model and the use of HRAPs for effluent polishing. These recommendations were established through the experimentation and modelling that were done in this research.

The following recommendations were determined for the use of the deterministic HRAP model:

1. Phosphate precipitation is an important mechanism in SRP removal. It is recommended that phosphate precipitation is included in a deterministic HRAP model.
2. The deterministic HRAP model should also include the contribution of the algal respiration, excretion and mortality processes to the soluble and particulate biodegradable non-living organics concentrations.
3. Evaporation can potentially have a significant effect on an HRAP in warm and sunny conditions and should be considered in the deterministic model.
4. Instead of estimating the rates and constants through a calibration process, it is recommended that the various rates and constants should be determined through analytical measurements.

The following recommendations were determined for the use of an HRAP for effluent polishing:

1. The theoretical model simulations showed that a pond depth between 0.2 m and 0.3 m, and an HRT larger than 4 days are recommended to achieve notable nutrient removal.
2. It is recommended that the HRAP is not shallower than 0.2 m. The simulations indicated that an algae culture in a pond shallower than 0.2 m might be unstable due to a combination of insufficient shading and excessive exposure to high-intensity sunlight.
3. A recommended HRAP surface area of 60 m2/m3/day was estimated as the required area for complete nitrogen assimilation from effluent quality wastewater.
4. A recommended HRAP surface area of 20 m2/m3/day was approximated for complete ammonia removal from effluent quality wastewater.
5. A cost-benefit analysis is recommended to determine the feasibility for an HRAP in a specific location.

REFERENCES

Blanc, R. & Leshem, U., 2013. *Utilizing algal oxygen production for advanced wastewater treatment in a Moving Bed Biofilm Reactor (MBBR) – the Biologically Aerated Reactor (BAR®).* Chicago, WEFTEC.

Bowie, G. L. et al., 1985. *Rates, Constants, and Kinetics Formulations in Surface Water Quality Modeling,* Athens, Georgia: United States Environmental Protection Agency.

Chapra, S. C., 2008. *Surface Water-Quality Modeling.* Long Grove: Waveland Press, Inc..

Clesceri, L. S., Greendberg, A. E. & Eaton, A. D., 1998. *Standard Methods for the Examination of Water and Wastewater.* 20th ed. Washington, DC: American Public Health Association.

Cole, T. M. & Wells, S. A., 2013. *CE-QUAL-W2: A Two-Dimensional, Laterally Averaged, Hydrodynamic and Water Quality Model, Version 3.71.* Portland: Portland State University.

Comeau, Y., 2008. Microbial Metabolism. In: M. Henze, M. C. M. Van Loosdrecht, G. A. Ekama & D. Brdjanovic, eds. *Biological Wastewater Treatment: Principles, Modelling and Design.* London: IWA Publishing, pp. 9-32.

Craggs, R., 2005a. Nutrients. In: A. Shilton, ed. *Pond Treatment Technology.* Cornwall: IWA Publishing, pp. 77-95.

Craggs, R., 2005b. Advanced integrated wastewater ponds. In: A. Shilton, ed. *Pond Treatment Technology.* Cornwall: IWA Publishing, pp. 282-310.

CSIR, 2010. *A CSIR perspective on water in South Africa - 2010,* s.l.: s.n.

Department of Water Affairs and Forestry, 1984. Requirements for the purification of waste water of effluent (Regulation No. 991). *Government Gazette, 18 May 1984, No. 9225*, pp. 12-16.

Department of Water Affairs, 2011. *Green Drop Handbook,* Pretoria: Department of Water Affairs (RSA).

Department of Water Affairs, 2013. National Water Act (36/1998): Revision of general authorisations in terms of section 39 of the Act (Requlation No. 665). *Government Gazette, 6 September 2013, No. 36820.*

Department of Water Affairs, 2014. *2013 Green Drop Report,* Pretoria: Department of Water Affairs (RSA).

Department of Water and Sanitation, 2015. *Green Drop System.* [Online] Available at: https://www.dwaf.gov.za/Dir_WS/GDS/GDS/Default.aspx [Accessed 17 February 2015].

Di Toro, D. M., 1978. Optics of Turbid Estuarine Waters: Approximations and Applications. *Warer Research,* 12(12), pp. 1059-1068.

Ekama, G. A. & Wentzel, M. C., 2008a. Organic Matter Removal. In: M. Henze, M. C. M. Van Loosdrecht, G. A. Ekama & B. D, eds. *Biological Wastewater Treatment: Principles, Modelling and Design.* London: IWA Publishing, pp. 53-86.

Ekama, G. A. & Wentzel, M. C., 2008b. Nitrogen Removal. In: M. Henze, M. C. M. Van Loosdrecht, G. A. Ekama & D. Brdjanovic, eds. *Biological Wastewater Treatment: Principles, Modelling and Design.* London: IWA Publishing, pp. 87-138.

Ekama, G. & Marais, G., 1977. The activated sludge process. Part II–dynamic behaviour. *Water SA,* 3(1), pp. 18-50.

Epperley, R. W., 1972. Temperature and Phytoplankton growth in the sea. *Fishery Bulletin,* 70(4), pp. 1063-1085.

Foehrenbach, J., 1972. Eutrophication. *Water Pollution Control Federation,* 44(6), pp. 1150-1159.

GeoSUN Africa, 2016. *Solar maps: Globar Horisontal Radiation.* [Online] Available at: http://geosun.co.za/solar-maps/ [Accessed 8 August 2016].

Green, F. B., Bernstone, T. J., Lundquist, T. J. & Oswald, W. J., 1996. Advanced integrated wastewater pond systems for nitrogen removal. *Water Science and Technology,* 33(7), pp. 207-217.

Henze, M., Van Loosdrecht, M. C. M., Ekama, G. A. & Brdjanovic, D., 2008. Wastewater Treatment Development. In: M. Henze, M. C. M. Van Loosdrecht, G. A. Ekama & D. Brdjanovic, eds. *Biological Wastewater Treatment: Principles, Modelling and Design.* London: IWA Publishing, pp. 1-8.

Howe, K. J. et al., 2012. *Principles of Water Treatment.* New Jersey: John Wiley & Sons, Inc..

Mara, D. D., 2004. *Domestic Wastewater Treatment in Developing Countries.* London: Earthscan.

Marais, G. & Ekama, G. A., 1976. The activated sludge process part I-steady state behaviour. *Water SA,* 2(4), pp. 164-200.

Matthews, M. W. & Bernard, S., 2015. Eutrophication and cyanobacteria in South Africa's standing water bodies: A view from space. *South African Journal of Science,* 111(5/6), p. 8.

Mayer, P. W. et al., 1999. *Residential end uses of water.* Denver, CO: AWWA Research Foundation and American Water Works Association.

Montgomery, D. C. & Runger, G. C., 2007. *Applied Statistics and Probability for Engineers.* 4th ed. s.l.:John Wiley & Sons, Inc..

Official Journal of European Communities, 1991. Council Directive 9 1 /271 /EEC of 21 May 1991 concerning urban waste water treatment. *Official Journal of European Communities,* Volume OJ L 135, pp. 40-52.

Osram, 2016. *Biolux T8 Product data sheet.* [Online] Available at: http://www.osram.com/osram_com/products/lamps/fluorescent-lamps/fluorescent-lamps-t8/fluorescent-lamps-t8-special-versions/biolux-t8/index.jsp [Accessed 2 March 2016].

Oswald, W. J., 1978. The Engineering Aspects of Microalgae. In: A. I. Laskin & H. A. Lechevalier, eds. *Handbook of Microbiology.* 2nd ed. Florida: CRC Press, pp. 519-552.

Park, J. B. K., Craggs, R. J. & Shilton, A. N., 2011. Wastewater treatment high rate algal ponds for biofuel production. *Bioresource Technology,* 102(1), pp. 35-42.

Render, D., 2015. *Rhodes High Rate Algal Pond* [Interview] (13 May 2015).

Riley, G. A. et al., 1956. Oceanography of Long Island Sound. *Bulletin of The Bingham Oseanographic Collection,* Volume 15, pp. 15-46.

Rose, P. D., Hart, O. O., Shipin, O. & Ellis, P. J., 2002. *Integrated Algal Ponding Systems and the Treatment of Domestic and Industrial Wastewaters Part 1: The AIWPS Model,* Pretoria: Water Research Commission.

Shilton, A., 2005. *Pond Treatment Technology.* London: IWA Publishing.

Tchobanoglous, G., Burton, F. L., Stensel, H. D. & Eddy, M. &., 2003. *Wastewater Engineering: Treatment and Reuse.* 4th ed. New York: McGraw-Hill.

Thomann, R. V. & Fitzpatrick, J. J., 1982. *Calibration and Verification of a mathematical model of the Eutriphication of the Potomac Estuary,* Washington, D.C.: HydroQual, Inc..

timeanddate.com, 2016a. *Cape Town, South Africa — Sunrise, Sunset, and Daylength.* [Online] Available at: http://www.timeanddate.com/sun/south-africa/cape-town [Accessed 9 August 2016].

timeanddate.com, 2016b. *Johannesburg, South Africa — Sunrise, Sunset, and Daylength.* [Online] Available at: http://www.timeanddate.com/sun/south-africa/johannesburg [Accessed 9 August 2016].

timeanddate.com, 2016c. *Durban, South Africa — Sunrise, Sunset, and Daylength.* [Online] Available at: http://www.timeanddate.com/sun/south-africa/durban [Accessed 9 August 2016].

Turton, A., 2015. Sitting on the Horns of a Dilemma: Water as a Strategic Resource in South Africa. *@Liberty*, 10 November, pp. 1-28.

WWIS, 2014a. *World Weather Information Service: Cape Town Climatological Information.* [Online]
Available at: http://worldweather.wmo.int/en/city.html?cityId=138 [Accessed 8 August 2016].

WWIS, 2014b. *World Weather Information Service: Johannesburg Climatological Information.* [Online]
Available at: http://worldweather.wmo.int/en/city.html?cityId=139 [Accessed 8 August 2016].

WWIS, 2014c. *World Weather Information Service: Durban Climatological Information.* [Online]
Available at: http://worldweather.wmo.int/en/city.html?cityId=137 [Accessed 8 August 2016].

APPENDICES

Appendix A: Typical Rates and Constants

Table A.1 - Typical values for the rates and constants applicable in the HRAP model

Stoichiometric Constants				
COD to VSS ratio in OHO biomass	f_{cv}	1.37-1.48 (1.48)	gCOD/ gVSS	(Comeau, 2008; Ekama & Wentzel, 2008a)
Nitrogen to VSS ratio in OHO biomass	a_{nv}	0.09-0.12 (0.10)	mgN/ mgVSS	(Ekama & Wentzel, 2008b)
Phosphorus to VSS ratio in OHO biomass	a_{pv}	0.01-0.03 (0.025)	mgP/ mgVSS	(Ekama & Wentzel, 2008b)
Ratio of VSS to algal biomass	f_{va}	50-100	mgVSS/ mgChl$a$	(Bowie, et al., 1985; Clesceri, et al., 1998)
Nitrogen to Chlorophyll a ratio in algal biomass	a_{na}	7-15	mgN/ mgChl$a$	(Bowie, et al., 1985)
Phosphorus to Chlorophyll a ratio in algal biomass	a_{pa}	0.5-1	mP/mgChl$a$	(Bowie, et al., 1985)
Ordinary Heterotopic Organisms (OHOs)				
Maximum specific growth rate at 20 °C	$\mu_{Hm,20}$	3-13.2 (6)	day^{-1}	(Tchobanoglous, et al., 2003)
Temperature correction factor for OHO growth	θ_{gX_a}	1.03-1.08 (1.07)	-	(Tchobanoglous, et al., 2003)
Endogenous respiration rate at 20 °C	$b_{H,20}$	0.24	day^{-1}	(Ekama & Wentzel, 2008a)
Temperature correction factor for endogenous respiration	θ_{rX_a}	1.029	-	(Ekama & Wentzel, 2008a)
Half saturation coefficient	K_s	5-40 (20)	mgCOD/L	(Tchobanoglous, et al., 2003)
Biomass Yield	Y_{Hv}	0.3-0.5 (0.45)	gVSS/ gCOD	(Tchobanoglous, et al., 2003; Ekama & Wentzel, 2008a)
Endogenous residue fraction	f_H	0.08-0.2 (0.2)	-	(Tchobanoglous, et al., 2003; Ekama & Wentzel, 2008a)
Ammonia Oxidising Organisms (ANOs)				
Maximum specific growth rate at 20 °C	$\mu_{Am,20}$	0.2-0.9 (0.75)	day^{-1}	(Tchobanoglous, et al., 2003)

Temperature correction factor for OHO growth	θ_{gX_n}	1.06-1.123 (1.07)	-	(Tchobanoglous, et al., 2003)
Endogenous respiration rate at 20 °C	$b_{A,20}$	0.04-0.15 (0.04,0.08)		(Ekama & Wentzel, 2008b; Tchobanoglous, et al., 2003)
Temperature correction factor for endogenous respiration	θ_{rX_n}	1.029-1.08 (1.04)		(Tchobanoglous, et al., 2003; Ekama & Wentzel, 2008b)
Half-saturation coefficient for the growth of ANOs	$K_{n,20}$	0.5-1 (0.74)	mgN/L	(Tchobanoglous, et al., 2003)
Temperature correction factor for the ANOs half-saturation coefficient	θ_{K_n}	1.03-1.123 (1.053)	-	(Tchobanoglous, et al., 2003)
Biomass Yield	Y_A	0.1-0.15 (0.1)	mgVSS/ mgN	(Tchobanoglous, et al., 2003; Ekama & Wentzel, 2008b)
Algae				
Maximum growth rate at 20 °C	$k_{ga,20}$	1.3-2.5	day^{-1}	(Bowie, et al., 1985)
Temperature correction factor for algal growth	θ_{ga}	1.066	-	(Epperley, 1972)
Respiration rate at 20 °C	$k_{rea,20}$	0.05-0.15	day^{-1}	(Bowie, et al., 1985)
Temperature correction factor for algal respiration	θ_{rea}	1.08	-	(Chapra, 2008)
Half saturation coefficient for algal growth	K_{sp}	0.0005-0.03	mgP/L	(Bowie, et al., 1985)
Half saturation coefficient for algal growth	K_{sn}	0.025	mgN/L	(Bowie, et al., 1985)
Half saturation for ammonia preference	K_{sam}	0.001-0.025	$mgNH_4$-N/L	(Thomann & Fitzpatrick, 1982; Cole & Wells, 2013)
Saturation light intensity	I_s	145-170	W/m^2	(Bowie, et al., 1985)
Light extinction in pure water	k_{ew}	0.04	m^{-1}	(Riley, et al., 1956)
Particulate Biodegradable COD				
Dissolution rate	k_p	0.1*	day^{-1}	(Chapra, 2008)
() - typical values * - model specific values				

Appendix B: Continuous Experiment Data

Table B.1 - Influent concentrations during the continuous operation

Influent Cycle		HRT (Days)	Parameter Concentration (mg/L)			
Start	End		SRP	NH_4-N	NO_3-N	COD
13-04-2016	15-04-2016	4	9.4	7.3	14.3	81.7
15-04-2016	19-04-2016	4	10.9	8.0	15.4*	83.1
19-04-2016	26-04-2016	4	9.5	6.6	12.6	77.8
26-04-2016	03-05-2016	4	10.7	8.0	15.8*	86.7
03-05-2016	10-05-2016	4	10.5	8.1	15.7*	85.5
10-05-2016	11-05-2016	4	9.1	6.9	13.2	73.3
17-05-2016	24-05-2016	10	9.1	6.9	13.2	73.3
24-05-2016	07-06-2016	10	9.7	6.6	13.2	76.8
07-06-2016	20-06-2016	10	8.7	6.7	12.5	74.3
* - outside recommended measurement range						

Table B.2 - Concentrations measured for the filtered effluent during continuous operation

Date	HRT (days)	Parameter Concentration (mg/L)				
		SRP	NH4-N	NO3-N	NO2-N	COD
13-04-2016	4	9.4	3.9	13.0	-	60
18-04-2016	4	9.0	3.0	12.9	-	25.5
26-04-2016	4	-	-	-	0.0	
05-05-2016	4	8.7	1.3	13.3	-	21.8
11-05-2016	4	8.9	1.6	13.2	-	18.8*
18-05-2016	10	10.0	0.09*	14.9*	-	26.3
24-05-2016	10	9.3	0.1*	14.3	3.0	22.3
30-05-2016	10	8.9	0.08*	13.9	2.5	23.9
03-06-2016	10	8.2	0.15*	13.9	2.1	21.8
09-06-2016	10	9.0	0.19*	13.6	1.6	20.5
17-06-2016	10	9.1	-	13.9	1.8	-
* - outside recommended measurement range						

Appendix C: Batch Experiment Data

Table C.1 - Concentrations and water levels measured in the batch experiment

Date	SRP (mgP/L)	NH4-N (mgN/L)	NO3-N (mgN/L)	NO2-N (mgN/L)	COD (mg/L)	Water level (mm)
20-06-2016 09:30	10.80	7.83	13.9	1.93	81.3	285
22-06-2016 08:08	10.93	5.31	14.72	2.14	30.2	280
24-06-2016 09:15	11.16	4.91	15.2	2.56	32.4	272
26-06-2016 09:45	11.26	4.76	15.62	2.91	32.6	265
28-06-2016 09:10	10.41	3.8	14.68	3.13	38.8	284
30-06-2016 07:07	10.61	3.23	15.2	3.52	32.1	276
04-07-2016 08:51	10.74	2.27	15.92	3.86	38.8	273
08-07-2016 08:31	11.55	1.56	17.06	4.15	38.7	254
11-07-2016 08:30	10.61	0.874	16.88	3.68	38.7	271
15-07-2016 08:26	10.67	0.449	21	0.504*	42	251
19-07-2016 09:26	9.69	0.125	20.2	0	33.7	278
22-07-2016 08:20	9.72	0.019	21.2	0	30.3	266
28-07-2016 08:16	8.32	0.02	18.88	0	30.9	286
* - outside recommended measurement range						

Table C.2 - Batch experiment concentrations after corrected for evaporation

Date	SRP (mgP/L)	NH4-N (mgN/L)	NO3-N (mgN/L)	NO2-N (mgN/L)	TIN (mgN/L)	COD (mg/L)
20-06-2016 09:30	10.7	7.7	13.8	1.9	23.4	80.5
22-06-2016 08:08	10.6	5.2	14.3	2.1	21.6	29.4
24-06-2016 09:15	10.5	4.6	14.4	2.4	21.4	30.6
26-06-2016 09:45	10.4	4.4	14.4	2.7	21.4	30.0
28-06-2016 09:10	10.3	3.7	14.5	3.1	21.3	38.3
30-06-2016 07:07	10.2	3.1	14.6	3.4	21.0	30.8
04-07-2016 08:51	10.2	2.2	15.1	3.7	20.9	36.8
08-07-2016 08:31	10.2	1.4	15.0	3.7	20.1	34.1
11-07-2016 08:30	10.0	0.8	15.9	3.5	20.2	36.4
15-07-2016 08:26	9.3	0.4	18.3	0.4	19.1	36.6
19-07-2016 09:26	9.4	0.1	19.5	0.0	19.6	32.5
22-07-2016 08:20	9.0	0.02	19.6	0.0	19.6	28.0
28-07-2016 08:16	8.3	0.02	18.7	0.0	18.8	30.7

Table C.3 - Batch experiment measured and adjusted chlorophyll *a* and VSS concentrations

Date	Measured		Water Level (mm)	Adjusted	
	Chl*a* (µg/L)	VSS (mg/L)		Chl*a* (µg/L)	VSS (mg/L)
20-06-2016	52	106	285	51	105
22-06-2016	-	107	285	-	104
24-06-2016	-	90	285	-	85
27-06-2016	-	80	285	-	79
30-06-2016	123	102	285	118	98
04-07-2016	-	76	285	-	72
08-07-2016	-	77	285	-	68
19-07-2016	544	115	285	525	111
28-07-2016	1570	103	285	1559	102

Appendix D: Model Calibration

Table D.1 - Ranges used in model calibration process

Parameter	Symbol	Round	Range		Step
Stoichiometric Constants					
Nitrogen to VSS ratio in OHO biomass	a_{nv}	1	0.09	0.12	0.01
		2	0.09	0.12	0.01
		3	0.09	0.12	0.01
Phosphorus to VSS ratio in OHO biomass	a_{pv}	1	0.01	0.03	0.01
		2	0.01	0.03	0.01
		3	0.01	0.03	0.01
Nitrogen to Chlorophyll *a* ratio in algal biomass	a_{na}	1	7	15	2
		2	7	7	0
		3	7	7	0
Phosphorus to Chlorophyll *a* ratio in algal biomass	a_{pa}	1	0.5	1	0.1
		2	1	1	0
		3	1	1	0
Ordinary Heterotopic Organisms (OHOs)					
Maximum specific growth rate at 20 °C	$\mu_{Hm,20}$	1	3	13	2
		2	3	13	2
		3	3	7	2
Half saturation coefficient	K_s	1	5	40	5
		2	5	40	5
		3	5	40	5
Biomass Yield	Y_{Hv}	1	0.3	0.5	0.1
		2	0.45	0.45	0
		3	0.45	0.45	0
Ammonia Oxidising Organisms (ANOs)					
Maximum specific growth rate at 20 °C	$\mu_{Am,20}$	1	0.2	1	0.2
		2	0.2	0.4	0.2
		3	0.2	0.2	0
Endogenous respiration rate at 20 °C	$b_{A,20}$	1	0.04	0.16	0.04
		2	0.04	0.16	0.04
		3	0.12	0.15	0.03
Half-saturation coefficient for the growth of ANOs	$K_{n,20}$	1	0.5	1	0.1
		2	0.5	1	0.1
		3	0.7	1	0.1
Biomass Yield	Y_A	1	0.1	0.15	0.025

		2	0.15	0.15	0
		3	0.15	0.15	0
Algae					
Maximum growth rate at 20 °C	$k_{ga,20}$	1	1.3	2.5	0.2
		2	1.3	1.7	0.2
		3	1.3	1.5	0.2
Respiration rate at 20 °C	$k_{rea,20}$	1	0.05	0.15	0.05
		2	0.1	0.15	0.05
		3	0.15	0.15	0
Saturation light intensity	I_s	1	145	170	5
		2	150	170	10
		3	150	170	10
Initial Concentrations					
Initial OHO concentration	X_{a_i}	1	5	20	5
		2	5	20	5
		3	1.5	5	0.5
Initial ANO concentration	X_{n_i}	1	0.2	0.8	0.1
		2	0.2	0.8	0.1
		3	0.2	0.8	0.1
Endogenous residue concentration	X_{e_i}	1	0	0	0
		2	0	0	0
		3	0	5	1

Table D.2 - Calibrated Rates and Constants

Stoichiometric Constants			
COD to VSS ratio in OHO biomass	f_{cv}	1.48	gCOD/gVSS
Nitrogen to VSS ratio in OHO biomass	a_{nv}	0.09	mgN/mgVSS
Phosphorus to VSS ratio in OHO biomass	a_{pv}	0.01	mgP/mgVSS
Ratio of VSS to algal biomass	f_{va}	75	mgVSS/mgChl*a*
Nitrogen to Chlorophyll *a* ratio in algal biomass	a_{na}	7	mgN/mgChl*a*
Phosphorus to Chlorophyll *a* ratio in algal biomass	a_{pa}	1	mP/mgChl*a*
Ordinary Heterotopic Organisms (OHOs)			
Initial OHO concentration	X_{a_i}	1.5	mgVSS/L
Initial endogenous residue concentration	X_{e_i}	5	mgVSS/L
Maximum specific growth rate at 20 °C	$\mu_{Hm,20}$	3	day^{-1}
Temperature correction factor for OHO growth	θ_{gX_a}	1.07	-
Endogenous respiration rate at 20 °C	$b_{H,20}$	0.24	day^{-1}

Temperature correction factor for endogenous respiration	θ_{rX_a}	1.029	-
Half saturation coefficient	K_s	40	mgCOD/L
Biomass Yield	Y_{Hv}	0.45	gVSS/gCOD
Endogenous residue fraction	f_H	0.2	-
Ammonia Oxidising Organisms (ANOs)			
Initial ANO concentration	X_{n_i}	0.21	mgVSS/L
Maximum specific growth rate at 20 °C	$\mu_{Am,20}$	0.2	day^{-1}
Temperature correction factor for OHO growth	θ_{gX_n}	1.07	-
Endogenous respiration rate at 20 °C	$b_{A,20}$	0.15	
Temperature correction factor for endogenous respiration	θ_{rX_n}	1.04	
Half-saturation coefficient for the growth of ANOs	$K_{n,20}$	1	mgN/L
Temperature correction factor for the ANOs half-saturation coefficient	θ_{K_n}	1.053	-
Biomass Yield	Y_A	0.15	mgVSS/mgN
Algae			
Maximum growth rate at 20 °C	$k_{ga,20}$	1.3	day^{-1}
Temperature correction factor for algal growth	θ_{ga}	1.066	-
Respiration rate at 20 °C	$k_{rea,20}$	0.15	day^{-1}
Temperature correction factor for algal respiration	θ_{rea}	1.08	-
Half saturation coefficient for algal growth	K_{sp}	0.03	mgP/L
Half saturation coefficient for algal growth	K_{sn}	0.025	mgN/L
Half saturation for ammonia preference	K_{sam}	0.025	$mgNH_4$-N/L
Saturation light intensity	I_s	170	W/m^2
Light extinction in pure water	k_{ew}	0.04	m^{-1}
Particulate Biodegradable COD			
Dissolution rate	k_p	0.1	day^{-1}

Appendix E: Climate Conditions Determination

Table E.1 - Average temperatures of cities chosen for evaluation

Month	**Cape Town**		**Johannesburg**		**Durban**	
	Min	Max	Min	Max	Min	Max
January	15.7	26.1	14.7	25.6	21.1	27.8
February	15.6	26.5	14.1	25.1	21.1	28
March	14.2	25.4	13.1	24	20.2	27.7
April	11.9	23	10.3	21.1	17.4	26.1
May	9.4	20.3	7.2	18.9	13.8	24.5
June	7.8	18.1	4.1	16	10.6	23
July	7	17.5	4.1	16.7	10.5	22.6
August	7.5	17.8	6.2	19.4	12.5	22.8
September	8.7	19.2	9.3	22.8	15.3	23.3
October	10.6	21.3	11.2	23.8	16.8	24
November	13.2	23.5	12.7	24.2	18.3	25.2
December	14.9	24.9	13.9	25.2	20	26.9
Average	11.4	22.0	10.1	21.9	16.5	25.2
Combined Average	16.7		16.0		20.8	

Appendix F: Nutrient Removal Charts for Johannesburg and Durban

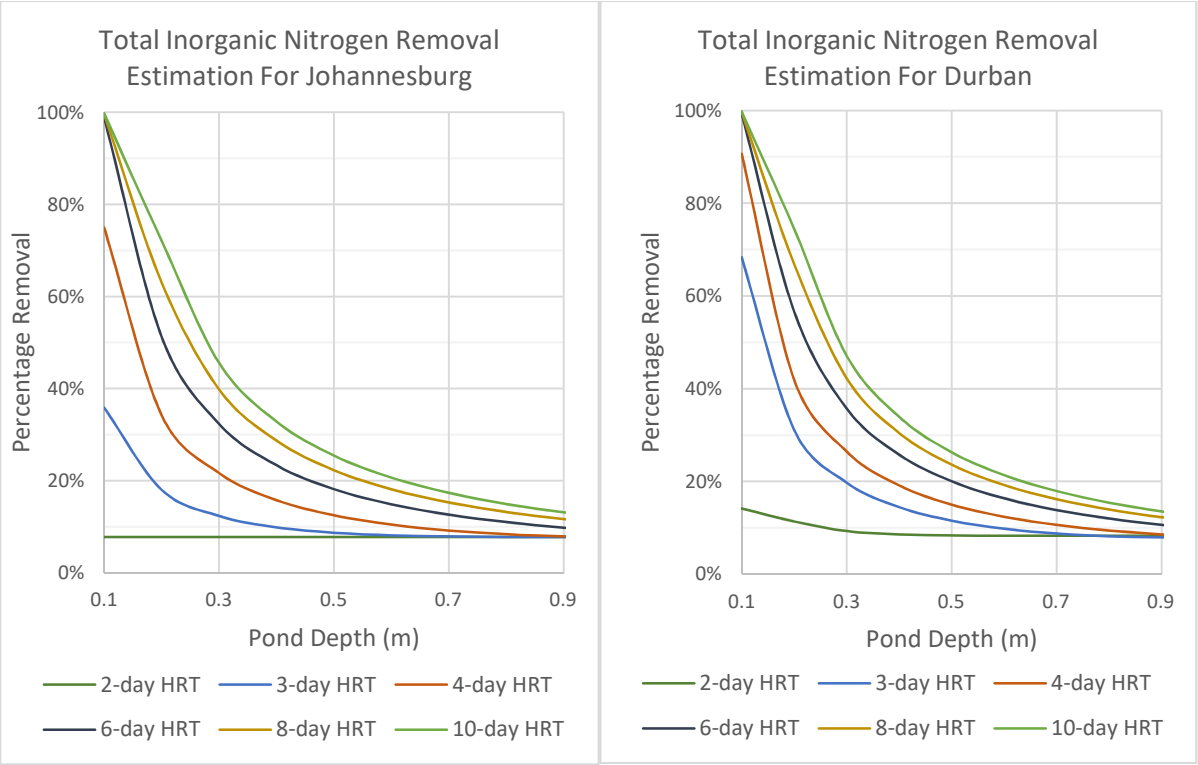

Figure F.1 - Estimation of Total Inorganic Nitrogen removal for an HRAP in Johannesburg and Durban

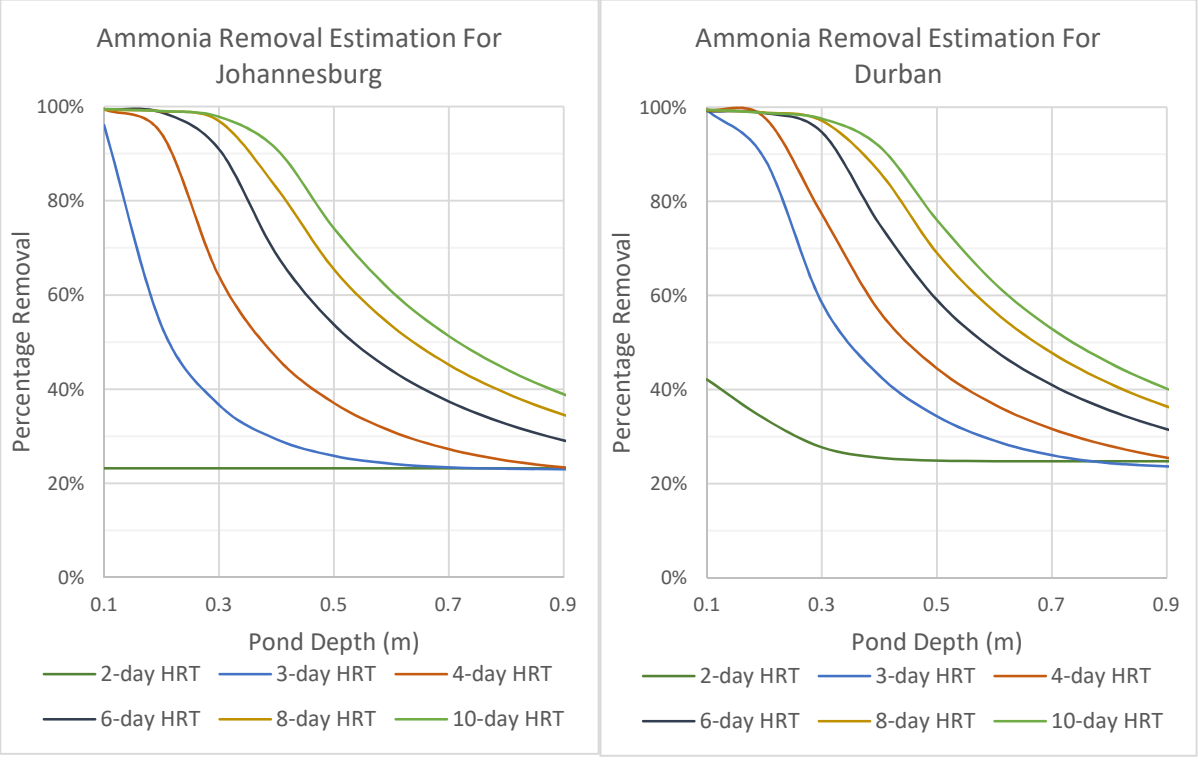

Figure F.2 - Estimation of ammonia removal for an HRAP in Johannesburg and Durban

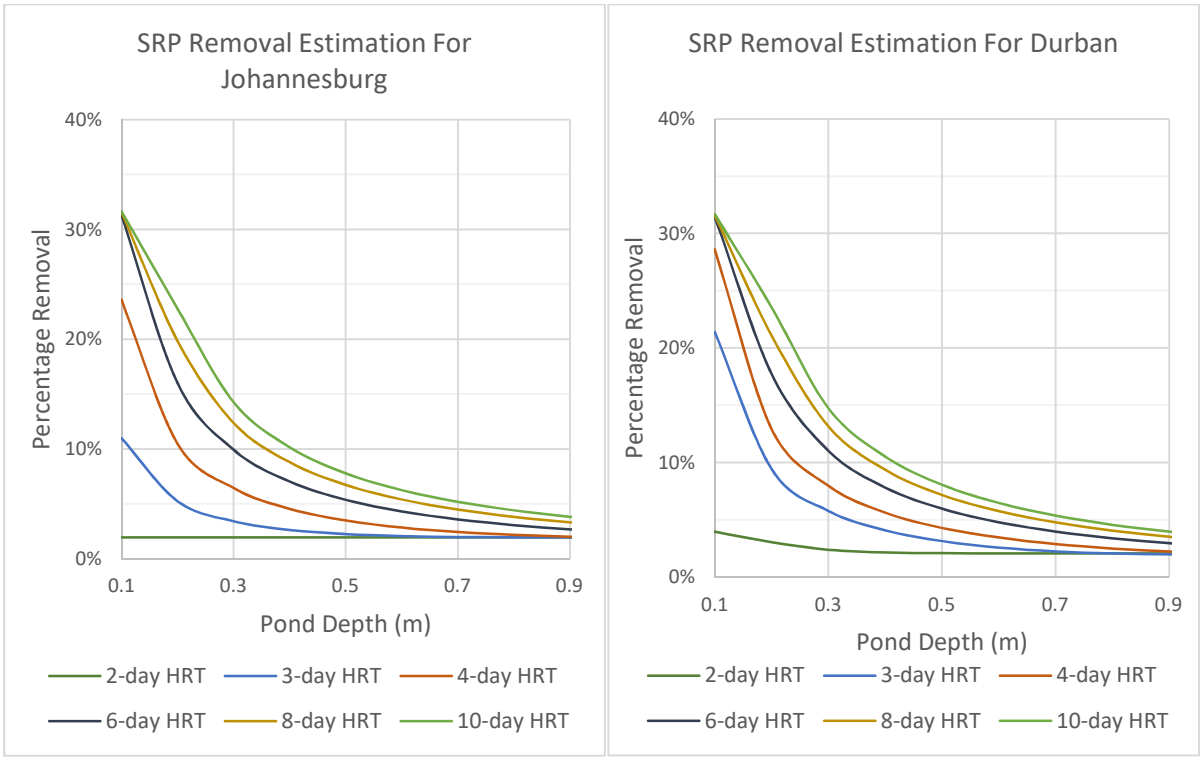

Figure F.3 - Estimation of SRP removal for an HRAP in Johannesburg and Durban

Appendix G: Area Requirement for Nutrient Removal

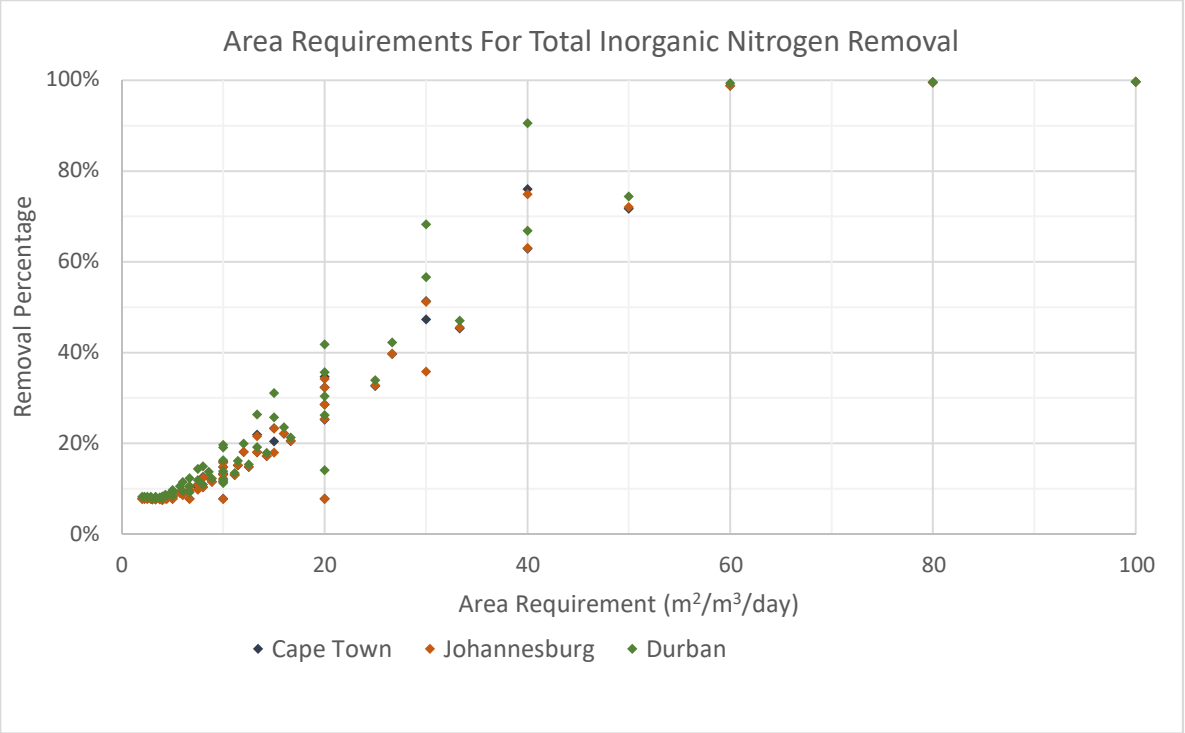

Figure G.1 - Full chart of area requirements for Total Inorganic Nitrogen removal

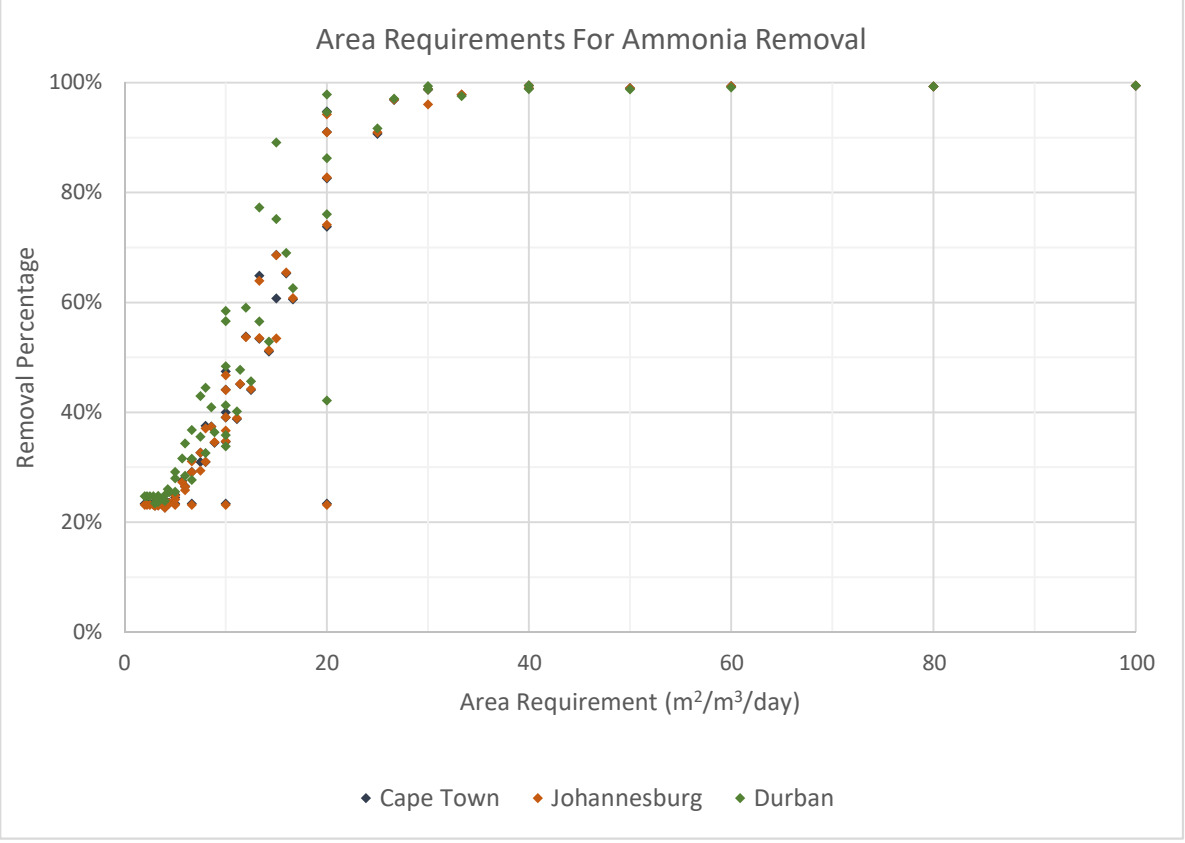

Figure G.2 - Full chart of area requirements for ammonia removal

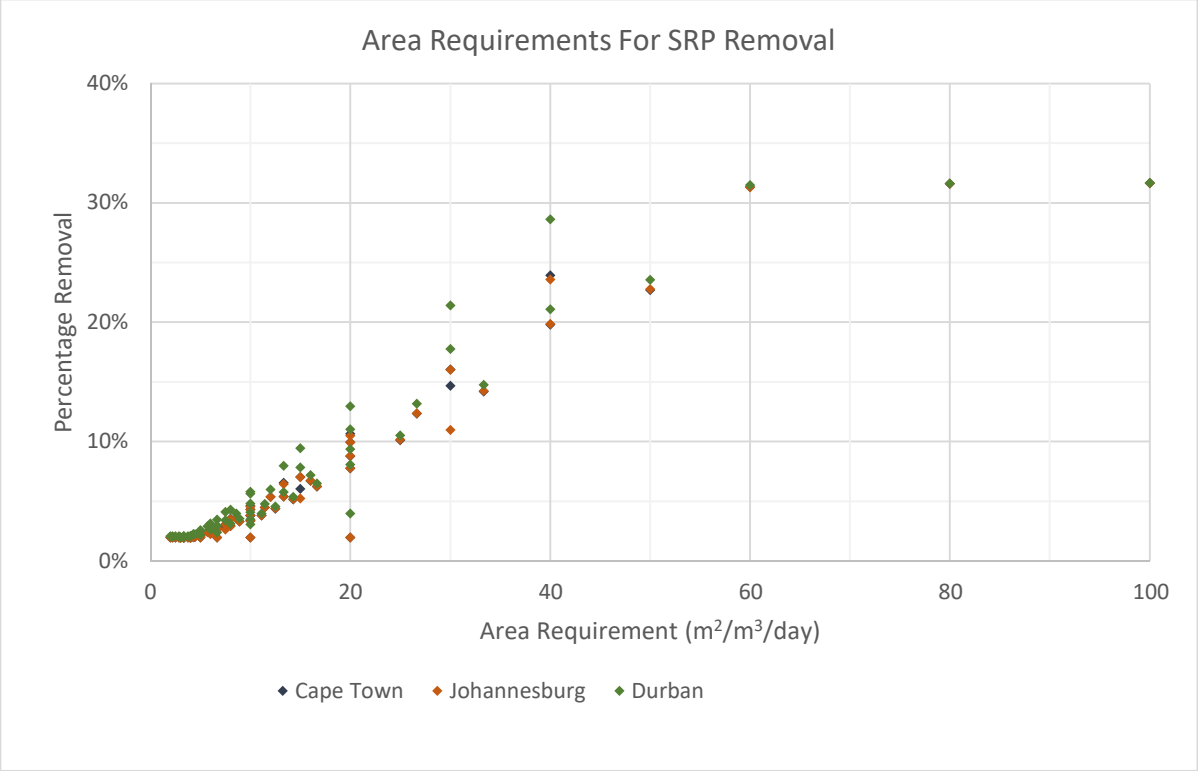

Figure G.3 - Full chart of area requirements for SRP removal

Appendix H: Model Code

```
Option Explicit
Sub model()

    Dim p, a, am, ni, Xa, Xer, cs, Xn, cp, pj, aj, amj, nij, Xaj, Xerj, csj, Xnj, cpj, ti, timeStep, simTime As Double
    Dim steps, i, rowEnd, currentRow As Long

    Dim total, indexDate, indexValue As Long

    Sheet3.Cells.Clear

    rowEnd = 1

    Do While Not Sheet6.Cells(rowEnd + 1, 1).Value = ""
        rowEnd = rowEnd + 1
    Loop

    timeStep = Sheet5.Range("t").Value
    simTime = Sheet6.Cells(rowEnd, 1).Value - Sheet6.Cells(2, 1).Value
    steps = Application.WorksheetFunction.RoundUp(simTime / timeStep, 0)

    p = Sheet5.Range("Pi").Value
    a = Sheet5.Range("Ai").Value
    am = Sheet5.Range("Nai").Value
    ni = Sheet5.Range("Nii").Value
    Xa = Sheet5.Range("Xai").Value
    cs = Sheet5.Range("csi").Value
    cp = Sheet5.Range("cpi").Value
    Xn = Sheet5.Range("Xni").Value
    Xer = Sheet5.Range("Xeri").Value

    Sheet3.Cells(1, 1).Value = "T"
    Sheet3.Cells(1, 2).Value = "Xa"
    Sheet3.Cells(1, 3).Value = "Xn"
    Sheet3.Cells(1, 4).Value = "A"
    Sheet3.Cells(1, 5).Value = "Xer"
    Sheet3.Cells(1, 6).Value = "cs"
    Sheet3.Cells(1, 7).Value = "cp"
    Sheet3.Cells(1, 8).Value = "P"
    Sheet3.Cells(1, 9).Value = "Am"
    Sheet3.Cells(1, 10).Value = "Ni"
    Sheet3.Cells(1, 11).Value = "VSS"

    ti = Sheet6.Cells(2, 1).Value
    currentRow = 2

    Sheet3.Cells(2, 1).Value = ti
    Sheet3.Cells(2, 2).Value = Xa
    Sheet3.Cells(2, 3).Value = Xn
    Sheet3.Cells(2, 4).Value = a
    Sheet3.Cells(2, 5).Value = Xer
    Sheet3.Cells(2, 6).Value = cs
    Sheet3.Cells(2, 7).Value = cp
    Sheet3.Cells(2, 8).Value = p
```

```
Sheet3.Cells(2, 9).Value = am
Sheet3.Cells(2, 10).Value = ni
Sheet3.Cells(2, 11).Value = getVSS(Xa, Xn, Xer, a, cp)

For i = 1 To steps

   If (ti + timeStep * i) >= Sheet6.Cells(currentRow + 1, 1).Value Then
      currentRow = currentRow + 1
   End If

   Xaj = Xa
   Xnj = Xn
   aj = a
   Xerj = Xer
   csj = cs
   cpj = cp
   pj = p
   amj = am
   nij = ni

   Xa = Xa + Dynamic.ohoChange(Xaj, csj, currentRow)
   Xn = Xn + Dynamic.anoChange(Xnj, amj, currentRow)
   a = a + Dynamic.algalChange(aj, Xaj, Xnj, Xerj, cpj, pj, amj + nij, currentRow)
   Xer = Xer + Dynamic.erChange(Xaj, Xerj, currentRow)
   cs = cs + Dynamic.sbCODchange(Xaj, csj, cpj, currentRow)
   cp = cp + Dynamic.pbCODchange(cpj, currentRow)
   p = p + Dynamic.srpChange(aj, pj, amj, nij, Xaj, Xnj, Xerj, cpj, csj, currentRow)
   am = am + Dynamic.ammoniaChange(aj, pj, amj, nij, Xaj, Xnj, Xerj, cpj, csj, currentRow)
   ni = ni + Dynamic.nitrateChange(aj, Xaj, Xnj, Xerj, pj, amj, nij, csj, cpj, currentRow)

   If p < 0 Then
      p = 0
   End If

   If am < 0 Then
      am = 0
   End If

   If ni < 0 Then
      ni = 0
   End If

   If cs < 0 Then
      cs = 0
   End If

   If cp < 0 Then
      cp = 0
   End If

   Sheet3.Cells(i + 2, 1).Value = ti + timeStep * i
   Sheet3.Cells(i + 2, 2).Value = Xa
   Sheet3.Cells(i + 2, 3).Value = Xn
   Sheet3.Cells(i + 2, 4).Value = a
   Sheet3.Cells(i + 2, 5).Value = Xer
```

```
    Sheet3.Cells(i + 2, 6).Value = cs
    Sheet3.Cells(i + 2, 7).Value = cp
    Sheet3.Cells(i + 2, 8).Value = p
    Sheet3.Cells(i + 2, 9).Value = am
    Sheet3.Cells(i + 2, 10).Value = ni
    Sheet3.Cells(i + 2, 11).Value = getVSS(Xa, Xn, Xer, a, cp)

Next i

Chart9.Axes(xlCategory).MaximumScale = Sheet6.Cells(rowEnd, 1).Value
Chart9.Axes(xlCategory).MinimumScale = Sheet6.Cells(2, 1).Value

Chart9.FullSeriesCollection(1).XValues = Range(Sheet3.Cells(2, 1), Sheet3.Cells(i + 1, 1))
Chart9.FullSeriesCollection(1).Values = Range(Sheet3.Cells(2, 2), Sheet3.Cells(i + 1, 2))
Chart9.FullSeriesCollection(1).IsFiltered = Not Sheet5.CheckBox1.Value
Chart9.FullSeriesCollection(2).XValues = Range(Sheet3.Cells(2, 1), Sheet3.Cells(i + 1, 1))
Chart9.FullSeriesCollection(2).Values = Range(Sheet3.Cells(2, 3), Sheet3.Cells(i + 1, 3))
Chart9.FullSeriesCollection(2).IsFiltered = Not Sheet5.CheckBox2.Value
Chart9.FullSeriesCollection(3).XValues = Range(Sheet3.Cells(2, 1), Sheet3.Cells(i + 1, 1))
Chart9.FullSeriesCollection(3).Values = Range(Sheet3.Cells(2, 4), Sheet3.Cells(i + 1, 4))
Chart9.FullSeriesCollection(3).IsFiltered = Not Sheet5.CheckBox3.Value
Chart9.FullSeriesCollection(4).XValues = Range(Sheet3.Cells(2, 1), Sheet3.Cells(i + 1, 1))
Chart9.FullSeriesCollection(4).Values = Range(Sheet3.Cells(2, 5), Sheet3.Cells(i + 1, 5))
Chart9.FullSeriesCollection(4).IsFiltered = Not Sheet5.CheckBox4.Value
Chart9.FullSeriesCollection(5).XValues = Range(Sheet3.Cells(2, 1), Sheet3.Cells(i + 1, 1))
Chart9.FullSeriesCollection(5).Values = Range(Sheet3.Cells(2, 6), Sheet3.Cells(i + 1, 6))
Chart9.FullSeriesCollection(5).IsFiltered = Not Sheet5.CheckBox5.Value
Chart9.FullSeriesCollection(6).XValues = Range(Sheet3.Cells(2, 1), Sheet3.Cells(i + 1, 1))
Chart9.FullSeriesCollection(6).Values = Range(Sheet3.Cells(2, 7), Sheet3.Cells(i + 1, 7))
Chart9.FullSeriesCollection(6).IsFiltered = Not Sheet5.CheckBox6.Value
Chart9.FullSeriesCollection(7).XValues = Range(Sheet3.Cells(2, 1), Sheet3.Cells(i + 1, 1))
Chart9.FullSeriesCollection(7).Values = Range(Sheet3.Cells(2, 8), Sheet3.Cells(i + 1, 8))
Chart9.FullSeriesCollection(7).IsFiltered = Not Sheet5.CheckBox7.Value
Chart9.FullSeriesCollection(8).XValues = Range(Sheet3.Cells(2, 1), Sheet3.Cells(i + 1, 1))
Chart9.FullSeriesCollection(8).Values = Range(Sheet3.Cells(2, 9), Sheet3.Cells(i + 1, 9))
Chart9.FullSeriesCollection(8).IsFiltered = Not Sheet5.CheckBox8.Value
Chart9.FullSeriesCollection(9).XValues = Range(Sheet3.Cells(2, 1), Sheet3.Cells(i + 1, 1))
Chart9.FullSeriesCollection(9).Values = Range(Sheet3.Cells(2, 10), Sheet3.Cells(i + 1, 10))
Chart9.FullSeriesCollection(9).IsFiltered = Not Sheet5.CheckBox9.Value
Chart9.FullSeriesCollection(10).XValues = Range(Sheet3.Cells(2, 1), Sheet3.Cells(i + 1, 1))
Chart9.FullSeriesCollection(10).Values = Range(Sheet3.Cells(2, 11), Sheet3.Cells(i + 1, 11))
Chart9.FullSeriesCollection(10).IsFiltered = Not Sheet5.CheckBox10.Value

i = 1

Do While Not Sheet7.Cells(i + 1, 1).Value = ""
    i = i + 1
Loop

Chart9.FullSeriesCollection(11).XValues = Range(Sheet7.Cells(2, 1), Sheet7.Cells(i, 1))
Chart9.FullSeriesCollection(11).Values = Range(Sheet7.Cells(2, 5), Sheet7.Cells(i, 5))
Chart9.FullSeriesCollection(11).IsFiltered = Not Sheet5.CheckBox11.Value
Chart9.FullSeriesCollection(12).XValues = Range(Sheet7.Cells(2, 1), Sheet7.Cells(i, 1))
Chart9.FullSeriesCollection(12).Values = Range(Sheet7.Cells(2, 6), Sheet7.Cells(i, 6))
Chart9.FullSeriesCollection(12).IsFiltered = Not Sheet5.CheckBox12.Value
```

```
    Chart9.FullSeriesCollection(13).XValues = Range(Sheet7.Cells(2, 1), Sheet7.Cells(i, 1))
    Chart9.FullSeriesCollection(13).Values = Range(Sheet7.Cells(2, 2), Sheet7.Cells(i, 2))
    Chart9.FullSeriesCollection(13).IsFiltered = Not Sheet5.CheckBox13.Value
    Chart9.FullSeriesCollection(14).XValues = Range(Sheet7.Cells(2, 1), Sheet7.Cells(i, 1))
    Chart9.FullSeriesCollection(14).Values = Range(Sheet7.Cells(2, 3), Sheet7.Cells(i, 3))
    Chart9.FullSeriesCollection(14).IsFiltered = Not Sheet5.CheckBox14.Value
    Chart9.FullSeriesCollection(15).XValues = Range(Sheet7.Cells(2, 1), Sheet7.Cells(i, 1))
    Chart9.FullSeriesCollection(15).Values = Range(Sheet7.Cells(2, 4), Sheet7.Cells(i, 4))
    Chart9.FullSeriesCollection(15).IsFiltered = Not Sheet5.CheckBox15.Value
    Chart9.FullSeriesCollection(16).XValues = Range(Sheet7.Cells(2, 1), Sheet7.Cells(i, 1))
    Chart9.FullSeriesCollection(16).Values = Range(Sheet7.Cells(2, 7), Sheet7.Cells(i, 7))
    Chart9.FullSeriesCollection(16).IsFiltered = Not Sheet5.CheckBox16.Value

    Sheet3.Cells(1, 13).Value = "Influent Data"
    total = (rowEnd - 2) * 2
    indexDate = 2
    indexValue = 2

    For i = 1 To total

        If i Mod 2 = 0 Then
            indexDate = indexDate + 1
        End If

        If Not i Mod 2 = 0 And Not i = 1 Then
            indexValue = indexValue + 1
        End If

        Sheet3.Cells(i + 1, 13).Value = Sheet6.Cells(indexDate, 1).Value
        Sheet3.Cells(i + 1, 14).Value = Sheet6.Cells(indexValue, 2).Value
        Sheet3.Cells(i + 1, 15).Value = Sheet6.Cells(indexValue, 3).Value
        Sheet3.Cells(i + 1, 16).Value = Sheet6.Cells(indexValue, 4).Value
        Sheet3.Cells(i + 1, 17).Value = Sheet6.Cells(indexValue, 5).Value
        Sheet3.Cells(i + 1, 18).Value = Sheet6.Cells(indexValue, 6).Value

    Next i

    Chart9.FullSeriesCollection(17).XValues = Range(Sheet3.Cells(2, 13), Sheet3.Cells(total + 1, 13))
    Chart9.FullSeriesCollection(17).Values = Range(Sheet3.Cells(2, 18), Sheet3.Cells(total + 1, 18))
    Chart9.FullSeriesCollection(17).IsFiltered = Not Sheet5.CheckBox17.Value
    Chart9.FullSeriesCollection(18).XValues = Range(Sheet3.Cells(2, 13), Sheet3.Cells(total + 1, 13))
    Chart9.FullSeriesCollection(18).Values = Range(Sheet3.Cells(2, 15), Sheet3.Cells(total + 1, 15))
    Chart9.FullSeriesCollection(18).IsFiltered = Not Sheet5.CheckBox18.Value
    Chart9.FullSeriesCollection(19).XValues = Range(Sheet3.Cells(2, 13), Sheet3.Cells(total + 1, 13))
    Chart9.FullSeriesCollection(19).Values = Range(Sheet3.Cells(2, 16), Sheet3.Cells(total + 1, 16))
    Chart9.FullSeriesCollection(19).IsFiltered = Not Sheet5.CheckBox19.Value
    Chart9.FullSeriesCollection(20).XValues = Range(Sheet3.Cells(2, 13), Sheet3.Cells(total + 1, 13))
    Chart9.FullSeriesCollection(20).Values = Range(Sheet3.Cells(2, 17), Sheet3.Cells(total + 1, 17))
    Chart9.FullSeriesCollection(20).IsFiltered = Not Sheet5.CheckBox20.Value

    Chart9.Activate
    Chart9.Refresh

End Sub
```

```
Function getVSS(Xa, Xn, Xer, a, cp) As Double
    Dim fcv, fva As Double

    fcv = Sheet1.Range("fcv").Value
    fva = Sheet1.Range("fva").Value

    getVSS = Xa + Xn + Xer + (a * fva) + (cp / fcv)
End Function

Function getFlow(row) As Double
    getFlow = Sheet6.Cells(row, 2).Value
End Function

Function ohoGrowthRate(cs) As Double
    Dim uH As Double
    Dim ks, t, thetaGXA As Double

    uH = Sheet1.Range("Uh").Value
    ks = Sheet1.Range("ks").Value
    t = Sheet5.Range("Temp").Value
    thetaGXA = Sheet1.Range("thetaGXA").Value

    ohoGrowthRate = uH * (thetaGXA ^ (t - 20)) * cs / (ks + cs)
End Function

Function ohoRespirationRate() As Double
    Dim bh, thetaRXA, temp As Double

    bh = Sheet1.Range("bh").Value
    temp = Sheet5.Range("Temp").Value
    thetaRXA = Sheet1.Range("thetaRXA").Value

    ohoRespirationRate = bh * thetaRXA ^ (temp - 20)
End Function

Function ohoChange(Xa, cs, row) As Double
    Dim Q As Double
    Dim V As Double
    Dim dt, kgx, krx As Double

    dt = Sheet5.Range("t").Value
    Q = Dynamic.getFlow(row)
    V = Sheet5.Range("V").Value

    kgx = ohoGrowthRate(cs)
    krx = ohoRespirationRate()

    ohoChange = (Xa * kgx - Xa * krx - Q / V * Xa) * dt
End Function

Function anoGrowthRate(am) As Double
    Dim uA, Kn, temp, thetaGXN, thetaKN As Double

    uA = Sheet1.Range("uA").Value
```

```
    temp = Sheet5.Range("Temp").Value
    Kn = Sheet1.Range("Kn").Value
    thetaGXN = Sheet1.Range("thetaGXN").Value
    thetaKN = Sheet1.Range("thetaKN").Value

    Kn = Kn * (thetaKN ^ (temp - 20))

    anoGrowthRate = uA * (thetaGXN ^ (temp - 20)) * am / (Kn + am)
End Function

Function anoRespirationRate() As Double
    Dim bA, thetaRXN, temp As Double

    bA = Sheet1.Range("bA").Value
    temp = Sheet5.Range("Temp").Value
    thetaRXN = Sheet1.Range("thetaRXN").Value

    anoRespirationRate = bA * thetaRXN ^ (temp - 20)
End Function

Function anoChange(Xn, am, row) As Double
    Dim Q As Double
    Dim V As Double
    Dim dt, kg, kr As Double

    dt = Sheet5.Range("t").Value
    Q = Dynamic.getFlow(row)
    V = Sheet5.Range("V").Value

    kg = anoGrowthRate(am)
    kr = anoRespirationRate()

    anoChange = (Xn * kg - Xn * kr - Q / V * Xn) * dt
End Function

Function erChange(Xa, Xer, row) As Double
    Dim f, kxr, dt, Q, V As Double

    Q = Dynamic.getFlow(row)
    V = Sheet5.Range("V").Value
    f = Sheet1.Range("fH").Value
    dt = Sheet5.Range("t").Value

    kxr = ohoRespirationRate()

    erChange = (f * kxr * Xa - Q / V * Xer) * dt
End Function

Function getSBCODIn(row) As Double
    getSBCODIn = Sheet6.Cells(row, 6).Value
End Function

Function sbCODchange(Xa, cs, cp, row) As Double
    Dim csin As Double
    Dim Q As Double
```

```
    Dim V As Double
    Dim dt, kgx, Yhv, kp As Double

    dt = Sheet5.Range("t").Value
    Q = Dynamic.getFlow(row)
    V = Sheet5.Range("V").Value
    csin = getSBCODIn(row)
    Yhv = Sheet1.Range("Yhv").Value
    kp = Sheet1.Range("kp").Value

    kgx = ohoGrowthRate(cs)

    sbCODchange = (Q / V * (csin - cs) - Xa * kgx / Yhv + kp * cp) * dt
End Function

Function getPBCODIn(row) As Double
    getPBCODIn = Sheet6.Cells(row, 7).Value
End Function

Function pbCODchange(cp, row) As Double
    Dim Q As Double
    Dim V, kp, dt, cpin As Double

    kp = Sheet1.Range("kp").Value
    dt = Sheet5.Range("t").Value
    V = Sheet5.Range("V").Value

    Q = Dynamic.getFlow(row)
    cpin = getPBCODIn(row)

    pbCODchange = (-kp * cp + Q / V * (cpin - cp)) * dt
End Function

Function phosphateIn(row) As Double
    phosphateIn = Sheet6.Cells(row, 3).Value
End Function

Function ammoniaIn(row) As Double
    ammoniaIn = Sheet6.Cells(row, 4).Value
End Function

Function nitrateIn(row) As Double
    nitrateIn = Sheet6.Cells(row, 5).Value
End Function

Function algaeGrowthRate(a, Xa, Xn, Xer, cp, n, p) As Double
    Dim kga, ftg, fl, fn As Double
    Dim thetaGA As Double
    Dim temp As Double
    Dim fld, d, lightS, Im, kea, Ia, ke, alpha0, alpha1, kew, fcv As Double
    Dim ksp, ksn As Double

    kga = Sheet1.Range("kga").Value
    fld = Sheet5.Range("fld").Value
    d = Sheet5.Range("d").Value
```

```
    lightS = Sheet1.Range("Is").Value
    Im = Sheet5.Range("Im").Value
    kew = Sheet1.Range("kew").Value
    fcv = Sheet1.Range("fcv").Value
    ksp = Sheet1.Range("ksp").Value
    ksn = Sheet1.Range("ksn").Value

    thetaGA = Sheet1.Range("thetaGA").Value
    temp = Sheet5.Range("Temp").Value
    ftg = (thetaGA ^ (temp - 20))

    Ia = Im * (2 / WorksheetFunction.pi())

    kea = kew + 0.174 * (Xa + Xn + Xer + cp / fcv)
    ke = kea + 0.0088 * a * 1000 + 0.054 * (a * 1000) ^ (2 / 3)

    alpha0 = Ia / lightS
    alpha1 = Ia / lightS * Exp(-ke * d)

    fl = 2.718 * fld * (Exp(-alpha1) - Exp(-alpha0)) / (ke * d)

    fn = WorksheetFunction.min(p / (p + ksp), n / (n + ksn))

    algaeGrowthRate = kga * fl * fn * ftg
End Function

Function algaeRespirationRate() As Double
    Dim thetaRA, kra As Double
    Dim temp, ftr As Double

    thetaRA = Sheet1.Range("thetaRA").Value
    temp = Sheet5.Range("Temp").Value
    kra = Sheet1.Range("kra").Value

    ftr = (thetaRA ^ (temp - 20))

    algaeRespirationRate = ftr * kra
End Function

Function nitrificationRate() As Double
    Dim thetaN, Kn, ftn As Double
    Dim temp As Double

    thetaN = Sheet1.Range("thetaN").Value
    temp = Sheet5.Range("Temp").Value
    Kn = Sheet1.Range("kn").Value

    ftn = (thetaN ^ (temp - 20))

    nitrificationRate = Kn * ftn
End Function

Function ammoniaPreference(am, ni) As Double
    Dim kam As Double
```

```
    kam = Sheet1.Range("ksam").Value

    ammoniaPreference = am * ni / ((kam + am) * (kam + ni)) + am * kam / ((am + ni) * (kam + ni))
End Function


Function algalChange(a, Xa, Xn, Xer, cp, p, n, row) As Double
    Dim kag, kra, dt, Q, V As Double

    dt = Sheet5.Range("t").Value
    Q = Dynamic.getFlow(row)
    V = Sheet5.Range("V").Value

    kag = algaeGrowthRate(a, Xa, Xn, Xer, cp, n, p)
    kra = algaeRespirationRate()

    algalChange = (kag - kra - Q / V) * a * dt
End Function

Function srpChange(a, p, am, ni, Xa, Xn, Xer, cp, cs, rowIn) As Double
    Dim kag, kra, dt, Q, V, Pin, apa, fH, fopc, Yhv, kgxa, apv, krxa, kgxn, krxn As Double

    dt = Sheet5.Range("t").Value
    V = Sheet5.Range("V").Value
    apa = Sheet1.Range("apa").Value
    apv = Sheet1.Range("apv").Value
    fH = Sheet1.Range("fH").Value
    fopc = Sheet1.Range("fopc").Value
    Yhv = Sheet1.Range("Yhv").Value

    Q = Dynamic.getFlow(rowIn)
    Pin = Dynamic.phosphateIn(rowIn)

    kra = algaeRespirationRate()
    kag = algaeGrowthRate(a, Xa, Xn, Xer, cp, am + ni, p)

    kgxa = Dynamic.ohoGrowthRate(cs)
    krxa = Dynamic.ohoRespirationRate()

    kgxn = Dynamic.anoGrowthRate(am)
    krxn = Dynamic.anoRespirationRate()

    srpChange = dt * ((apa * kra * a) + (apv * krxa * Xa * (1 - fH)) + (apv * krxn * Xn) - (apa * kag * a) - (apv * kgxa * Xa) - (apv *
                                    kgxn * Xn) + Q / V * (Pin - p) + (fopc * Xa * kgxa / Yhv))
End Function

Function ammoniaChange(a, p, am, ni, Xa, Xn, Xer, cp, cs, rowIn) As Double
    Dim kag, kra, kgxa, kgxn, krxa, krxn, dt, Q, V, ana, amin, fam, fH, anv, Yhv, Yn, fonc As Double

    dt = Sheet5.Range("t").Value
    V = Sheet5.Range("V").Value
    ana = Sheet1.Range("ana").Value
    anv = Sheet1.Range("anv").Value
    fH = Sheet1.Range("fH").Value
    Yhv = Sheet1.Range("Yhv").Value
```

```
    Yn = Sheet1.Range("Yn").Value
    fonc = Sheet1.Range("fonc").Value

    amin = Dynamic.ammoniaIn(rowIn)
    Q = Dynamic.getFlow(rowIn)

    fam = ammoniaPreference(am, ni)

    kag = algaeGrowthRate(a, Xa, Xn, Xer, cp, am + ni, p)
    kra = algaeRespirationRate()

    kgxa = Dynamic.ohoGrowthRate(cs)
    krxa = Dynamic.ohoRespirationRate()

    kgxn = Dynamic.anoGrowthRate(am)
    krxn = Dynamic.anoRespirationRate()

    ammoniaChange = dt * ((ana * kra * a) + (anv * krxa * Xa * (1 - fH)) + (anv * krxn * Xn) - (fam * ana * kag * a) - (anv * fam *
                    kgxa * Xa) - (anv * fam * kgxn * Xn) + (fonc * Xa * kgxa / Yhv) - (Xn * kgxn / Yn) + Q / V * (amin - am))
End Function

Function nitrateChange(a, Xa, Xn, Xer, p, am, ni, cs, cp, rowIn) As Double
    Dim kag, kgxa, kgxn, dt, Q, V, niin, ana, anv, fam, Yn As Double

    dt = Sheet5.Range("t").Value
    V = Sheet5.Range("V").Value
    ana = Sheet1.Range("ana").Value
    anv = Sheet1.Range("anv").Value
    Yn = Sheet1.Range("Yn").Value

    Q = Dynamic.getFlow(rowIn)
    niin = Dynamic.nitrateIn(rowIn)

    fam = ammoniaPreference(am, ni)

    kag = algaeGrowthRate(a, Xa, Xn, Xer, cp, am + ni, p)
    kgxa = Dynamic.ohoGrowthRate(cs)
    kgxn = Dynamic.anoGrowthRate(am)

    nitrateChange = dt * (Q / V * (niin - ni) + (Xn * kgxn / Yn) - ((1 - fam) * ana * kag * a) - ((1 - fam) * anv * kgxa * Xa) - ((1 - fam)
                    * anv * kgxn * Xn))
End Function
```